UNIVERSITY OF CALIFORNIA SAN DIEGO

SAN DIEGO STATE UNIVERSITY

Functional and Anatomical Substrates of Cognitive Abilities in Autism Spectrum Disorder

A dissertation submitted in partial satisfaction of the requirements for the degree Doctor of Philosophy

in

Clinical Psychology

by

Maya Anne Reiter

Committee in charge:

University of California San Diego

Professor Jay Giedd
Professor Frank Haist

San Diego State University

Professor Ralph-Axel Müller, Chair
Professor Ruth Carper
Professor Inna Fishman
Professor Jillian Lee Wiggins

2022

The dissertation of Maya Anne Reiter is approved, and it is acceptable in quality and form for publication on microfilm and electronically.

_____

_____

_____

_____

_____

_____

_____

_____
Chair

University of California San Diego

San Diego State University

2022

TABLE OF CONTENTS

LIST OF TABLES

LIST OF FIGURES

ACKNOWLEDGEMENTS

For the instrumental guidance and support I've received from many individuals throughout and before my time in graduate school, I am extremely grateful. I would first like to acknowledge Dr. Ralph-Axel Müller, my dissertation chair, for his invaluable scientific insight and instruction over the years it took to produce this work. Thank you for developing my ability to articulate, generate, fund, and publish, ideas. Many thanks also to Dr. Vanessa Malcarne, Dr. Mike Taylor, Dr. George Matt, and my clinical supervisors at the JDP for the professional and personal guidance they've provided. I also would like to thank my dissertation committee, my coauthors, and Dr. Inna Fishman, and Dr. Ruth Carper for their collaboration, mentorship and support over the years. Thank you also to my research mentors at the University of Washington, especially to Dr. Natalia Kleinhans, Dr. Stephen Dager, Dr. Annette Estes, Dr. Tara Madhyastha, and Dr. Corey Fagan, for their support of my work and training since before I began my doctoral studies. To the love of my life, James, my family, and my friends who have been by my side every step of the way- thank you for your unwavering support, kind and well-timed words, and for always believing in me and my dreams. And finally, to my grandfather Allen, who would have so loved to see me graduate, thank you for always being my number 1 fan, for your sense of humor, kindness, and compassion, and for sharing with me many stories from your remarkable life.

Please note that Chapter 2, in full, is a reprint of the material as it appears in Biological Psychiatry: Cognitive Neuroscience and Neuroimaging 2018. Reiter, Maya Anne; Mash Lisa; Linke, Annika; Fong, Christopher; Fishman, Inna; Müller, Ralph-Axel, Elsevier Inc., 2018. The dissertation author was the primary investigator and author of this paper.

VITA

2022	**Doctor of Philosophy** in Clinical Psychology San Diego State University/ University of California San Diego Joint Doctoral Program in Clinical Psychology Major Area of Study: Neuropsychology Dissertation Chair: Ralph-Axel Müller, Ph.D. Dissertation Title: *Functional and Anatomical Substrates of Cognitive Abilities in Autism Spectrum Disorder*
2021-2022	**Predoctoral Internship** Long Beach VA Healthcare System Major Area of Study: Clinical Psychology
2018	**Master of Science** in Clinical Psychology San Diego State University Thesis Chair: Ralph-Axel Müller, Ph.D. Thesis Title: *Distinct Patterns of Atypical Functional Connectivity in Lower-Functioning Autism*
2014	**Bachelor of Science** in Psychology, Cum Laude University of Washington

PEER-REVIEWED PUBLICATIONS

*Tung, R., ***Reiter, M. A.**, Linke, A. C., Kohli, J., Kinnear, M., Carper, R., & Müller, R.-A. (2021). Functional connectivity within an anxiety network in middle-aged adults with autism and associations with anxiety symptom severity. *Autism Research*.

**equal contribution in first-authorship*

St. John, T., Estes, A., Begay, K. K., Munson, J., **Reiter M. A.**, Dager, Stephen R., & Kleinhans, N.M (2021). Characterizing social functioning in school-age children with sensory processing abnormalities. *Journal of Autism and Developmental Disorders.* doi: 10.1007/s10803-021-05050-4

Reiter M. A., Jahedi, A., Fredo, J., Fishman, I., Bailey, B., & Müller, R.-A. (2020). Performance of machine learning classification models of autism using resting-state fMRI is contingent on sample heterogeneity. *Neural Computing and Applications. 33,* 3299–3310. doi: 10.1007/s00521-020-05193-y

Reiter, M. A., Mash, L. E., Linke, A. C., Fong, C. H., Fishman, I., & Müller, R.-A. (2018). Distinct patterns of atypical functional connectivity in lower functioning autism. *Biological Psychiatry: Cognitive Neuroscience and Neuroimaging, 4*, 251–259. doi:10.1016/j.bpsc.2018.08.009

Müller R.-A., & **Reiter, M. A.** Brain changes in adolescence—It is about time to get serious in autism spectrum disorder research. [Editorial]. (2018). *Autism Research, 12*, v–vi. doi:10.1002/aur.2042

Mash, L. E., **Reiter, M. A.**, Linke, A. C., Townsend G., & Müller, R.-A. (2018). Multimodal approaches to functional connectivity in autism spectrum disorders: An integrative perspective. *Developmental Neurobiology, 78*, 456–473. doi:10.1002/dneu.22570

Reiter, S., Eli, I., Mahameed, M., Emodi-Perlman, A., Friedman-Rubin, P., **Reiter, M. A.**, & Winocur, E. (2018). Pain catastrophizing and pain persistence in temporomandibular disorder patients. *Journal of Oral & Facial Pain and Headache, 32*, 309–320. doi:10.11607/ofph.1968

Reiter, S., Winocur, E., Akrish, S., Reiter, A., **Reiter, M. A.**, Lahav, M., & Emodi-Perlman, A. (2018).קריטריונים אבחוניים להפרעות תפקודיות במערכת הלעיסה: גרסה עברית [Diagnostic criteria for temporomandibular disorders: Hebrew version]. In R. Ohrbach (Ed.), *Diagnostic criteria for temporomandibular disorders: Assessment instruments*. Retrieved from https://ubwp.buffalo.edu/rdc-tmdinternational/tmd-assessmentdiagnosis/dc-tmd/dc-tmd-translations/

Kleinhans, N. M., **Reiter, M. A.**, Neuhaus, E., Pauley, G., Martin, N., Dager, S. R. (2016). Subregional differences in intrinsic amygdala hyperconnectivity and hypoconnectivity in autism spectrum disorder. *Autism Research, 9*, 760–772. doi:10.1002/aur.1589

Askren, M. K., McAllister-Day, T. K., Koh, N., Mestre Z., Dines J. N., Korman, B. A., Melhorn, S. J., Peterson, D. J., Peverill, M., Qin, X., Rane, S. D., Reilly, M. A., **Reiter, M. A.**, . . . & Madhyastha, T. (2016). Using Make for reproducible and parallel neuroimaging workflow and quality-assurance. *Frontiers in Neuroinformatics, 10*, doi:10.3389/fninf.2016.00002

Borghesani, P. R., Madhyastha, T. M., Aylward, E. H., **Reiter, M. A.**, Swarny, B. R., Schaie, K. W., & Willis, S. L. (2013). The association between higher order abilities, processing speed, and age are variably mediated by white matter integrity during typical aging. *Neuropsychologia, 51*, 1435–1444. doi:10.1016/j.neuropsychologia.2013.03.005

ABSTRACT OF THE DISSERTATION

Functional and Anatomical Substrates of Cognitive Abilities in Autism Spectrum Disorder

by

Maya Anne Reiter
Doctor of Philosophy in Clinical Psychology

University of California San Diego, 2022
San Diego State University, 2022

Professor Ralph-Axel Müller, Chair

Neuroimaging research on Autism Spectrum Disorder (ASD) includes predominantly individuals with higher cognitive abilities (HCA), despite high prevalence of Lower Cognitive Abilities (LCA) in ASD, diminishing ecological validity of prior research. We aimed to increase understanding of brain-behavior relationships associated with cognitive abilities (CA) and earlier developmental abilities preceding CA, in children and adolescents with ASD.

Study 1 contrasted resting-state functional connectivity (FC) in children with and without ASD (6-15 years) in LCA and HCA subsamples. Participants with ASD+LCA showed decreased

FC between pericalcarine visual cortex (VC) and posterior superior temporal sulcus (pSTS), bilaterally, compared to ASD+HCA peers. Study 2 investigated relationships between cognitive developmental abilities and FC of VC in toddlers and preschoolers (18-55 months) with and without ASD, searching for earlier signs of atypical brain-behavior relationships involving VC in ASD. Independent component analysis of resting-state fMRI scans (collected during natural sleep) was used to generate bias-free VC seeds for FC analyses. A strong positive relationship between VC FC (with pSTS) and cognitive developmental abilities observed in typically developing (TD) children was absent in the ASD group, and VC FC was inversely related to ASD symptom severity. Study 3 tested for atypical relationships between VC neuroanatomy and CA in ASD. Using anatomical MRI scans from ASD and TD children (7-18 years), we derived surface area, cortical thickness, and local gyrification index in four occipital VC regions. An atypical relationship between CA and left lingual gyrus cortical thickness was observed in the ASD group. There were no significant ASD-TD group differences in VC anatomical measures after multiple-comparison correction, however, group-difference effect-sizes were markedly larger in LCA subsamples when participants were stratified by IQ.

Overall, findings provide evidence that VC anatomy and VC FC (with regions involved in multisensory integration) are atypically related to CA in children and adolescents with ASD. Moreover, atypical relationships between VC FC and cognitive developmental abilities in autism can be detected as early as the first years of life. Including participants with LCA in neuroimaging research, despite difficulties collecting MRI data in this population, is critical to improving insight into brain structure and functioning in ASD.

Chapter 1: Introduction

Autism Spectrum Disorder

Autism spectrum disorder (ASD) is a neurodevelopmental disorder with a current prevalence rate of 2% (Maenner et al., 2020), characterized by early-appearing deficits in social communication and restricted and repetitive behaviors and interests (American Psychiatric Association, 2013). Autism is currently diagnosed behaviorally, as there is no identified biomarker of the condition that could be observed at the individual level. Gold-standard diagnostic procedures include use of the Autism Diagnostic Observation Schedule, a semi-standardized behavioral observation where the examiner rates an individual's social responses to a variety of standardized social scenarios (Lord et al., 2012a; Lord et al., 1989), a standardized semi-structured clinical interview to establish evidence of early symptoms such as the Autism Diagnostic Interview-Revised (Lord, Rutter, & Le Couteur, 1994), and expert clinical judgement. Behavioral evidence of ASD is often present prior to the age of earliest reliable diagnosis [estimated to be around 14 months (Pierce et al., 2019)], beginning with motor delays, followed by atypical visual orienting, aberrant responses to social stimuli, and finally, the core diagnostic symptoms of the disorder - restrictive repetitive behaviors and social communication deficits (Girault & Piven, 2020). Although ASD occurs on a spectrum from very mild to extremely severe, most individuals require some form of lifelong support [e.g., familial, community, public services, health systems etc. (Lord, Elsabbagh, Baird, & Veenstra-Vanderweele, 2018)]. Moreover, up to 70% of individuals with ASD have at least one comorbid diagnosis (Hossain et al., 2020; Simonoff et al., 2008) with psychiatric disorders (Hossain et al., 2020; Leyfer et al., 2006), and intellectual disabilities (Matson & Shoemaker, 2009) being some of the most common co-occurring conditions.

The modalities of anatomical and functional Magnetic Resonance Imaging

The current dissertation utilizes anatomical and functional Magnetic Resonance Imaging (aMRI and fMRI, respectively). While diffusion MRI, electroencephalogram, magnetoencephalography, positron emission tomography, electrocorticography, and other imaging modalities are important adjunctive aids to understanding neural development in ASD, these are beyond the scope of the current dissertation. A brief description of the aMRI and fMRI methodologies incorporated in this dissertation is provided below.

Anatomical MRI (aMRI) can be used to study anatomy or structure of the brain and cortex. The neuroanatomical cortical metrics examined in the current dissertation included total brain volume, cortical thickness (CT), surface area (SA) and a local gyrification index (LGI). Although anatomical MRI methods measure structure rather than function, aMRI measures relate to function because throughout development brain function drives plasticity, which in turn changes anatomy (Zatorre, Fields, & Johansen-Berg, 2012). While CT and SA are both related to brain volume, they have different genetic (Panizzon et al. 2009) and environmental determinants (Raznahan et al. 2012), and different developmental trajectories. They are generally found to be influenced by separate aspects of cortical development (Geschwind & Rakic, 2013) and are biologically dissociable in developmental neuroimaging studies of clinical populations (Raznahan et al. 2016; (Xiao et al., 2017). Understanding the distinct developmental properties of CT and SA is an imperative consideration in interpreting earlier neuroimaging literature which often reported only cortical volume. Estimates of SA broadly reflect columnar and minicolumnar organization of cortex (Rakic, 1988), whereas CT is more closely related to synaptic density, synaptic pruning and intracranial myelination (Tahedl, 2020). LGI estimates reflect the degree of cortical folding over

a given area; LGI is preferable, in terms of differentiating between clinical groups, to other metrics of gyrification such as local curvature and sulcal depth (Shimony et al., 2016).

Functional MRI (fMRI) measures the blood-oxygen-level-dependent (BOLD) signal, which is influenced by the hemodynamic response (a homeostatic process that adjusts or increases focal blood flow to support biological, including neural, systems following activation), over time (Ogawa, Lee, Kay, & Tank, 1990)]. The physical basis for the BOLD signal lies in the difference in magnetic properties between oxygenated hemoglobin (which is diamagnetic) and deoxygenated hemoglobin (which is paramagnetic). The amount of oxygen in the blood thus affects the local MRI signal. FMRI data (the BOLD timeseries) are used to study the brain in action over time. In task-based fMRI research, researchers examine changes in the BOLD signal in relation to presented stimuli (the term functional activity refers to this response or relationship). Resting-state fMRI (rsfMRI), on the other hand, is collected in the absence of a task and believed to reflect intrinsic, or spontaneous, ongoing neural activity. A prolific body of research examines how synchronized (i.e. correlated) the BOLD signal is in different regions of the brain over time. If two regions show correlated BOLD signal time series, they are considered to be *functionally connected*. Resting-state functional connectivity MRI research additionally presumes that spontaneous fluctuations in the BOLD signal are synchronized within functionally specialized brain networks, reflecting history of co-activation (Raichle et al., 2001). Functional connectivity within and between regions of these functional networks (e.g., denoting the degree of within-network integration and between-network segregation or differentiation) has been shown to coherently relate to behavior and psychopathology (Menon, 2011). In the current dissertation, analysis of rsfMRI data primarily considered intrinsic functional connectivity.

Cognitive impairment in ASD: Common but understudied using MRI

About one third of children with autism are estimated to have intellectual disability (ID), with a further ~25% exhibiting intellectual abilities in the borderline range, referred to hereafter as lower cognitive abilities [LCA] (Maenner et al., 2020). Longitudinal studies following participants with ASD from early childhood to adulthood suggest that general cognitive abilities (including early developmental skills measured in preschool age) are predictive of later adaptive functioning, independence, and overall quality of life and well-being in ASD (Ben-Itzchak & Zachor, 2020; Lord, McCauley, Pepa, Huerta, & Pickles, 2020). Although among the people on the autism spectrum those with LCA experience the most significant impairments, require the most support, and actually constitute the majority of the population, little is known about specific brain anomalies associated with this phenotype. Three of the contributing factors to the current gap in knowledge are described:

1) There is a sparse amount of high quality neuroimaging data collected on individuals with ASD and lower cognitive abilities (ASD+LCA) available, to date. Obtaining MRI data of sufficient quality for research analysis requires participants to tolerate the loud and confining MRI environment, remain very still during the MRI scan, and respond to instructions of the examiner – all of which can be highly challenging for participants with ASD+LCA. Due to practical difficulties associated with scanning individuals with LCA, samples used to study the population have largely been restricted to those with average or above average CA, misrepresenting the true distribution of cognitive abilities in ASD (Jack & Pelphrey, 2017). Neuroimaging data collected from individuals with ASD and lower cognitive abilities are scarce. For example, only a small proportion (c. 11%) of imaging datasets included in the publicly available Autism Brain Imaging Data Exchange (ABIDE 1&2) were obtained from individuals

with IQ scores ≤ 85. This proportion is even lower when considering data quality (Di Martino et al., 2017b; Di Martino et al., 2014). Restricted range of IQ scores, present in most ASD studies, hinders studying relationships between functional connectivity and neuroanatomy and cognitive abilities in ASD, as well as differences from TD peers in such relationships (interaction effects). Although MRI data from individuals with ASD and LCA are challenging to collect, select groups worldwide have succeeded in acquiring smaller datasets of sufficient quality on this population. Use of inter-group cooperation and data-sharing initiatives may facilitate necessary efforts to increase research on ASD+LCA.

2) Brain-behavior relationships related to cognitive abilities in ASD have rarely been explored due to focus on group-level differences (ASD vs. TD) in the majority of studies, as pointed out by S. A. Bedford et al. (2020). A common practice in neuroimaging research studies on ASD is matching ASD and TD groups on IQ to (understandably) reduce the likelihood that differences across groups could constitute a confounding variable. However, TD populations, by definition, do not exhibit clinically relevant cognitive impairments, whereas ASD populations often do. Thus, IQ matching with TD samples is possible only for a narrower range of individuals on the autism spectrum, which may be problematic. Alternative approaches could include contrasting ASD groups with differing cognitive ability profiles [individuals with ASD and LCA compared to those with ASD and higher cognitive ability (HCA)], and even contrasting individuals with ASD and LCA with TD peers despite significant differences in IQ scores (both approaches were used in Study 1 of this dissertation). These experimental designs may be justified due to an absence of other good options and given that IQ differences are emblematic of the population studied just as are deficits in social cognition.

3) There is currently only a limited amount of neuroimaging research on the neural substrates of developmental abilities in ASD during the first few years of life. Collecting neuroimaging data in children younger than 6 years of age is difficult for similar reasons to those impeding collection of MRI data in older individuals with cognitive difficulties, as well as due to additional challenges unique to studying toddlers and preschoolers. However, more and more groups have been successful in collecting neuroimaging data from children with ASD under the age of 6, which is promising.

A Review of the Neuroimaging Literature on ASD

Much MRI research, many remaining unknowns

Over the past decades, thousands of neuroimaging studies have attempted to identify biomarkers of ASD and neural correlates of symptom severity and variability in outcome. It is widely accepted that ASD is characterized by atypical brain development, which manifests in distinct brain structure and functioning differences. However, currently, these differences can only be detected at the group level. Despite the vast number of studies on ASD using fMRI and aMRI methods, no distinct neural signature or biomarker of ASD has yet been established (Uddin, Dajani, Voorhies, Bednarz, & Kana, 2017). One aspect of this may be because multiple ASD subtypes and comorbidities are likely associated with distinct etiologies (Lenroot & Yeung, 2013; Lombardo, Lai, & Baron-Cohen, 2019). In view of this complexity, conflicting findings reported in the neuroimaging literature on ASD are not altogether surprising. While research on brain development during the first years of life in ASD has been increasing over the past two decades, much is still unknown about where, when, and how the deviations from the path of typical development occur. Findings from the anatomical MRI and fMRI literatures are reviewed below

from a developmental perspective, to provide context for the three studies comprising the current dissertation.

Atypical structural brain development in ASD

Atypical brain development in ASD may have a prenatal origin (Bonnet-Brilhault et al., 2018; Courchesne, Gazestani, & Lewis, 2020), and MRI studies of infants at risk for ASD suggest that differences in neuroanatomy in ASD become increasingly measurable (using currently available methods) during the first year/s of life (Bonnet-Brilhault et al., 2018; Courchesne et al., 2020; Wolff, Jacob, & Elison, 2018a). Certain neural changes precede the emergence of the core symptoms of ASD, and temporally coincide with prodromal developmental delays (motor delays, atypical visual orienting, and atypical response to social stimuli) during the first year and a half of life in ASD (Girault & Piven, 2020).

Atypical cortical and subcortical brain volume in ASD: One of the most consistently reported neuroanatomical findings in ASD is enlarged total brain volume during the first years of life (Courchesne, Carper, & Akshoomoff, 2003; Ecker, 2017; Lange et al., 2015). However, divergence in brain volume from typical development has been found to change across the lifespan. In one longitudinal study examining infants at high risk for ASD (using a sibling prospective design), no differences in brain volume were found at the age of 6 months between high-risk infants who went on to develop ASD and high-risk infants who did not. However, by the age of 12 months, the high-risk infants showed larger brain volumes compared to control groups (Shen et al., 2013). Other research in older children and adults has shown that early brain overgrowth appears to be just one stage of an atypical growth trajectory, with a cross-over to decreased total brain volume in ASD (compared to TD peers) occurring during childhood, due to differing rates of change in brain volume across the two populations (Lange et al., 2015; Prigge et al., 2021)

With regards to volume of subcortical gray matter structures, including the hippocampus, amygdala, and basal ganglia, Prigge et al. (2021) reported higher subcortical gray matter volume in ASD before age 20, at which point subcortical gray matter volumes become comparable across groups. The most commonly reported finding is amygdala overgrowth during first years of life in ASD (Schumann, Barnes, Lord, & Courchesne, 2009; Wolff et al., 2018). Indeed, a meta-analysis found that, as age increases in ASD, amygdala volume decreases relative to controls (Stanfield et al., 2008); however, it is not clear whether amygdala volumes are decreased compared to TD individuals in adulthood. Notably, a large-scale study by van Rooij et al. (2018) including 1,571 participants with ASD between the ages of 2-64 years (mean age 15.8 years, with the age distribution greatly skewed towards adolescence), found that amygdala, putamen, pallidum, and nucleus accumbens volumes were decreased compared to TD individuals, however, more research is needed in order to understand how amygdalar volume in ASD compares to what is observed in typical development across the lifespan.

Atypical cortical thickness, surface area, and local gyrification in ASD: To our knowledge, there are only two studies quantifying cortical thickness (CT), surface area (SA), and local gyrification (LGI) in infants and toddlers with ASD. One of these reported that early brain overgrowth in ASD (compared to same-aged typically developing peers) was associated with higher cortical surface area (but not cortical thickness) in temporal, frontal, parietal, and occipital regions in 2-year-old toddlers with ASD (Hazlett et al., 2011). On the other hand, a more recent study found that in toddlers at around the same age, cortical thickness in similar regions was more informative than surface area for a machine learning classification algorithm for ASD (Xiao et al., 2017). While some have hypothesized that brain overgrowth in ASD during the first years of life

may begin with increases in surface area followed by atypical increases in cortical thickness (Hazlett et al., 2011; Wolff et al., 2018), further research is warranted.

The literature on older children, adolescents, and adults with ASD also includes conflicting findings with respect to morphology. However, there are some findings which have been reasonably well replicated (Donovan & Basson, 2017). There are multiple studies examining cortical thickness in children and adults with ASD, and fewer studies on surface area. However, results of available studies need to be reviewed with cautious attention to age, as both CT and SA relate strongly to brain volume (Geschwind & Rakic, 2013), which has been shown to change across age, and differentially so in ASD (Lange et al., 2015; Prigge et al., 2021). Moreover, there are dramatic changes in CT and SA in neurotypical development across the lifespan (Frangou et al., 2022; Storsve et al., 2014; Tamnes et al., 2017), thus, any abnormalities detected in ASD need to be directly referenced to age-dependent normative values. Widespread differences in CT and SA have been reported in many brain regions; however, the pattern of the divergence from TD individuals (i.e., increased or decreased) is not always consistent (Stanfield et al., 2008). As mentioned, one reason for this may be that the effects are highly sensitive to age. Although currently there is not sufficient evidence to define conclusive age-related trajectories of regionally specific alterations in CT and SA in ASD, several studies conducted in children and adults examining group differences in CT are synthesized below.

In a study of male children with ASD and matched controls between 8 and 12 years of age, Hardan, Muddasani, Vemulapalli, Keshavan, and Minshew (2006) found increased CT in boys with ASD compared to controls in temporal and parietal regions, but not in frontal or occipital regions. A different study conducted in a similar age group used machine learning to construct classification algorithms based on volumetric measurements and cortical thickness, with mixed

results (Jiao et al., 2010), including decreased cortical thickness in right pars triangularis, orbitofrontal gyrus, and parahippocampal gyrus, and increased CT in anterior cingulate cortex and precuneus. In adolescents and young adults with ASD between the ages of 14-33 years, Hyde, Samson, Evans, and Mottron (2010) also found a mixed pattern of CT divergence from typical development in the ASD group; authors found increased cortical thickness in fusiform gyrus, posterior superior temporal sulcus, Heschl's gyrus, lingual gyrus, middle occipital gyrus, posterior cingulate gyrus, medial frontal gyrus, medial orbital frontal gyrus, middle frontal gyrus, and inferior parietal lobule, and decreased cortical thickness in fewer regions, mostly involving pre- and post-central gyri in sensorimotor regions (Hyde et al., 2010). Finally, a study of adults with ASD between the ages of 21 and 45 years found cortical thinning compared to TD adults in regions belonging to the mirror neuron system involved in social cognition (Hadjikhani, Joseph, Snyder, & Tager-Flusberg, 2006); specifically, decreased cortical thickness was observed in regions including the superior temporal sulcus, precentral gyrus (motor face area), postcentral gyrus (sensory face area), inferior occipital gyrus, orbitofrontal cortex, anterior cingulate gyrus, superior parietal lobule, and temporal gyri. Although the findings presented above may grossly follow the pattern of early overgrowth accompanied by subsequent decrease in gray matter volume starting during adolescence and continuing on into adulthood, further research is needed. Among other things, findings appear to be regionally specific and may relate to very different functional systems, which form discrete brain-behavior relationships that are currently poorly understood.

Atypical development of brain functioning in ASD

Functional brain connectivity, examined using either task-based fMRI or resting-state fMRI (rsfMRI), has been shown to be atypical in individuals with ASD in many hundreds of empirical studies in children and (to a lesser extent) adults. Overarching theories that have

attempted to categorize abnormal brain functioning in ASD have generally either not been supported by subsequent studies [e.g., the theory of global under-connectivity (Just, Cherkassky, Keller, & Minshew, 2004)], or have not yet been widely accepted [e.g., the theory of decreased network integration and segregation (Rudie et al., 2012; Shih et al., 2011)]. Methodological approaches (Müller et al., 2011), age (Uddin, Supekar, & Menon, 2013), gender (Alaerts, Swinnen, & Wenderoth, 2016), cognitive ability (Reiter et al., 2018), ASD population heterogeneity (Lenroot & Yeung, 2013; Lombardo, Lai, et al., 2019), more specifically cohort differences that vary across study site (He, Byrge, & Kennedy, 2020; King et al., 2019) have all been named as factors that may account for the multitude of discrepant functional connectivity findings. A comprehensive review of the atypical functional connectivity literature in ASD extending beyond the most consistently reported findings is therefore beyond the scope of this review, however, particular attention will be given to the smaller literature on toddlers and to presenting fMRI findings that have been more robustly replicated, as these findings were used to define the hypotheses for Study 1 of this dissertation, which then guided the experimental designs for Studies 2 and 3.

FMRI research during the first years of life in ASD: Compared to the amount of research on neuroanatomy (mostly brain volume) during the first years of life in ASD, fMRI research on functional connectivity in ASD during this stage of life is far more limited. The earliest work examining functional brain development during the first years of life in ASD focused on neurodevelopmental substrates of language. This is not surprising given that speech delay and persisting impairments are very common in individuals with ASD (Tager-Flusberg, Paul, & Lord, 2005), although this symptom is no longer included among the diagnostic criteria (American Psychiatric Association, 2013). Notably, acquisition of language in typical development has been

shown to involve interaction of brain regions extending beyond those used in the adult brain (i.e., outside the language networks) including visual regions in the occipital cortex, among other regions (Redcay, Haist, & Courchesne, 2008). Thus, interactions between auditory, visual, and other neural networks are involved in the acquisition of language and disruptions in these interactions may characterize this atypical developmental process in ASD. In the first ever fMRI study of language processing in the brain in 2-3 year-olds with ASD during natural sleep, Redcay and Courchesne (2008) presented forward and backward speech stimuli to toddlers during an fMRI scan. They found significantly lower activation to speech stimuli within language regions in the ASD group, as well as atypically increased activations in medial prefrontal cortex as well as right inferior frontal gyrus. A trend towards decreased lateralization of response in language regions (increased recruitment of the right hemisphere) was also observed (Redcay & Courchesne, 2008). In a later study, the same group found that toddlers at risk for developing ASD displayed lower left-hemisphere response to speech, as well as abnormally right-lateralized temporal cortex response to language, which became more pronounced with age, peaking at between 3-4 years of age (Eyler, Pierce, & Courchesne, 2012). A third study by this group demonstrated that hypoactivity in superior temporal cortices in response to speech was associated with poor language outcome in ASD at a later age, while absence of this pattern in toddlers with ASD portended good language outcomes (Lombardo et al., 2015).

In addition to the work reviewed above on the neural substrates of language, more recent studies examining the development of neural networks in ASD have just begun, and this body literature is currently still small. One of the current models regarding atypical connectivity of resting state networks in ASD suggests that the ASD brain is characterized by a pattern of decreased network integration and segregation (Rudie et al., 2012; Shih et al., 2011), and the

emerging findings observed in toddlers with ASD may provide tentative support for this model during the first years of life in ASD. One study found reduced functional connectivity between left and right hemispheres in putative language areas (Dinstein et al., 2011), suggesting reduced integration within language networks in toddlers with ASD. In another study using an infant sibling paradigm, rsfMRI data were used to examine the neural substrates of initiation of joint attention (IJA), an early emerging autism deficit, in infants at risk for developing ASD (Eggebrecht et al., 2017). Authors found relationships between poor IJA and atypical between-network functional connectivity between the visual network and dorsal attention network, and between the visual network and the posterior cingulate cortex, the posterior node of the default mode network, (Eggebrecht et al., 2017). Increased connectivity between the visual and dorsal attention networks was associated with poorer IJA, possibly suggesting that decreased network segregation early in life in ASD may be implicated in emergence of this fundamental social skill. A study by Lombardo et al. (2019) found that hypoconnectivity involving occipito-temporal cortex and the DMN, in a subtype of ASD toddlers with social visual engagement difficulties, was associated with higher symptom severity. These important studies highlight the key role of visual networks in the emergence of early ASD symptoms. Indeed, another study in 3-year-olds with ASD, which examined functional connectivity of the visual cortex, also found weaker functional connectivity between visual cortex and sensorimotor regions compared to TD controls (Shen et al., 2016). In contrast to the study by Shen et al. (2016), a recent study in a cohort of similarly aged toddlers found the exact opposite pattern of group differences (i.e., increased functional connectivity between visual and sensorimotor networks in ASD); greater functional connectivity between visual cortex and sensorimotor areas was associated positively with symptom severity (Chen, Linke, Olson, Ibarra, Reynolds, et al., 2021). In conclusion, despite some conflicting findings regarding

the pattern of disrupted visual cortex connectivity in toddlers with ASD, available findings suggest that atypical functional connectivity of visual cortex can be detected as early as at 12 months of age, and that this may have strong developmental consequences that affect individuals with ASD throughout their lives.

Research in older children and adolescents: Studies on later stages of childhood and adolescence have shown that functional connectivity within and between resting-state networks including the default-mode, salience, and dorsal attention networks is atypical in ASD [several of many examples include (Abbott et al., 2016; Assaf et al., 2010; Dichter, 2012; Doyle-Thomas et al., 2015; Mash, Reiter, Linke, Townsend, & Müller, 2018; Monk et al., 2009; Weng et al., 2010b; Yerys et al., 2015)]. Atypical connectivity of the default mode network (DMN) in ASD has been widely reported (Padmanabhan, Lynch, Schaer, & Menon, 2017), and many studies show underconnectivity between anterior (medial prefrontal cortex, mPFC) and posterior (posterior cingulate cortex, PCC) midline hubs of the DMN in ASD (Abbott et al., 2016; Assaf et al., 2010; Dichter, 2012; Doyle-Thomas et al., 2015; Jung et al., 2014; Monk et al., 2009; Weng et al., 2010b; Yerys et al., 2015). The DMN is a task-negative network that is active during rest and de-activated during tasks requiring directed attention (Raichle et al., 2001). Anti-correlation between task-negative DMN and task-positive networks (TPNs) is associated with higher cognitive function in typically developing (TD) populations (Hampson, Driesen, Roth, Gore, & Constable, 2010) and is attenuated in many clinical disorders including ASD, depression, and neurodegenerative disease (Menon, 2011; Raichle et al., 2001; Whitfield-Gabrieli & Ford, 2012). Notably, diminished anti-correlation (reduced segregation) between TPNs and task-negative networks (TNNs) has been reported during tasks (Kennedy, Redcay, & Courchesne, 2006) and at rest (Abbott et al., 2016) in ASD. The anterior insula, a key hub of the salience network (SN), has been found to coordinate

switching between TPNs and TNNs in TD individuals (Sridharan, Levitin, & Menon, 2008) – a mechanism that may be affected in ASD [see examples - (Odriozola et al., 2016; Uddin, Kelly, Biswal, Castellanos, & Milham, 2009)]. Indeed, results of a recent review suggest that atypical functional connectivity of insular cortex is linked to many behaviors and characteristics associated with ASD such as impairments in social cognition and executive functioning (Nomi, Molnar-Szakacs, & Uddin, 2019).

Regions most frequently identified as atypically functionally connected in ASD: Despite the prevalence of conflicting findings reported in the fMRI literature on ASD, atypical functional connectivity of certain regions has been replicated across studies. For example, atypical anatomical development and functional connectivity of the posterior superior temporal sulcus (pSTS) has received high levels of attention (Redcay, 2008), with atypical pSTS connectivity repeatedly linked to impaired social cognition (Alaerts et al., 2015b; Alaerts et al., 2014; Shih et al., 2011), as well as to low cognitive ability in ASD (Reiter et al., 2018). The amygdala has also long been considered of key relevance in ASD (Baron-Cohen et al., 2000). Functional connectivity of the amygdala has been implicated in abnormal face-processing (Aoki, Cortese, & Tansella, 2015), sensory sensitivity (Green et al., 2015), negative valence (Kleinhans et al., 2016), and autism symptoms (Fishman, Linke, Hau, Carper, & Müller, 2018) in ASD. Notably, atypical functional connectivity of the amygdala is also one of the earliest detectible patterns of functional connectivity reported that has been associated with impairments in social cognition, as it has been found in children with ASD as young as 3 years old (Shen et al., 2016). As described earlier, structural enlargement of the amygdala during the first years of life is one of the more replicated findings in the structural MRI literature (Schumann et al., 2009; Wolff et al., 2018).

Functional connectivity of visual cortex (VC) in ASD: Despite considerable evidence that individuals with ASD activate visual cortex during tasks more than TD peers, who rely more heavily on frontal regions (Samson, Mottron, Soulieres, & Zeffiro, 2012), visual cortex (referring henceforth to lower-order visual processing regions located in the occipital lobe) has received much less attention in literature reviews on atypical functional connectivity in ASD. There are currently numerous reviews published on the amygdala, pSTS, and DMN in ASD but none on connectivity of visual cortex. Research suggests that visual processing in ASD is atypical (Simmons et al., 2009), with some isolated domains of superior ability, for example in spatial reasoning (J. L. Stevenson & Gernsbacher, 2013) and visual search (O'Riordan, Plaisted, Driver, & Baron-Cohen, 2001). Increased visual cortex activation (Samson et al., 2012) and connectivity (Keehn et al. 2013) have been reported during cognitive tasks in ASD and are associated with poorer task performance. Atypical recruitment of visual cortex during auditory processing has also been observed in children and adolescents with ASD and linked to more severe phenotypes (Keehn et al., 2017). Moreover, increased visual region connectivity with the extended language network was associated with lower language abilities (Y. Gao et al., 2019). Notably, atypically increased functional connectivity involving visual cortex and the default-mode network have been replicated in children with ASD and average to high cognitive abilities (Abbott et al., 2016; Yerys et al., 2015). As noted, increased connectivity between these same networks at the age of 12 months was associated with a better initiation of joint attention in infants at risk for ASD (Eggebrecht et al., 2017). It may be that interactions between visual networks and the DMN adaptively change across development in typically developing individuals, and presence of previously adaptive patterns of brain function at older ages in ASD reflects severe neurodevelopmental delay. In conclusion,

atypical functional connectivity of visual cortex with multiple neural networks has been associated with a wide range of deficits observed in ASD, and warrants further study.

Brain structure and function in ASD accompanied by LCA

A very limited literature documenting aMRI and fMRI abnormalities in individuals with ASD and lower cognitive abilities (LCA) currently exists. At the gross neuroanatomical level, children with ASD and comorbid intellectual disability (in one study of 41 participants) show high rates (44%) of abnormal findings on MRI scans (e.g., enlargement of the ventricles, abnormal signal intensities, and arachnoid cysts), as rated by neurologists (Erbetta et al., 2015). However, observed MRI abnormalities were not sufficient to distinguish children with ASD and intellectual disabilities from children with intellectual disabilities alone (Erbetta et al., 2015), which highlights the fact that clinical examination of MRI scans at the individual level is currently insufficient to distinguish ASD from intellectual disability. One limitation of the study by Erbetta et al. (2015) was the absence of a comparison between higher and lower functioning individuals with ASD. To our knowledge, only one study exists that contrasts surface-based morphometry in autistic children with higher and lower cognitive abilities (Nordahl et al., 2007). This study examined 3 groups of children with ASD stratified by IQ (group A mean IQ = 56; group B mean IQ = 89; group C mean IQ = 97) and a typically developing (TD) group (mean IQ = 115). Nordahl et al. (2007) found that groups A and B showed similarly atypical cortical folding in the inferior frontal gyrus compared to the TD group. Abnormal cortical folding was more pronounced in the LCA group (A) compared to group B. Remarkably, group C (with higher CA) showed an entirely different pattern of abnormalities in cortical folding compared to the TD group, suggesting that ASD cognitive ability subgroups may not simply exhibit a continuum of a single neurobiological abnormality (Nordahl

et al., 2007). To our best knowledge, these two studies are the only available articles on morphology in individuals with ASD+LCA.

As for the functional MRI literature, the only task-based fMRI study of minimally verbal children with ASD found that within auditory language-implicated regions, speech sounds produced less functional activity (neural response) compared to song-sounds in minimally verbal individuals with ASD (Lai, Pantazatos, Schneider, & Hirsch, 2012). Apart from study 1 of the current dissertation [(Reiter et al., 2018) presented below], there are only 2 published studies using rsfMRI in the ASD+LCA population to date, to our knowledge (Gabrielsen et al., 2018; G. Li, Rossbach, Jiang, & Du, 2018). Functional activity can also be examined with resting-state by calculating regional homogeneity (ReHo), which measures the degree to which the time series of neighboring voxels are synchronized, and amplitude of low-frequency fluctuation (ALFF), which measures the amplitude of a time series of a given voxel. G. Li et al. (2018) found that compared with a typically developing group, the group of children with ASD+LCA (mean age 8.8 years $\pm$ 3.11, $n_{ASD+LCA}$ = 15, mean FSIQ 50 $\pm$ 11.25) showed higher ReHo in the precuneus and inferior parietal gyrus, as well as significantly higher ALFF in right middle temporal gyrus, angular gyrus, and inferior parietal gyrus; no correlations between ReHo or ALFF and symptom severity were observed. Gabrielsen et al. (2018) found reduced functional connectivity within the DMN, salience, auditory, and frontoparietal networks in the ASD+LCA group ($n_{ASD+LCA}$ = 17), suggesting decreased integration within major resting state networks in ASD+LCA; this study also found patterns of overconnectivity between DMN and the dorsal attention network, suggesting some patterns of decreased network segregation in ASD+LCA.

Aims of the current dissertation

Brain-behavior relationships related to cognitive abilities in ASD are poorly understood, and the current dissertation aimed to characterize some of these relationships utilizing both anatomical and functional MRI data. The existing dearth in research on individuals with ASD and LCA undermines the ecological validity of prior neuroimaging research on ASD – it is currently unclear to what extent findings presented in the large body of ASD research generalize to the broader population with lower CA. In particular, it is unclear whether or not individuals with ASD+LCA show atypicalities in brain functioning that are simply more pronounced than those shown by their higher cognitive ability peers, or whether ASD+LCA is characterized by distinct patterns of atypical functional connectivity. Study 1 of the current dissertation aimed primarily to begin to answer some of these questions. At the time it was published, Study 1 was the first study on resting-state functional connectivity in an entire sample of 22 individuals with ASD and LCA. (Notably, in the 4 years since its publication, only 2 other studies have been published on resting-state functional connectivity in individuals with ASD and LCA or ID, demonstrating the inherent difficulties in conducting research on this population.) Following up on findings from Study 1, Study 2 aimed to examine relationships between functional connectivity (in particular visual cortex functional connectivity, given hypotheses generated in Study 1) and cognitive developmental abilities in toddlers and preschoolers with and without ASD. In Study 2, we sought to test whether evidence of patterns of visual cortex functional connectivity associated with ASD+LCA in childhood and adolescence could be detected earlier in life than during the age range studied in Study 1. Finally, in Study 3, we sought to expand upon findings reported in Studies 1 and 2 by incorporating a second neuroimaging modality to test for distinct relationships between morphology of visual cortex and cognitive abilities in children and adolescents with ASD.

Overall, we sought to broaden the scope of imaging research onto some etiological variants that may be only found among individuals with lower cognitive abilities through inclusion of segments of the ASD population that have been traditionally underrepresented in research (children and adolescents with lower CA and toddlers with ASD and developmental delays). Improved understanding of the neural mechanisms associated with cognitive abilities and their precursors in ASD may help inform development of targeted and timed interventions seeking to improve quality of life in ASD. Finally, this dissertation is motivated by what its author believes is an ethical responsibility of researchers, that is, to utilize publicly funded research to generate data and findings that represent the full spectrum of individuals with ASD and speak to the interests of as many stakeholders in the community as possible. In addition to filling important gaps in the literature current dissertation strives to increase emphasis on neurodiversity in the scientific literature on ASD.

Chapter 2 (Study 1): Distinct Patterns of Atypical Functional Connectivity in Lower-Functioning Autism

Abstract

Background: Functional MRI research on Autism Spectrum Disorders (ASDs) has been largely limited to individuals with near-average intelligence. Although cognitive impairment is common in ASD, functional network connectivity in this population remains poorly understood. Specifically, it remains unknown whether lower-functioning individuals exhibit exacerbated connectivity abnormalities similar to those previously detected in higher-functioning samples, or specific, divergent patterns of connectivity. **Methods:** Resting-state fMRI data from 88 children (44 ASD, 44 typically developing, TD; average age: 11 years) were included. Based on IQ, individuals with ASDs were assigned to a lower (L-ASD, mean IQ = 77$\pm$6) or higher (H-ASD, mean IQ = 123$\pm$8) functioning group. Two TD comparison groups were matched to these groups on head-motion, handedness, and age. Seeds in the medial prefrontal cortex, posterior cingulate cortex, posterior superior temporal sulcus, insula, and amygdala were used to contrast whole-brain functional connectivity across groups. **Results:** L-ASD (compared to H-ASD) participants showed significant underconnectivity within the default mode network and the ventral visual stream. H-ASD (compared to matched TD) participants showed significantly decreased anti-correlations between default mode, salience, and task-positive regions. Effect sizes of detected differences were large (Cohen's $d > 1.46$). **Conclusions:** Lower and higher functioning individuals with ASDs demonstrated distinct patterns of atypical connectivity. Findings suggest a gross pattern of predominantly reduced network integration in L-ASD (affecting default mode and visual networks), and predominantly reduced network segregation in H-ASD. Results indicate the need for stratification by general functional level in ASD studies of functional connectivity.

Chapter 2, in full, is a reprint of the material as it appears in Biological Psychiatry: Cognitive Neuroscience and Neuroimaging 2018:

Introduction

Functional MRI (fMRI) research on Autism Spectrum Disorders (ASDs) has primarily focused on samples of individuals with Full Scale Intelligence Quotient (FSIQ) scores around or above average. Unfortunately, such samples misrepresent the true distribution of cognitive abilities in this population (Jack & Pelphrey, 2017). The CDCP (Center for Disease Control and Prevention, 2014) estimates that 31% of individuals with ASDs have an intellectual disability (IQ ≤ 70), with an additional 23% functioning in the borderline (71 ≤ FSIQ ≤ 85 (Alloway, 2010)) range. However, only a small proportion of ASD cases (roughly 11%, and even fewer when considering data quality) in the Autism Brain Imaging Data Exchange (ABIDE 1&2) obtained FSIQ scores ≤ 85 (Di Martino et al., 2017b; Di Martino et al., 2014). Imaging research in lower functioning individuals is a pressing priority for public-health (Chakrabarti, 2017). Although this segment of the autism spectrum experiences the most significant impairments, little is known about specific brain anomalies associated with low general level of functioning in ASDs. Moreover, theories attempting to characterize the neural abnormalities contributing to ASDs are likely incomplete, if derived from studies of unrepresentative high-functioning samples. Inclusion of more representative samples may allow for stronger theory-driven hypotheses in future research.

Resting-state fMRI (rsfMRI) is widely used to study brain function in the absence of an explicit task. RsfMRI detects intrinsic (task-independent) low frequency fluctuations of the Blood Oxygen Level Dependent signal that are synchronized within functional brain networks (Biswal, Yetkin, Haughton, & Hyde, 1995; Van Dijk et al., 2010). One advantage of rsfMRI in the study of L-ASD individuals is the absence of any task-related confounds (e.g., engagement, performance).

However, obtaining high-quality rsfMRI data from this population is challenging, as even submillimeter amounts of motion may confound detected BOLD signal correlations (Power et al., 2014). L-ASD individuals are often apprehensive of the scanning environment and may struggle to remain still during scans (A. D. Cox, Virues-Ortega, Julio, & Martin, 2017; Nordahl et al., 2016), especially in the absence of a distracting video or task (Huijbers, Van Dijk, Boenniger, Stirnberg, & Breteler, 2016). While improved behavioral protocols combined with advanced MRI sequences can lead to higher success rates in data acquisition (A. D. Cox et al., 2017; Nordahl et al., 2016), data-sharing initiatives remain essential for obtaining samples with sufficient statistical power in this population.

Atypical functional connectivity has been detected in many fMRI studies of ASDs (Hull, Jacokes, Torgerson, Irimia, & Van Horn, 2017; Mash et al., 2018). However, to our knowledge, no previous intrinsic functional connectivity (iFC) studies have focused specifically on L-ASD individuals. We selected five regions of interest (ROIs) commonly linked to atypical connectivity in the ASD iFC literature as seed-regions for iFC analyses (Hull, Jacokes, Torgerson, Irimia, & Van Horn, 2017). Atypical connectivity of the default mode network (DMN) in ASD has been widely reported (Padmanabhan et al., 2017), with many studies showing underconnectivity between anterior (medial prefrontal cortex, mPFC) and posterior (posterior cingulate cortex, PCC) midline hubs of the DMN in ASD (Assaf et al., 2010; Dichter, 2012; Doyle-Thomas et al., 2015; Jung et al., 2014; Monk et al., 2009; Weng et al., 2010b; Yerys et al., 2015). The DMN is a task-negative network that is active during rest and de-activated during tasks requiring directed attention (Raichle et al., 2001). Anti-correlation between task-negative DMN and task-positive networks (TPNs) marks higher cognitive function in Typically Developing (TD) populations (Hampson et al., 2010) and is attenuated in many clinical disorders including ASDs, depression,

and neurodegenerative disease (Menon, 2011; Raichle et al., 2001; Whitfield-Gabrieli & Ford, 2012). Notably, diminished anti-correlation between TPNs and task-negative networks (TNNs) has been reported during tasks (Kennedy et al., 2006) and at rest (Abbott et al., 2016) in ASDs. The anterior insula, a key hub of the salience network (SN), has been found to coordinate switching between TPNs and TNNs in TD individuals (Sridharan et al., 2008) – a mechanism that may be affected in ASDs (Uddin & Menon, 2009). The amygdala (Baron-Cohen et al., 2000) and posterior superior temporal sulcus (Redcay, 2008) have also been considered of key relevance in ASDs. The amygdala has been implicated in abnormal face-processing (Aoki et al., 2015), sensory sensitivity (Green et al., 2015), and negative valence (Kleinhans et al., 2016). Atypical anatomical development and functional connectivity of the posterior Superior Temporal Sulcus (pSTS) have been linked to impaired social cognition in ASDs (Alaerts et al., 2015b; Alaerts et al., 2014; Shih et al., 2011).

The present study aimed to take a first step towards filling the large gap in the neuroimaging literature on iFC in L-ASD. The extensive iFC literature on ASD has not generated a clear picture of the relationship between cognitive abilities and iFC, with only few published studies directly examining FSIQ-related effects. For example, Anderson et al. (2011) used machine learning to build a diagnostic classifier (including DMN regions, superior parietal lobule, fusiform gyrus and anterior insula), which was significantly correlated with verbal (but not performance) IQ. However, in a much larger sample (n = 964, mean performance IQ = 106) Nielsen et al. (2013) presented a classifier (involving similar regions) that showed only weak correlation with verbal (r = -.07) and performance IQ (r = -.03). FSIQ has predominantly been studied as a nuisance variable in studies of individuals of near-average FSIQ (e.g., (Salmi et al., 2013; Weng et al., 2010), both reporting no IQ-effects on results).

In samples predominantly including individuals with near-average FSIQ, effects of general level of cognitive functioning may remain undetected, especially given numerous other factors of variability related to etiological heterogeneity, demography, and treatment history. In the present study, we therefore opted to contrast the tails of the FSIQ distribution in available ASD datasets, i.e., participants with FSIQs ≤85 and ≥115 (1 standard deviation below and above the mean(Alloway, 2010)) to better isolate links between general functional abilities and functional network connectivity in ASDs.

To help understand iFC differences between the L-ASD and higher functioning ASD (H-ASD) groups, we also tested these groups against suitable TD comparison groups (with differing FSIQ levels). In the absence of previous findings to guide predictions, a default hypothesis was that connectivity patterns differentiating ASD from TD samples would be aggravated in L-ASD participants. However, we also anticipated the possibility of distinctive patterns of atypical iFC found only in L-ASD (but not H-ASD) participants. Such insight into differing iFC patterns could ultimately inform targeted interventions for more severely impacted individuals with ASDs.

Methods

Participants: Participants were 88 (44 ASD, 44 TD) children and adolescents, age 6-15 years, selected from in-house data and two other sites contributing to the Autism Brain Imaging Data Exchange-II (ABIDE-II, (Di Martino et al., 2017). Participants were split into four groups, each including 22 individuals: L-ASD, H-ASD, A-TD (average FSIQ TD), and H-TD (higher FSIQ TD). Participant demographics are shown in Table 2.1. For in-house data (n = 9 per group), ASD diagnosis was confirmed using expert clinical judgement in conjunction with the Autism Diagnostic Observation Scale (Gotham, Risi, Pickles, & Lord, 2007; Lord et al., 2012) and the Autism Diagnostic Interview-Revised (Lord et al., 1994). Diagnostic labels from the ABIDE

databases were retained. Inclusion criteria for ABIDE sites were (1) contribution of >5 L-ASD individuals in the eligible age range with usable anatomical and rsfMRI data (see details below) and (2) rsfMRI data acquired while participant's eyes were open (given effects of eye-status on iFC (Nair et al., 2017)). Only 2 sites from ABIDE-II (and none from ABIDE-I (Di Martino et al., 2014)) met these criteria: : New York University (NYU), group 1 (n = 7 per group), and Oregon Health and Sciences University (OHSU) (n = 6 per group). All ASD individuals from these sites with usable rsfMRI data and FSIQ ≤ 85 were included in the L-ASD group. The H-ASD, H-TD, and A-TD groups were matched to the L-ASD group on age, gender, handedness, and head-motion. In order to minimize potential effects of scanning site, all groups were also matched for age and motion within individual sites (Supplemental Tables 2.S1-2.S3). Participants in the H-ASD and H-TD groups had FSIQ scores ≥115, but due to matching constraints, 3/22 ASD and 4/22 TD participants with slightly lower scores (between 106-114) had to be included. FSIQ matching could not be reasonably implemented for the L-ASD group because individuals with FSIQ ≤85 may not be considered 'typically developing' (Jarrold & Brock, 2004). Therefore, an A-TD group was included for further comparison, and a secondary analysis controlling for FSIQ was performed for the contrast of this group with the L-ASD group. This strategy is common in the study of developmental disorders that negatively affect FSIQ, as for example in Fetal Alcohol Syndrome (Crocker, Riley, & Mattson, 2015).

Ethical considerations: The in-house study was approved by San Diego State University and University of California at San Diego's Institutional Review Boards, and all participants provided informed consent to partake in this research. See Supplemental Table 2.S4 for description of MRI scanning parameters at each site.

rsfMRI Preprocessing: The first five volumes of each resting-state scan were discarded for T1 equilibration. Images were preprocessed using Analysis of Functional NeuroImages (AFNI) (R. W. Cox, 1996) (http://afni.nimh.nih.gov**)** and FSL 5.0 (Smith et al., 2004) (http://www.fmrib.ox.ac.uk/fsl**)** suites. In-house rsfMRI data were field-map corrected and slice-time corrected, and all data were motion-corrected, and resampled to MNI152 3 mm isotropic standard space, using FSL's FLIRT (functional to anatomical) and FNIRT (anatomical to standard) normalization tools. Images were spatially smoothed to a global full-width-at-half-maximum of 6 mm, and temporally smoothed using a bandpass filter of $.008 < f < .08$ Hz. Subject level regression of sixteen nuisance variables was performed for denoising. Regressors included six rigid-body motion parameters estimated during motion correction and mean time series from white-matter and ventricular cerebrospinal fluid (CSF) masks obtained from FSL's FAST, eroded by one voxel, each with a first derivative. All sixteen nuisance regressors were band-pass filtered using the same second-order Butterworth filter ($.008 < f < .08$ Hz) (Satterthwaite et al., 2013) used for temporal smoothing of the functional images. Additionally, individual volumes with frame-wise displacement > .5 mm were censored. Time series segments with <10 contiguous time points after censoring were also removed. Only participants with at least 80% of volumes retained after censoring were included in analyses, except for one participant (79% retained volumes), whose data were retained for matching purposes. All four groups were well matched on Root Mean Square Displacement (RMSD), a summary measure of motion throughout the scan (Table 2.1).

Table 2.1: Participant demographics (a) and t-tests (b)

a.

All Sites	**Age Mean(SD) [min – max]**	**FSIQ Mean(SD) [min – max]**	**RMSD Mean(SD) [min – max]**	**ADOS Tot Mean(SD) [min – max]**	**Left Handed n(%)**	**Female n(%)**
L-ASD (n=22)	11.1 (2.7) [7 – 15.5]	77 (6) [61 – 85]	.070 (.030) [.017 – .133]	14 (5) [5 – 24]	4 (19.0%)[a]	4 (18.2%)
H-ASD (n=22)	11.1 (2.8) [7 – 15]	123 (8) [106 – 138]	.068 (.025) [.032 – .106]	11 (4) [6 – 21]	2 (9.1%)	3 (13.6%)
A-TD (n=22)	11.0 (2.8) [6 – 15]	99 (7) [88 – 112]	.064 (.025) [.030 – .141]	----------	2 (9.1%)	7 (31.8%)
H-TD (n=22)	10.8 (2.0) [8 – 14]	124 (8) [108 – 144]	.064 (.019) [.033 –.097]	----------	1 (4.5%)	5 (22.7%)

b.

	Group 1	**Group 2**	**Age (t, p)**	**FSIQ (t, p)**	**RMSD (t, p)**	**Sex (χ^2, p)**	**Handedness (χ^2, p)**	**ADOS Total (t, p)**
Contrast 1	*L-ASD*	*H-ASD*	-.001, .99	-20.98, <.001*	.23, .82	.17, .68	.89, .35	2.56, .02*
Contrast 2	*L-ASD*	*A-TD*	.13, .90	-11.65, <.001*	.77, .44	1.09, .30	.89, .35	-------- -----
Contrast 3	*H-TD*	*H-ASD*	-.40, .69	.41, .68	-.70, .49	.61, .43	.36, .55	-------- -----
Contrast 4	*H-TD*	*A-TD*	-.28, .78	10.89, <.001*	-.030, .98	.46, .50	.36, .55	-------- -----

[a]Handedness data was not available for one participant in the L-ASD group. * indicates $p < .05$

Seeds: Left and right amygdala masks were created using the Harvard-Oxford subcortical atlas, and thresholded at 50% probability. Location and volume of other seeds was determined based on relevant literature (as cited). Left and right anterior insula seeds were 8 mm radius spheres centered around MNI coordinates (x = ±39, y = 23, z = -4) (Uddin et al., 2015). Left and right pSTS seeds were 10 mm radius spheres centered at MNI coordinates (x = ±47, y = -60, z = 4) (Alaerts et al., 2014). DMN seeds (mPFC and PCC) were 6 mm radius spheres centered around MNI coordinates (x = 0, y = 50, z = 0 - mPFC) and (x = −6, y = -50, z = 36 - PCC) located in the anterior and posterior DMN midline nodes, as identified by Independent Component Analysis of a sample of nearly 30,000 human subjects (Smith et al., 2009).

Statistical Analysis: We tested for differences in whole-brain functional connectivity across four contrasts of interest (Supplemental Figure 2.S1): (1) L-ASD vs. H-ASD, (2) L-ASD vs. A-TD, (3) H-ASD vs. H-TD, and (4) A-TD vs. H-TD. This design was implemented to address the guiding question of this study, i.e., is atypical iFC simply more pronounced in L-ASD than H-ASD, or do individuals with L-ASD show distinct patterns of iFC?

Mean timeseries were extracted from the mPFC, PCC, bilateral pSTS, bilateral amygdala, and bilateral insula, and correlated with all other voxels in the brain for each participant (Supplemental Figs. 2a-h). Across comparison groups, differences in iFC between the seed region and all other brain voxels were examined using t-tests implemented by AFNI's 3dttest++. A gray matter mask was used to constrain all analyses to gray matter, cerebellum, and brainstem (excluding white matter and CSF). We controlled for Type 1 error in accordance with recent recommendations (R. W. Cox, Chen, Glen, Reynolds, & Taylor, 2017), addressing concerns regarding inflated false-positive rates in fMRI research (Eklund, Nichols, & Knutsson, 2016). A voxel-wise threshold for significance was set at $\alpha < .005$, and the additional cluster-size thresholds

(number of contiguous significant voxels) were determined using permutation testing with AFNI's 3dttest++ function and the "Clustsim" argument (Supplemental Table 2.S5).

Results

We found significant iFC differences for the contrasts L-ASD vs. H-ASD, L-ASD vs. A-TD, and H-ASD vs. H-TD, but not for A-TD vs. H-TD (Table 2.2 and Figure 2.1). Overall, significant findings were robust across the three scanning sites, and inclusion of a site covariate did not change the results presented below. No significant iFC differences were detected for the amygdala seeds. See Supplemental Figures 2.2-2.4 for group-average connectivity maps for all seeds (2a-h), scatterplots illustrating data results by site (3a-c), and scatterplots depicting connectivity across all four groups for clusters of significant group differences (4a-c).

Contrast 1: H-ASD vs. L-ASD: Compared to the H-ASD group, the L-ASD group showed significant underconnectivity between mPFC seed and precuneus/posterior cingulate gyrus (Figure 2.1). However, within the L-ASD group, no corresponding correlation between FSIQ and FC was detected after post-hoc analysis. Underconnectivity was also observed bilaterally between the pSTS seeds and pericalcarine cortex. These effects were significant with and without controlling for symptom severity (ADOS-2 Total score, see Supplemental Figure 2.S5). No inverse effects of significantly increased connectivity in the L-ASD group were detected.

Contrast 2: L-ASD vs. A-TD: The L-ASD group showed mPFC overconnectivity with pericalcarine cortex compared to A-TD participants, who showed mostly negative correlations between these regions. This group difference remained significant after controlling for FSIQ (Supplemental Figure 2.S6). As this result spatially overlapped with the underconnectivity cluster for the pSTS seeds in Contrast 1, we tested the correlation between the two effects in the L-ASD group. Pearson correlation showed no association (r = -.142, t = -.63, p = .54).

Contrast 3: H-ASD vs. H-TD: Compared to the H-TD group, the H-ASD group showed significantly greater connectivity between PCC and right superior frontal gyrus (SFG), right anterior insula, and left Crus-I of the cerebellum. However, within the H-ASD group no corresponding correlations between FSIQ and these FC patterns were detected post-hoc. Significant group differences in iFC between the PCC and right SFG and left Crus-I reflected a shift from mostly negative to mostly positive connectivity in the H-ASD group compared to the H-TD group. Group differences in iFC between the PCC and right insula were driven by mostly negative iFC in the H-TD group, but near-zero iFC scores in the H-ASD group.

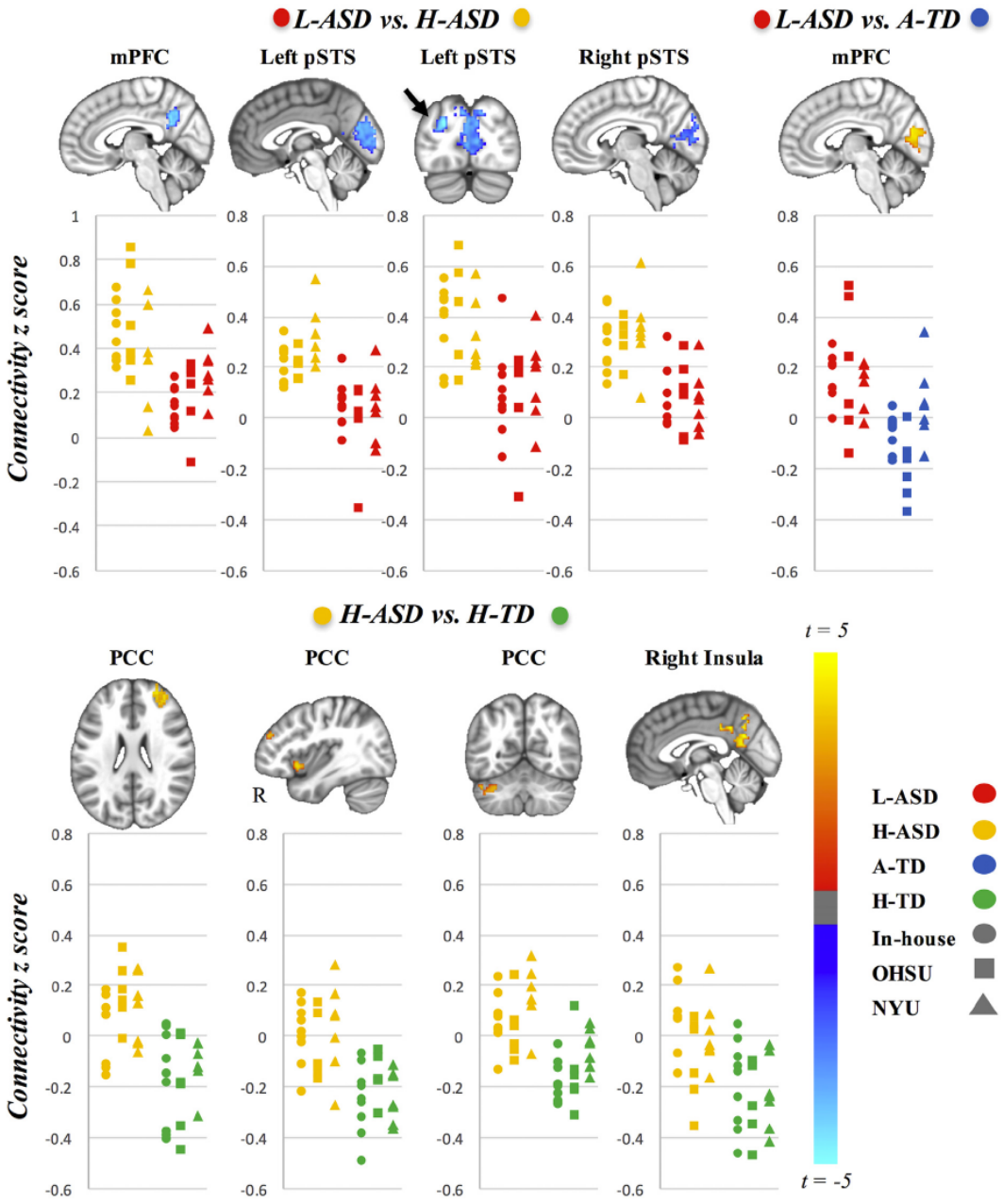

Figure 2.1: Group differences in seed to whole-brain functional connectivity. Contrast #1: L-ASD (lower IQ ASDs) vs. H-ASD (higher IQ ASDs); contrast #2: L-ASD vs. A-TD (average IQ TD); and, contrast #3: H-ASD vs. H-TD (higher IQ TD). Data are presented in neurological orientation (L=L). Statistical significance was set at voxelwise $p < .005$, whole-brain cluster corrected at $p < .05$). Scatter plots depicting individual connectivity scores for both groups contrasted across all sites are provided for illustrative purposes (H-ASD = yellow; L-ASD = red; H-TD = green; A-TD = blue. Note that the top panels (excluding the top left panel) involve differences in functional connectivity in the L-ASD group involving early visual cortex.

Table 2.2: Group differences in seed to whole-brain functional connectivity. Group differences in seed to whole-brain functional connectivity - All clusters reported were significant at the criterion threshold of alpha = .05 ($p < .005$, voxel extent). Cluster size is reported in voxels (3mm isotropic resolution). The t-score, value, and MNI mm coordinates are reported for the peak voxel of the cluster (columns 4-8). Group-level parameter estimates (mean and standard deviation) of cluster-wise mean z-scores (columns 9-10). Cohen's d is reported for each cluster as an estimated effect size. Peak regions were labeled using the Talairach and Harvard-Oxford Cortical and Subcortical atlases. For large clusters, other regions covered by the cluster are reported in parentheses. Supplemental figures 5-6 present results for the L-ASD vs. H-ASD contrast with ADOS total entered as a covariate, and for the L-ASD vs. A-TD contrast with FIQ included in the model as a covariate.

Contrast	Seed	Size	peak t	Peak β	mm x	mm y	mm z	Mean $z^1(sd^1)$	Mean $z^2(sd^2)$	Cohen's d	Peak Regions
L-ASD[1] (n=22) vs. H-ASD[2] (n=22)	mPFC	104	-4.45	-.36	8	-50	30	.20 (.13)	.46 (.20)	1.54	Precuneus
	Left pSTS	566	-5.03	-.38	-12	-80	42	.03 (.13)	.25 (.10)	1.90	Cuneal Cortex (other: Pericalcarine Cortex)
		70	-4.69	-.36	-18	-86	24	.12 (.18)	.39 (.17)	1.54	Left Lateral Occipital Cortex, Superior Division
	Right pSTS	340	-4.91	-.45	24	-86	36	.08 (.12)	.32 (.12)	2.00	Right Lateral Occipital Cortex, Superior Division (other: Cuneal Cortex, Pericalcarine Cortex).
L-ASD[1] (n=22) vs. A-TD[2] (n=22)	mPFC	127	4.34	.28	8	-78	16	.16 (.15)	-.06 (.15)	1.46	Cuneal Cortex (other: Pericalcarine Cortex)
H-ASD[1] (n=22) vs. H-TD[2] (n=22)	PCC	90	4.93	.36	30	54	28	.10 (.14)	-.15 (.16)	1.66	Right Superior Frontal Gyrus
		85	4.77	.30	38	16	-8	.00 (.14)	-.22 (.11)	1.75	Right Insula
		75	4.63	.31	-34	-72	-26	.09 (.12)	-.13 (.11)	1.91	Left Crus-I
	Right Insula	164	4.24	0.28	2	-56	18	.01 (.15)	-.22 (.15)	1.53	Precuneus (other: Posterior Cingulate Cortex)

Post-hoc analyses: H-ASD vs. A-TD. As in the main contrasts, the two ASD groups were compared to different TD groups, we performed a Supplemental analysis contrasting the H-ASD with the A-TD group (the same TD group as in contrast 2). Unlike the mPFC-pericalcarine overconnectivity observed in the L-ASD vs. A-TD comparison, the H-ASD group showed mPFC overconnectivity with right inferior frontal gyrus extending into insular cortex (Supplemental Figure 2.S7).

Interactions with Symptom Severity. We investigated whether seed-to-whole-brain FC related differently to ASD symptom severity (ADOS-2 total scores) in the L-ASD vs. H-ASD groups. We found no significant interactions in the relationship between symptom severity and seed-to-whole-brain FC in the L-ASD vs. H-ASD.

Age Effects. Linear regression showed no significant relationships between age and functional connectivity between the regions presented above across the entire sample (Supplemental Table 2.S6). Additionally, there were no age by diagnosis (ASD vs. TD, Supplement), or age by functioning level (H-ASD vs. L-ASD) interactions with FC (Supplemental Tables 2.S7-2.S8).

Discussion

Although hundreds of imaging studies have examined functional connectivity in individuals with ASDs with average or above-average intelligence, no systematic research on lower functioning segments of the ASD population is currently available. The present study has taken a first step towards filling this knowledge gap by examining a multisite sample of exclusively lower-functioning individuals (FSIQ ≤85). Our primary research question, whether L-ASD individuals would simply show more severe forms of the same regional patterns of atypical iFC as seen in higher-functioning individuals (H-ASD), could be answered in the negative. In fact, L-

ASD participants showed extensive differences in iFC, for several seed regions, in direct comparison with the H-ASD group. Moreover, the L-ASD and H-ASD groups showed distinct patterns of atypical connectivity with the mPFC compared to an A-TD group. Finally, in comparison with the FSIQ-matched H-TD group, the H-ASD group showed overconnectivity for PCC and right insula in regions that showed more neurotypical levels of iFC in the L-ASD group (Supplemental Figure 2.S4c). These findings strongly suggest that L-ASD is characterized by *distinctive* patterns of atypical network organization, rather than simply 'more of the same' abnormalities detected in the many previous studies with mostly higher-functioning participants.

In the L-ASD group, atypical connectivity of lower-order visual cortex was remarkable. Compared to the H-ASD group, L-ASD individuals exhibited underconnectivity within parts of the ventral visual stream and the DMN, suggesting reduced network integration in lower-functioning individuals. However, compared to the TD groups, both ASD groups exhibited inter-network overconnectivity, although across different networks. L-ASD individuals exhibited overconnectivity between DMN and visual regions, whereas the H-ASD group showed over-connectivity between the DMN and SN as well as task-positive regions. Notably, the H-ASD group exhibited mostly diminished anti-correlations compared to H-TD individuals (indicating reduced network segregation) between these networks. Our results also indicate that iFC of lower-order visual cortex is affected in different ways in lower- vs. higher-functioning children with ASDs (Supplemental Figure 2.S4a).

In contrast, no significant differences in iFC were found between the two TD groups that differed on FSIQ. FSIQ relationships with iFC, especially involving fronto-parietal regions, have been reported for larger samples TD of children (e.g. (C. Li & Tian, 2014). In the present study, which included only smaller TD samples that primarily served as comparison groups with ASD

samples, an expected trend towards stronger anti-correlations between rSFG (part of task positive fronto-parietal network) and PCC (task-negative DMN hub) in H-TD compared with A-TD groups was observed. Remarkably, this trend was reversed in ASD, with higher mean iFC in H-ASD than in L-ASD samples (Supplemental Figure 2.S4c). The overall pattern of findings further supports the conclusion that lower general level of functioning in ASDs may be associated with *specific* alterations in brain network organization.

DMN underconnectivity in lower functioning children with ASDs: Independent of ASD symptom severity, the L-ASD group showed reduced connectivity between midline hubs of the DMN, when compared to the H-ASD group. (A concordant effect in the comparison L-ASD vs. A-TD group remained below corrected significance.) Underconnectivity between the main DMN nodes (mPFC, PCC) is among the best-replicated imaging findings in previous ASD studies that included mixed samples with mostly higher functioning participants (Abbott et al., 2016; Assaf et al., 2010; Dichter, 2012; Doyle-Thomas et al., 2015; Falahpour et al., 2016; Joshi, Gabrieli, Biederman, & Whitfield-Gabrieli, 2015; Jung et al., 2014; Monk et al., 2009; Washington et al., 2014; Weng et al., 2010b; Yerys et al., 2015). Our findings suggest that DMN underconnectivity findings broadly reported in the literature may have been primarily driven by participants with lower or average IQ, whereas many children with ASDs and above-average intelligence tend to show relatively high levels of within-network DMN iFC. Indeed, mean iFC was slightly *higher* in the H-ASD group when compared to A-TD and H-TD groups (Supplemental Figure 2.S4a).

Atypical connectivity of visual cortex in L-ASD: Behavioral studies suggest atypical visual processing in ASDs (Simmons et al., 2009), with some islands of superior abilities, for example in spatial reasoning (J. L. Stevenson & Gernsbacher, 2013) and visual search (O'Riordan

et al., 2001). In addition to pronounced underconnectivity within the DMN, the L-ASD group exhibited lower iFC bilaterally between the pSTS and pericalcarine, compared to the H-ASD group. However, the L-ASD group showed overconnectivity between similar visual regions and the anterior DMN hub (mPFC), in comparison with the A-TD group. The pericalcarine cortex is the location of primary visual cortex, surrounding the calcarine fissures in the occipital lobes; this region receives visual input from the thalamus via the optic radiation and transmits information to higher-order processing regions. The findings described above are broadly consistent with evidence of the atypical role of early visual cortex in ASDs (Lundstrom, Reichenberg, Anckarsater, Lichtenstein, & Gillberg, 2015; Samson et al., 2012), and more specifically with altered connectivity between pSTS and lower-order visual cortex (Alaerts et al., 2014; Shih et al., 2011). Our finding of weak iFC between lower-order visual cortices and pSTS in the L-ASD group may reflect reduced processing along the ventral visual stream, which is important for object identification and higher-order visual processing (Ungerleider & Haxby, 1994). Specifically, reduced iFC with pSTS in L-ASD may affect audio-visual integration, biological motion and face perception, and – in the left hemisphere – language (Redcay, 2008).

In contrast to underconnectivity within ventral visual stream, pericalcarine cortex was overconnected with mPFC in L-ASD participants in comparison with the A-TD group (with a concordant difference in mean iFC in comparison with the H-ASD group; Supplemental Figure 2.S4b). While further supporting an atypical role of visual cortex in L-ASD, a functional interpretation of this specific finding is uncertain. No link between this effect and visual-pSTS underconnectivity was found, suggesting that high levels of iFC between mPFC and visual cortex do not reflect a compensatory mechanism for reduced ventral stream integration in L-ASD. Although atypically increased iFC between DMN and visual cortex has been reported before in

higher-functioning children with ASDs (Abbott et al., 2016; Yerys et al., 2015), these were findings for PCC seeds, and not for the anterior DMN hub in mPFC, as in the present study. More generally however, increased visual cortex activation (Samson et al., 2012) and occipital connectivity (Keehn et al. 2013) have been reported during cognitive tasks in ASDs.

Functional networks: Less integrated in L-ASD, less segregated in H-ASD? It should be noted that, for optimal contrast with L-ASD, our H-ASD group represented the upper tail of the FSIQ distribution in ASD neuroimaging studies and therefore differed from cohorts included in most studies (with a mean FSIQ of 123, 1 standard deviation above the mean of the total ASD sample across all sites included in ABIDE (Di Martino et al., 2017b; Di Martino et al., 2014)). Compared to L-ASD, the H-ASD group had more robust iFC within the DMN and parts of ventral processing stream, suggesting greater network integration. In contrast, the pattern of differences in comparison with H-TD participants indicated reduced network segregation in the H-ASD group. H-TD participants mostly showed anti-correlations between the posterior DMN hub in PCC and SN (right insula), a task-positive region in right superior frontal gyrus (rSFG), and left cerebellar Crus-1 – a region that has been related to visual processing (D'Mello & Stoodley, 2015). These anti-correlations were absent or even reversed in the H-ASD group, suggesting reduced segregation between functionally differentiated networks. Surprisingly, iFC in the L-ASD participants was more similar to the TD groups across all of these clusters (Supplemental Figure 2.S4c).

The overall pattern of our results suggests that previous findings of reduced network integration accompanied by reduced network segregation in ASDs (Fishman, Datko, Cabrera, Carper, & Müller, 2015; Hull, Jacokes, Torgerson, Irimia, Van Horn, et al., 2017; Rudie et al., 2013; Shih et al., 2011) may be differentially driven by individuals with lower vs. higher general

level of functioning. While we found evidence of predominantly reduced network integration in L-ASD (lower iFC between nodes of the same network), network anomalies in H-ASD participants predominantly reflected reduced segregation (higher iFC or reduced anticorrelations between networks).

Limitations: As in all studies of ASDs, caution is needed, as many factors of variability (e.g. etiological heterogeneity, and treatment history) probably also affect network organization and connectivity and could not be controlled in this study. The sample size available from combined scanning sites was relatively small, which limited statistical power. General conclusions regarding the large low-functioning population with ASDs must therefore be drawn with caution, although the consistency of many findings across scanning sites was encouraging. Additional research investigating the relationship between functional connectivity in L-ASD and more specific behavioral measures than FSIQ is warranted.

While previous research has shown atypical effects of age on FC in ASD (Nomi & Uddin, 2015), we found no effects of age in the current study; it is possible that detection of such effects requires larger samples. Larger studies are also required in order to examine FC differences in L-ASD across a wider array of brain regions, as FC patterns have been shown to be regionally distinct, even when multiple regions are sampled from a single network's hub (Lynch et al., 2013). Usable data were available for only three L-ASD participants with FSIQ <70. Improved acquisition and analysis protocols permitting inclusion of individuals with intellectual disability will be crucial in future studies, as paradoxically, neuroimaging over the past decades has largely excluded children who suffer from the most severe forms of the disorder and present the most urgent public health need.

Conclusions: Our findings suggest that neural network connectivity in children with ASDs and lower general functional abilities may be associated with distinctly atypical patterns, which differ from those found in higher-functioning ASDs. Whereas effects detected in relevant comparisons indicated reduced network integration (within DMN and ventral visual stream) in L-ASD, they showed reduced network segregation (between DMN, SN, and one task-positive frontal region) in H-ASD. More broadly, our results indicate the need for better stratification of ASD study designs and analyses with respect to general levels of functioning, as combination of lower and higher-functioning individuals in most previous studies may have confounded or obscured functional network anomalies.

Acknowledgements: Chapter 2, in full, is a reprint of the material as it appears in Biological Psychiatry: Cognitive Neuroscience and Neuroimaging 2018. Reiter, Maya Anne; Mash Lisa; Linke, Annika; Fong, Christopher; Fishman, Inna; Müller, Ralph-Axel, Elsevier Inc., 2018. The dissertation author was the primary investigator and author of this paper.

Supplemental Tables 2.S1-2.S3: Participant demographics and descriptive information (a) and contrast t-tests (b) by scanning site.

2.S1a. Participant demographics and descriptive information

NYU	**Age (SD) [min – max]**	**FSIQ (SD) [min – max]**	**RMSD (SD) [min – max]**	**ADOS Total (SD) [min – max]**	**Left Handed**	**Female**
L-ASD (n=7)	8.8 (1.90) [7 – 12]	75 (4) [67 – 80]	.086 (.034) [.028 – .133]	13 (6) [5 – 22]	0 (0%)*	2 (28.6%)
H-ASD (n=7)	8.6 (1.9) [7 – 12]	123 (12) [106 – 138]	.082 (.020) [.044 – .106]	9 (3) [6 – 12]	1 (14.3%)	0 (0%)
A-TD (n=7)	8.6 (2.4) [6 – 13]	98 (7) [91 – 108]	.067 (.037) [.030 – .141]	----------	0 (0%)	1 (14.3%)
H-TD (n=7)	9.3 (1.3) [8 – 11]	128 (8) [119 – 144]	.060 (.021) [.034 – .093]	----------	0 (0%)	0 (0%)

* Handedness data was not available for one participant in the L-ASD group.

2.S1b. Contrast t-tests

	Group 1	**Group 2**	**Age (t, p)**	**FSIQ (t, p)**	**RMSD (t, p)**	**ADOS Total (t, p)**
Contrast 1	*L-ASD*	*H-ASD*	.20, .85	-10.01, <.001*	.29, .78	1.61, .13
Contrast 2	*L-ASD*	*A-TD*	.19, .85	-7.78, <.001*	1.03, .32	----------
Contrast 3	*H-TD*	*H-ASD*	.81, .43	.79, .44	1.99, .07	----------
Contrast 4	*H-TD*	*A-TD*	.70, .49	7.43, <.001*	.387, .70	----------

* indicates $p < .05$

2.S2a. Participant demographics and descriptive information

OHSU	**Age (SD) [min–max]**	**FSIQ (SD) [min–max]**	**RMSD (SD) [min–max]**	**ADOS Tot (SD) [min– max]**	**Left Handed**	**Female**
L-ASD (n=6)	11.3 (3.1) [7 – 14]	80 (5) [72 – 84]	.065 (.032) [.035 – .115]	13 (4) [9 – 20]	0 (0%)	1 (16.7%)
H-ASD (n=6)	10.8 (2.5) [7 – 14]	125 (7) [116 – 136]	.069 (.024) [.039 - .103]	11 (2) [8 – 14]	0 (0%)	1 (16.7%)
A-TD (n=6)	11.0 (1.8) [8 – 13]	104 (7) [94 – 112]	.070 (.018) [.047 – .095]	----------	0 (0%)	3 (50%)
H-TD (n=6)	10.7 (2.2) [8 – 14]	127 (3) [122 – 130]	.073 (.016) [.058 - .097]	----------	0 (0%)	2 (33%)

2.S2b. Contrast t-tests

	Group 1	**Group 2**	**Age (t, p)**	**FSIQ (t, p)**	**RMSD (t, p)**	**ADOS Total (t, p)**
Contrast 1	*L-ASD*	*H-ASD*	.31, .76	-12.99, <.001*	-2.48, .81	.59, .56
Contrast 2	*L-ASD*	*A-TD*	.23, .82	-7.10, <.001*	-.31, .76	----------
Contrast 3	*H-TD*	*H-ASD*	-.12, .90	.64, .54	.34,.74	----------
Contrast 4	*H-TD*	*A-TD*	-.29, .78	7.54, <.001*	3.42, .74	----------

* indicates $p < .05$

2.S3a. Participant demographics and descriptive information

SDSU	**Age (SD) [min–max]**	**FSIQ (SD) [min–max]**	**RMSD (SD) [min–max]**	**ADOS Tot (SD) [min–max]**	**Left Handed**	**Female**
L-ASD (n=9)	12.6 (2.0) [10– 15]	77 (8) [61 – 85]	.062 (.023) [.017 – .094]	16 (4) [8 – 24]	4 (44.4%)	1 (11.1%)
H-ASD (n=9)	13.1 (1.8) [10 – 15]	121 (5) [112 – 130]	.058 (.027) [.032 - .106]	12 (5) [8 – 21]	1 (11.1%)	2 (22.2%)
A-TD (n=9)	12.8 (2.4) [8 – 15]	98.1 (6) [88 – 106]	.060 (.019) [.035 - .100]	----------	2 (22.2%)	3 (33.3%)
H-TD (n=9)	12.0 (1.7) [10 – 14]	119 (9) [108 – 132]	.060 (.020) [.033 - .093]	----------	1 (11.1%)	3 (33.3%)

2.S3b. Contrast t-tests

	Group 1	**Group 2**	**Age (t, p)**	**FSIQ (t, p)**	**RMSD (t, p)**	**ADOS Total (t, p)**
Contrast 1	*L-ASD*	*H-ASD*	-.55, .59	-13.86, <.001*	.35, .73	2.05, .06
Contrast 2	*L-ASD*	*A-TD*	.17, .87	6.40, <.001*	-.36, .72	----------
Contrast 3	*H-TD*	*H-ASD*	-1.39, .18	-.69, .50	.21, .83	----------
Contrast 4	*H-TD*	*A-TD*	-.88, .39	6.06, <.001*	0.20, .83	----------

* indicates $p < .05$

Supplemental Table 2.S4: Anatomical and resting state scan parameters by site

Scanner		NYU	OHSU	SDSU
		Siemens Allegra 3T	Siemens TrioTim 3T	GE MR750 3T
Headcoil		8Ch	12Ch	8Ch
Anatomical	TR (ms)	2530	2300	8.136
	TE (ms)	3.25	3.58	3.172
	Flip Angle	7	10	8
	Field of view (mm)	256x256	256x240	256x256
	Resolution (mm)	1.3x1x1.3	1x1x1.1	1x1x1
	Slices	128	160	172
	Slice Thickness (mm)	1.33	1.10	1.0
	Scan Time (min)	8:07	9:14	4:54
Resting	TR (ms)	2000	2500	2000
	TE (ms)	15	30	30
	Flip Angle	90	90	90
	Field of view (mm)	240x240	240x240	220x220
	Resolution (mm)	3x3x4	3.8x3.8x3.8	3.4x3.4x3.4
	Slices	33	36	42
	Slice Thickness (mm)	4.0	3.8	3.4
	Volumes	175	120	180
	Scan Time	6:00	5:07	6:10

*TR = repetition time; TE = echo time

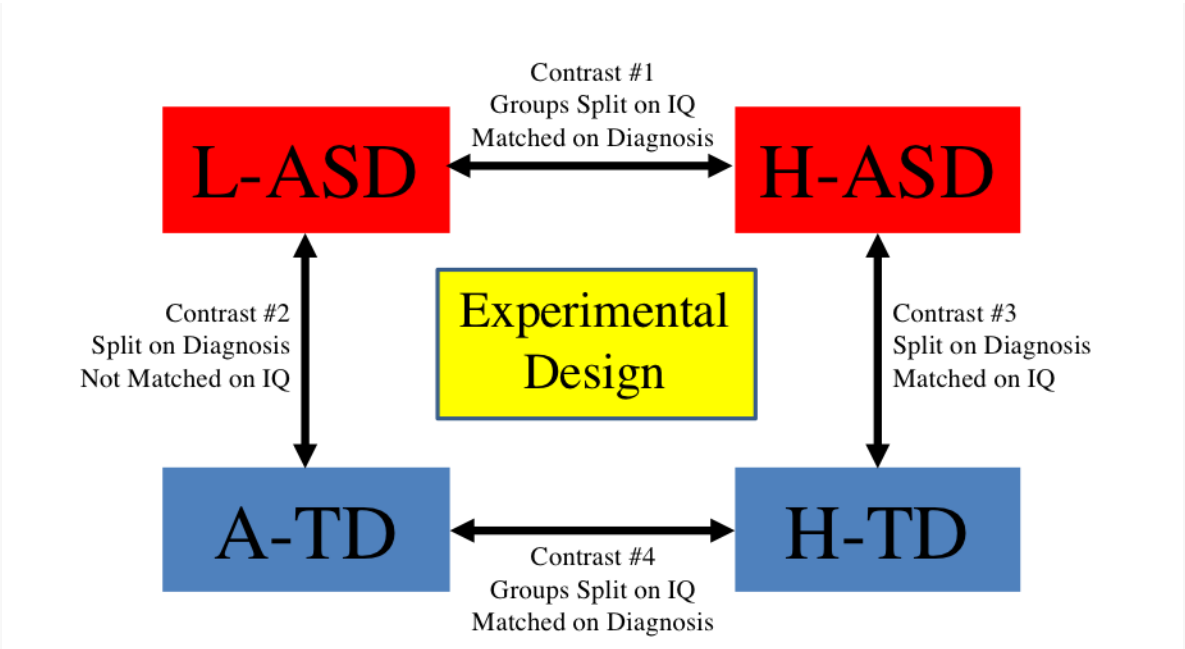

Supplemental Figure 2.S1: Experimental design of the present study. Each of the four groups above (n = 22 x 4) included 3 equally-sized samples of individuals from the SDSU (n = 9), NYU (n = 7), and OHSU (n = 6) scanning sites. All four groups were matched on head-motion, age, gender, and handedness, both within and across scanning sites. Differences in iFC were tested across four contrasts of interest #1 (L-ASD vs. H-ASD), #2 (L-ASD vs. A-TD); #3 (H-ASD vs. H-TD), #4 (A-TD vs. H-TD).

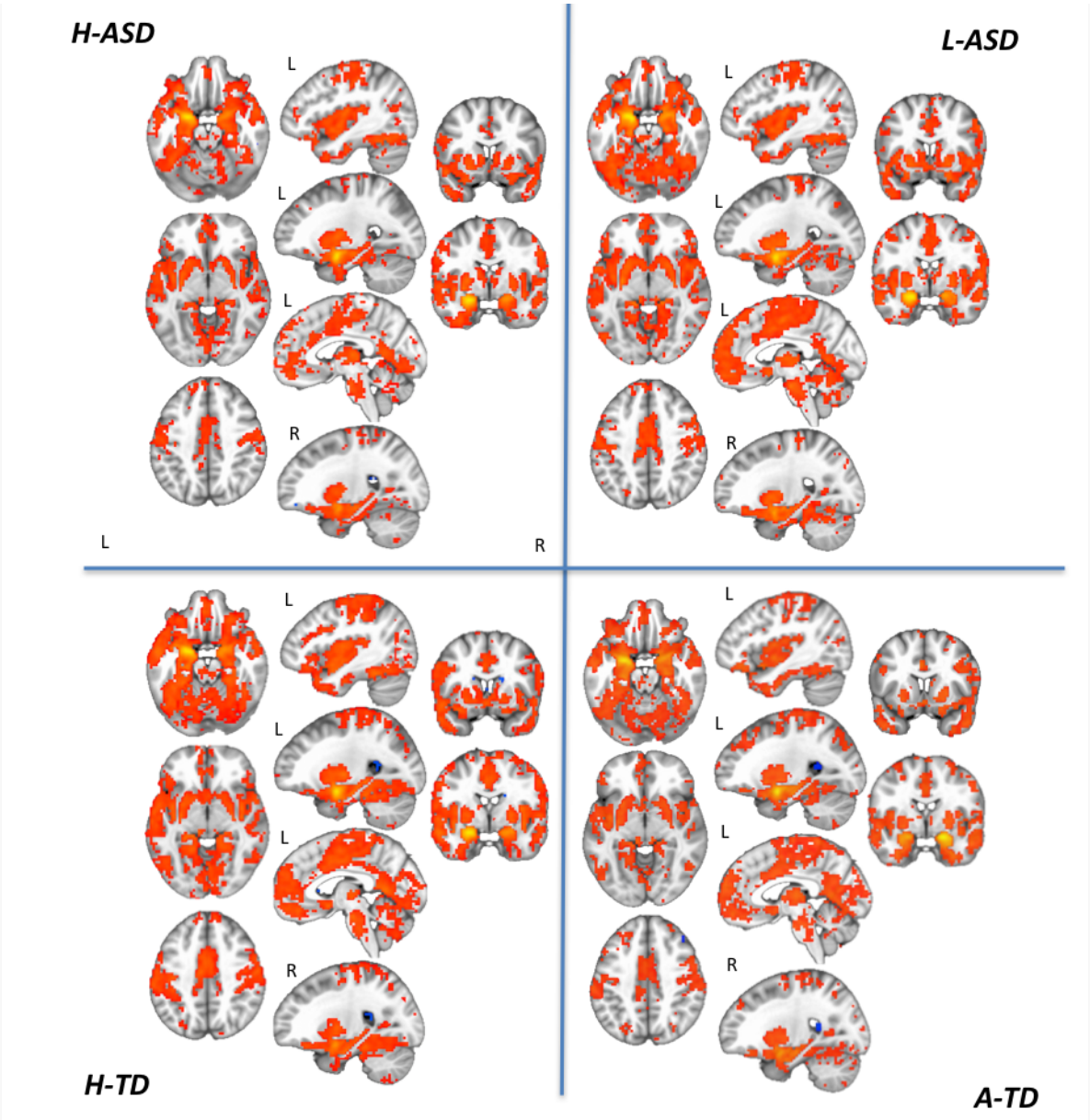

Supplemental Figure 2.S2a: Group mean maps of seed to whole-brain connectivity for H-ASD (top-left), L-ASD (top-right), H-TD (bottom-left), & A-TD (bottom right). All group mean maps were thresholded at $p < 0.005$ voxel extent. Red-yellow clusters represent positive correlations with the left Amygdala seed mean time course, and blue-light blue clusters represent negative correlations with the seed. All images are presented in neurological orientation (left = left).

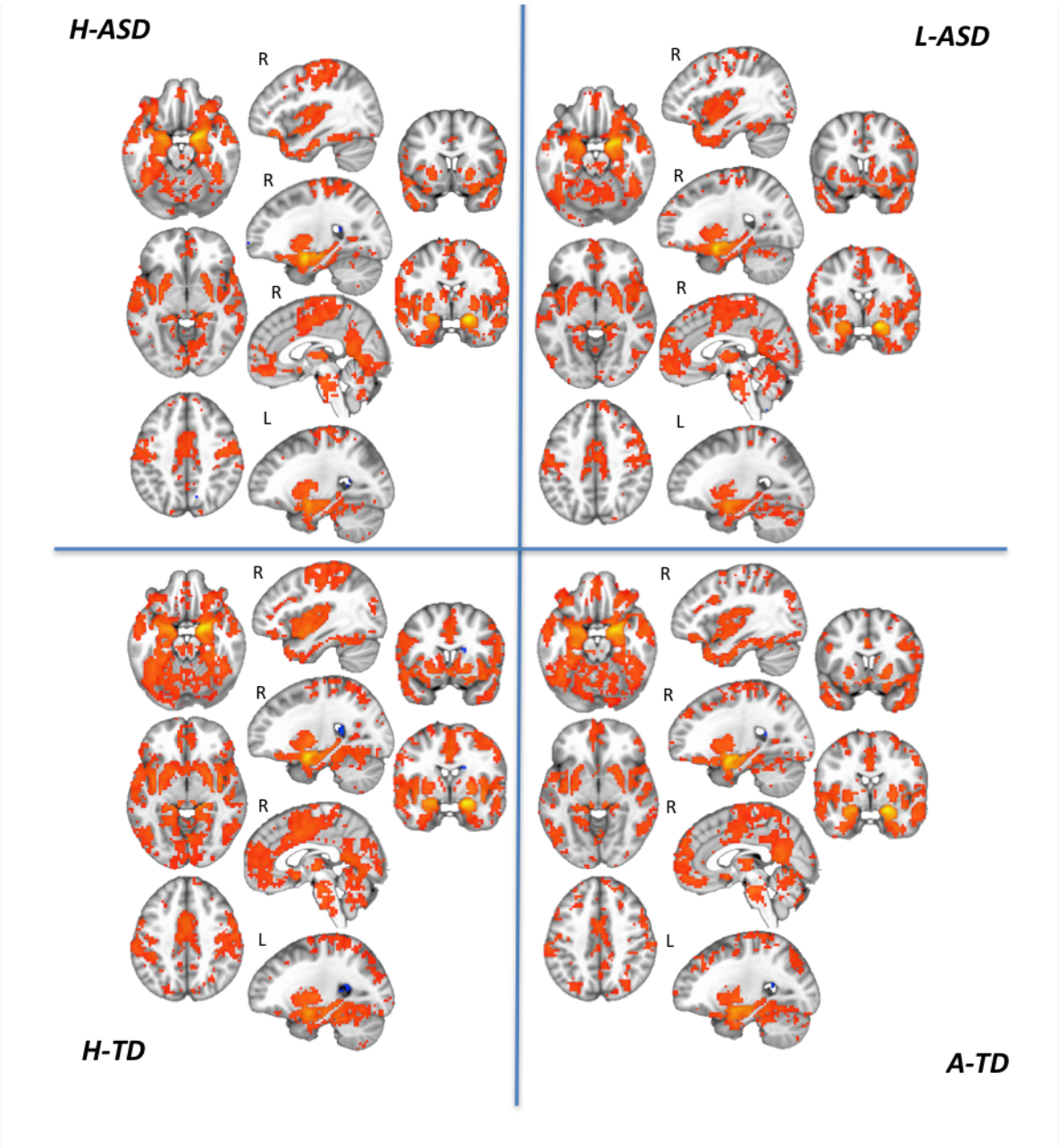

Supplemental Figure 2.S2b: Group mean maps of seed to whole-brain connectivity for H-ASD (top-left), L-ASD (top-right), H-TD (bottom-left), & A-TD (bottom right). All group mean maps were thresholded at $p < 0.005$ voxel extent. Red-yellow clusters represent positive correlations with the right Amygdala seed mean time course, and blue-light blue clusters represent negative correlations with the seed. All images are presented in neurological orientation (left = left).

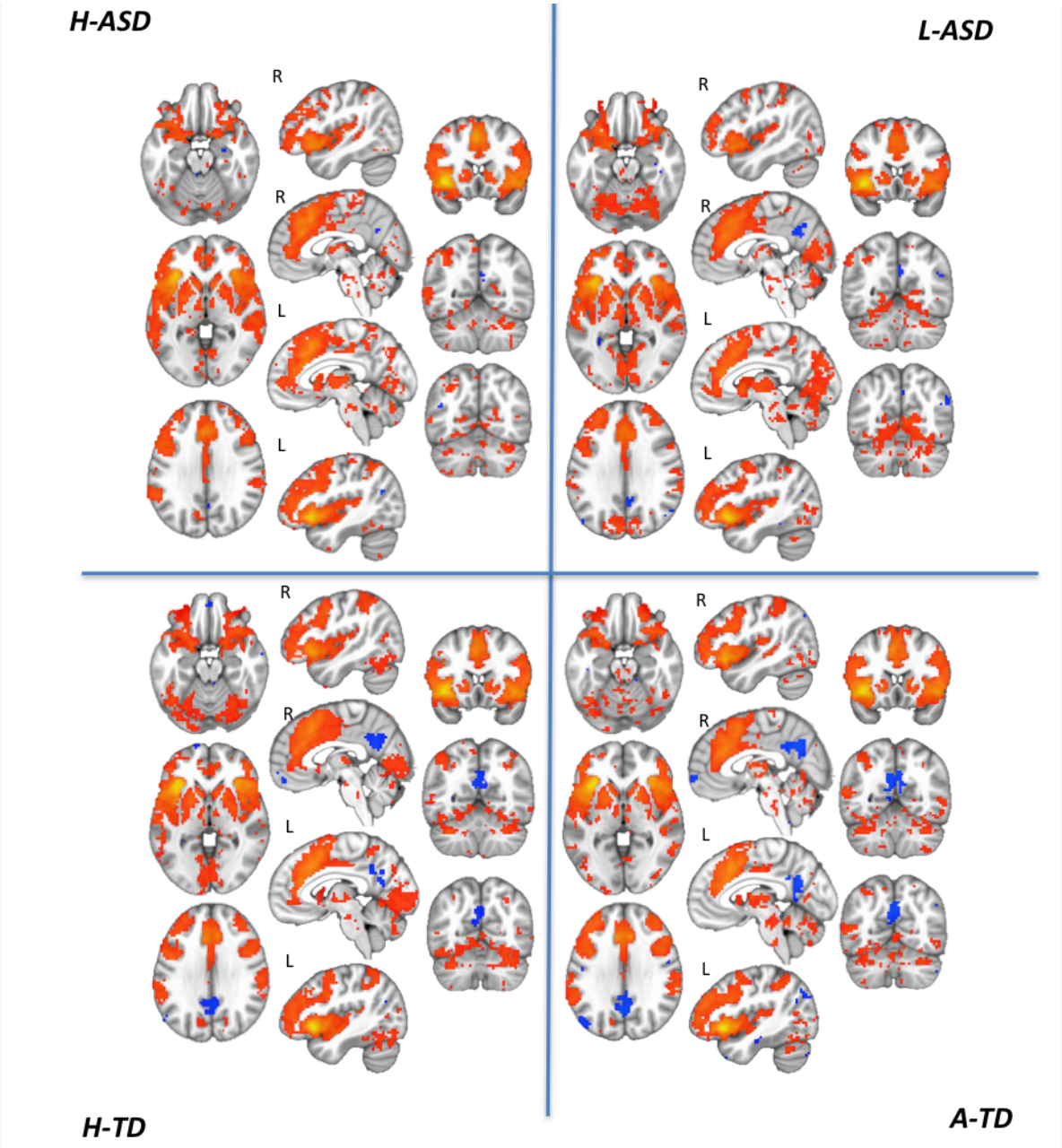

Supplemental Figure 2.S2c: Group mean maps of seed to whole-brain connectivity for H-ASD (top-left), L-ASD (top-right), H-TD (bottom-left), & A-TD (bottom right). All group mean maps were thresholded at $p < 0.005$ voxel extent. Red-yellow clusters represent positive correlations with the left Insula seed mean time course, and blue-light blue clusters represent negative correlations with the seed. All images are presented in neurological orientation (left = left).

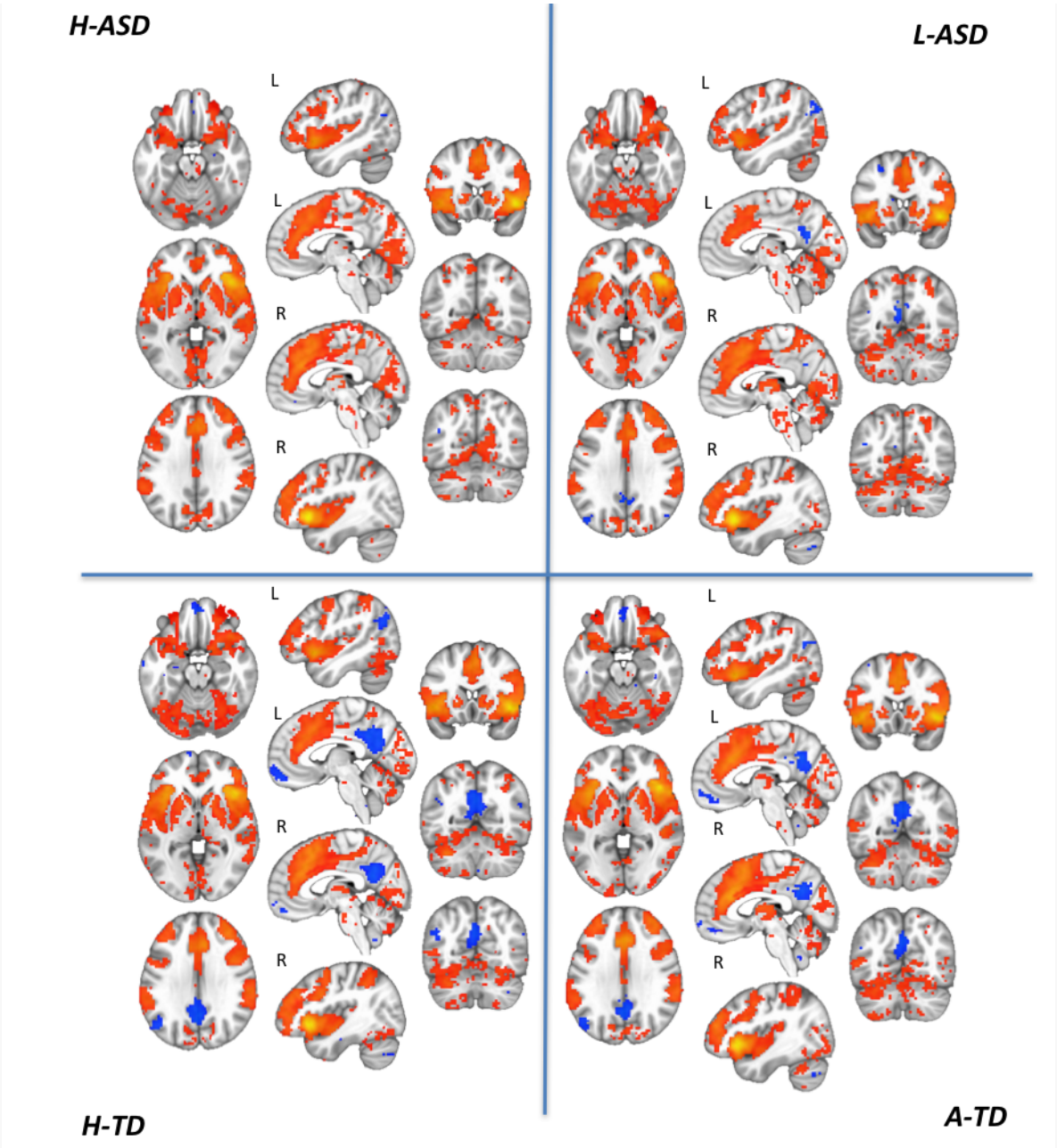

Supplemental Figure 2.S2d: Group mean maps of seed to whole-brain connectivity for H-ASD (top-left), L-ASD (top-right), H-TD (bottom-left), & A-TD (bottom right). All group mean maps were thresholded at $p < 0.005$ voxel extent. Red-yellow clusters represent positive correlations with the right Insula seed mean time course, and blue-light blue clusters represent negative correlations with the seed. All images are presented in neurological orientation (left = left).

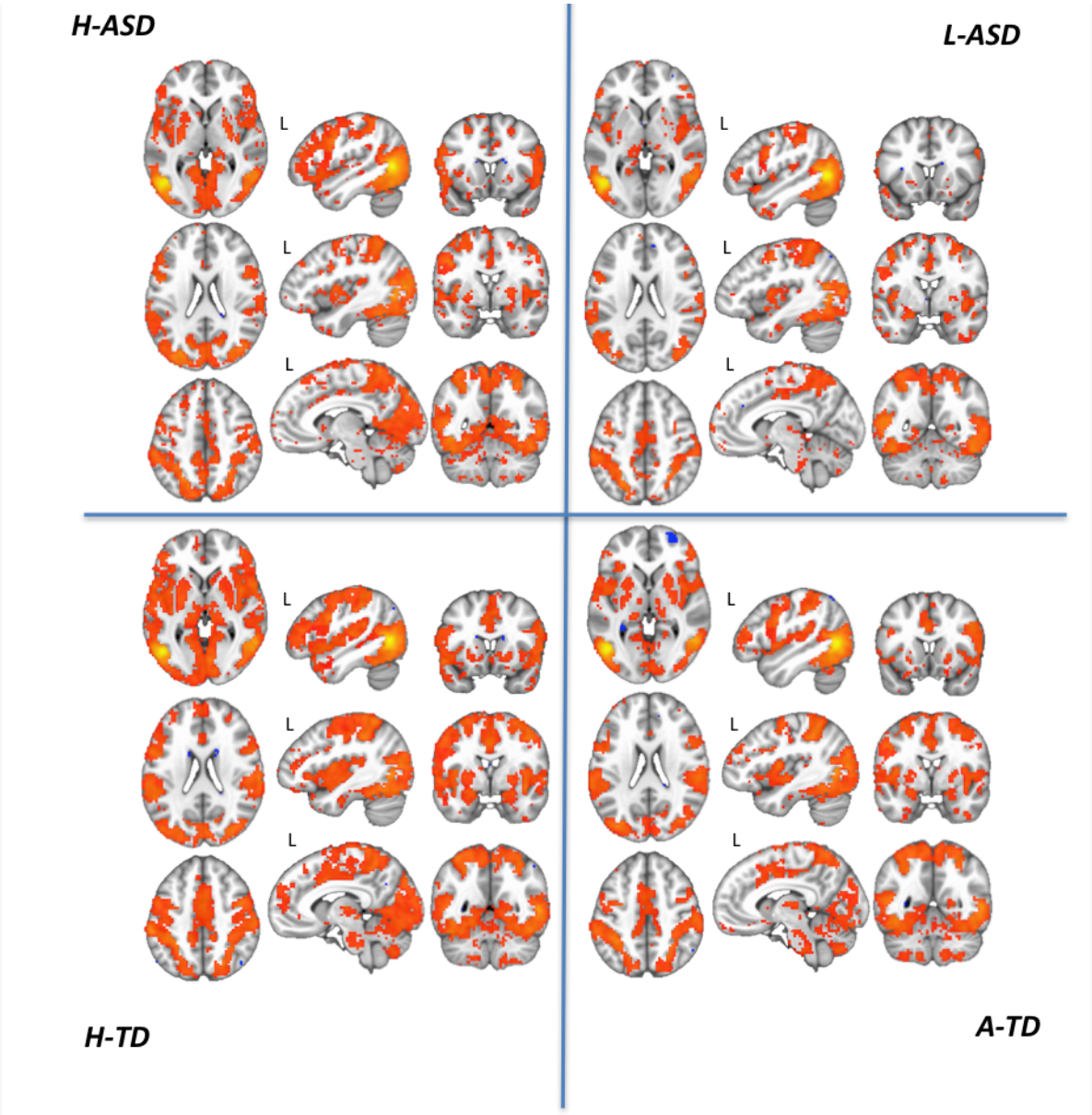

Supplemental Figure 2.S2e: Group mean maps of seed to whole-brain connectivity for H-ASD (top-left), L-ASD (top-right), H-TD (bottom-left), & A-TD (bottom right). All group mean maps were thresholded at $p < 0.005$ voxel extent. Red-yellow clusters represent positive correlations with the left pSTS seed mean time course, and blue-light blue clusters represent negative correlations with the seed. All images are presented in neurological orientation (left = left).

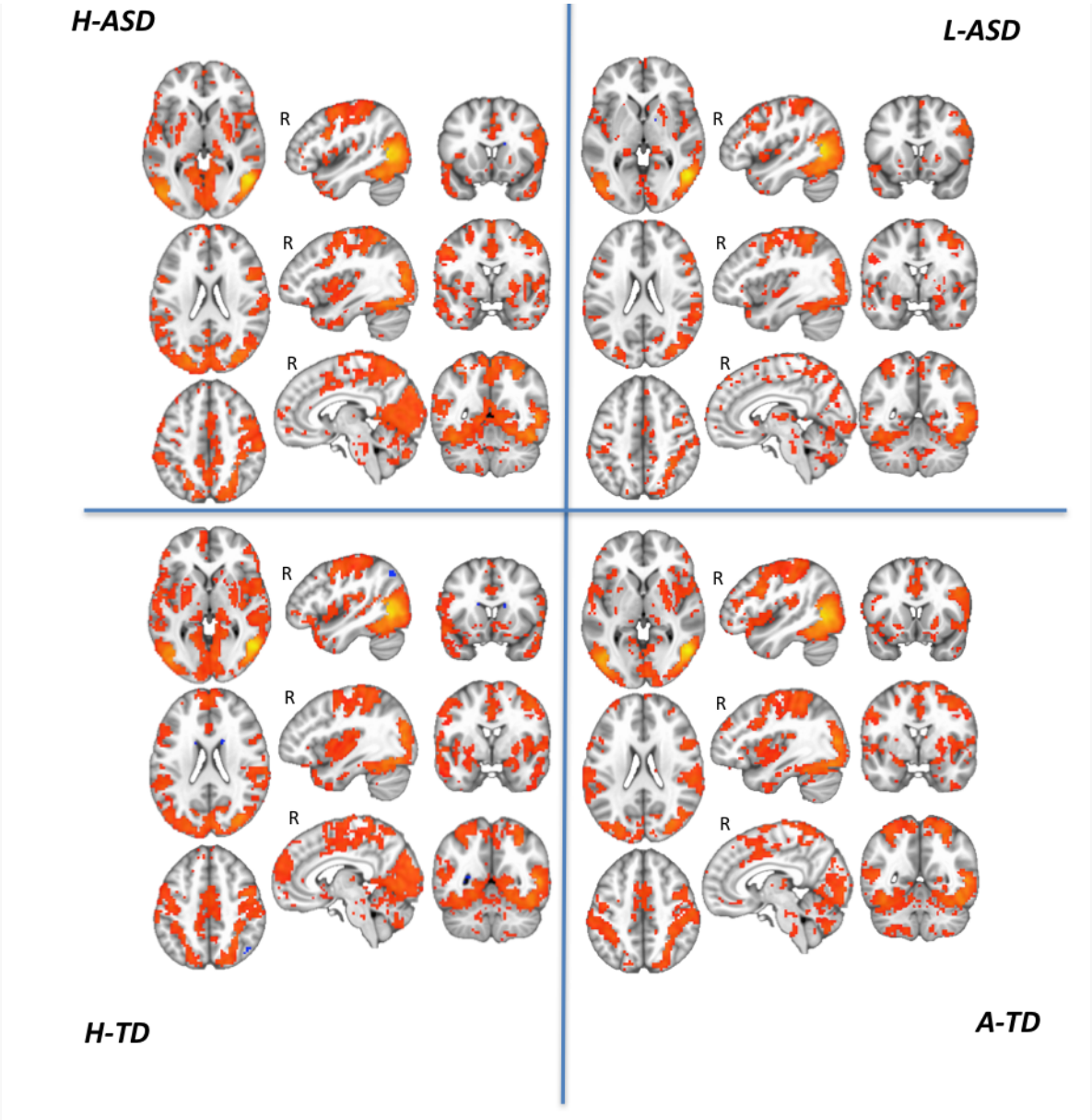

Supplemental Figure 2.S2f: Group mean maps of seed to whole-brain connectivity for H-ASD (top-left), L-ASD (top-right), H-TD (bottom-left), & A-TD (bottom right). All group mean maps were thresholded at $p < 0.005$ voxel extent. Red-yellow clusters represent positive correlations with the right pSTS seed mean time course, and blue-light blue clusters represent negative correlations with the seed. All images are presented in neurological orientation (left = left).

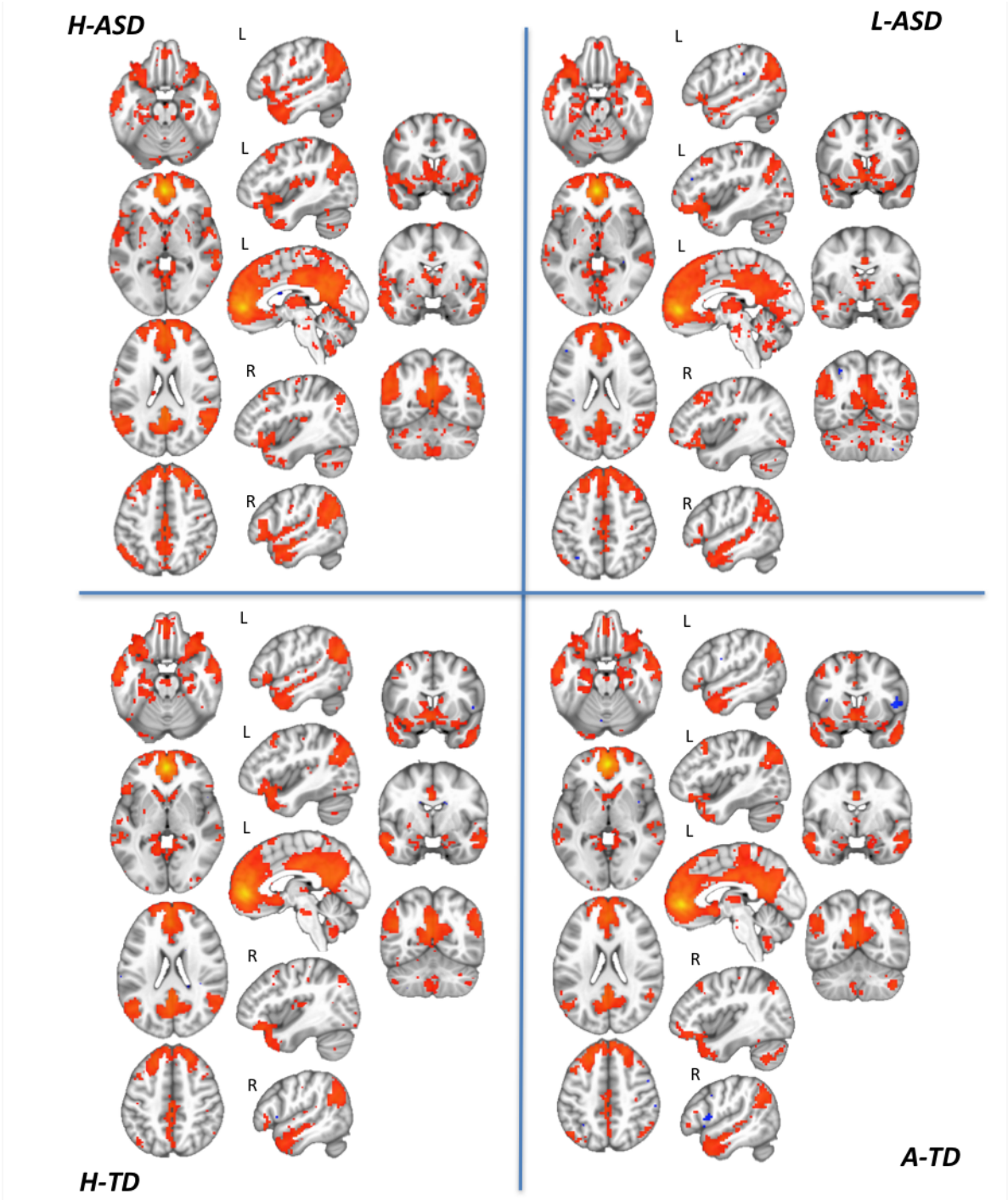

Supplemental Figure 2.S2g: Group mean maps of seed to whole-brain connectivity for H-ASD (top-left), L-ASD (top-right), H-TD (bottom-left), & A-TD (bottom right). All group mean maps were thresholded at $p < 0.005$ voxel extent. Red-yellow clusters represent positive correlations with the Medial Prefrontal Cortex seed mean time course, and blue-light blue clusters represent negative correlations with the seed. All images are presented in neurological orientation (left = left).

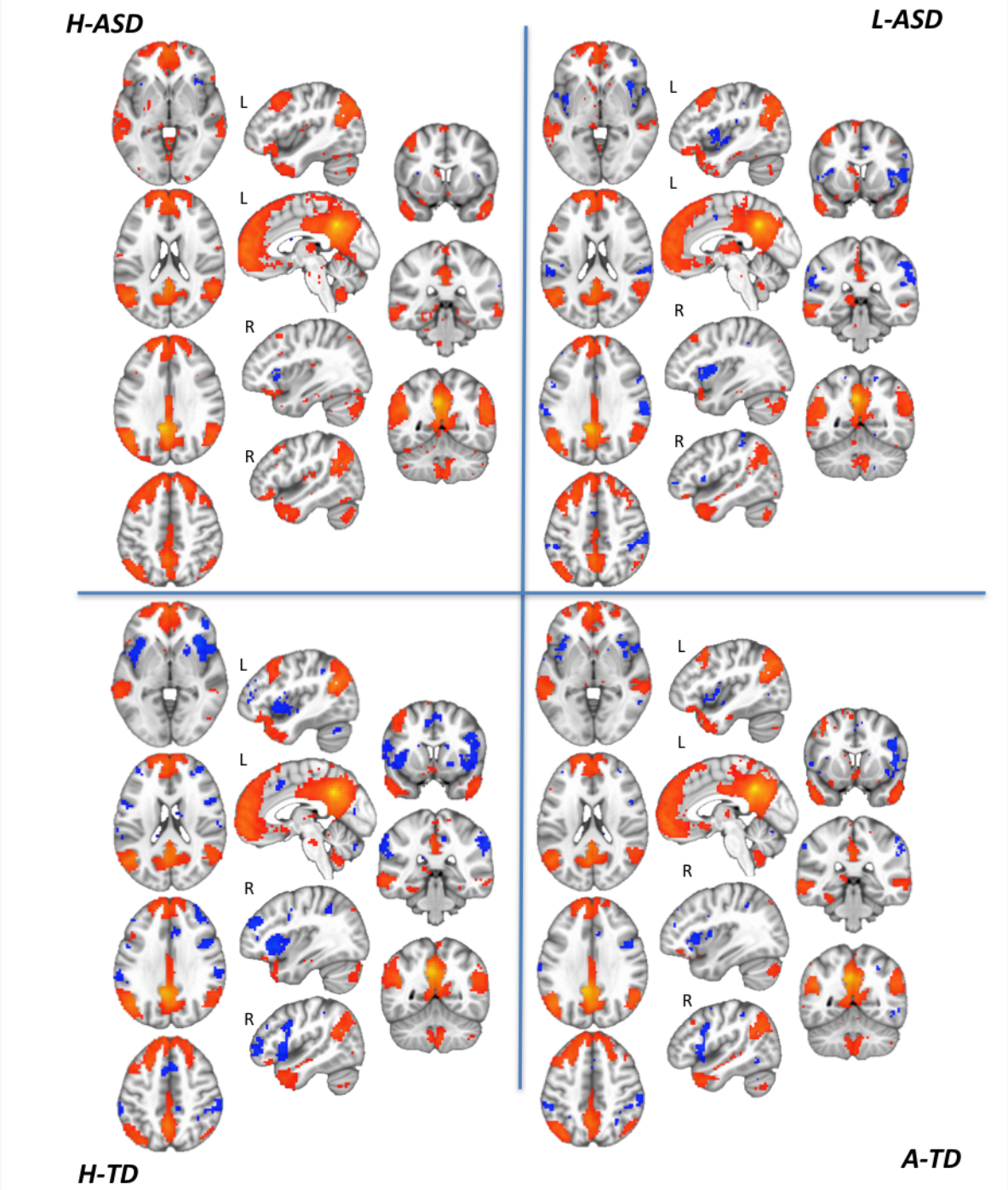

Supplemental Figure 2.S2h: Group mean maps of seed to whole-brain connectivity for H-ASD (top-left), L-ASD (top-right), H-TD (bottom-left), & A-TD (bottom right). All group mean maps were thresholded at $p < 0.005$ voxel extent. Red-yellow clusters represent positive correlations with the Posterior Cingulate Cortex seed mean time course, and blue-light blue clusters represent negative correlations with the seed. All images are presented in neurological orientation (left = left).

Supplemental Table 2.S5: Cluster-size thresholds from all analyses with significant clusters at alpha < .05. Obtained via AFNI 3dttest++ with the Clustsim option.

Contrast	Seed	Cluster Size Threshold (voxels)	Clustering Method	Voxel-wise p-Value Threshold
L-ASD < H-ASD	mPFC	63	Faces of adjacent voxels must touch to be included in the same cluster (NN1 bi-sided)	.005
	Left STS	70		
	Right STS	71		
L-ASD > A-TD	mPFC	68		
H-ASD > H-TD	PCC	65		
	Right Insula	66		

Supplemental Tables 2.S6-2.S8: Age Effects

For each result cluster reported in Table 2.2 in the main manuscript, age was modeled as a predictor variable for the response variable "functional connectivity" (per individual connectivity z-scores between the seed and group difference result cluster). Alpha of .05 for each model was used as the significance criterion. Across the entire sample, there were no significant relationships between age and functional connectivity between regions reported in the results section. The results are described in a table below:

Table 2.S6: Relationship between age and seed-cluster connectivity z-scores in full sample (N = 88)

Seed	Cluster	Beta Value	t Value	p Value
mPFC	PCC	.001	.20	.84
Left pSTS	Pericalcarine	.001	.25	.80
Left pSTS	Precuneus	.009	1.21	.23
Right pSTS	Pericalcarine	.010	1.52	.131
mPFC	Pericalcarine	-.013	-1.88	.06
PCC	Superior Frontal Gyrus	-.0003	-.04	.97
PCC	Right Insula	-.001	-.23	.82
PCC	Left Crus 1	-.009	-1.5	.136

We also tested whether there were any age X group (ASD vs. TD), or age X functioning level (L-ASD vs. H-ASD) interactions/age-related changes in FC. Diagnosis (ASD vs. TD) X age, and ASD group (L-ASD vs. H-ASD) X age linear regression interaction models were specified. We found no significant age X diagnosis, or age X ASD group interactions for the FC results reported in this study. These results are described in the tables below:

Table 2.S7: Group (ASD vs. TD) by age interactions in seed-cluster connectivity z-scores (N = 88)

Seed	Cluster	Interaction Beta Value	t Value	p Value
mPFC	PCC	.004	.25	.80
Left pSTS	Pericalcarine	-.008	-.66	.51
Left pSTS	Precuneus	-.003	-.24	.81
Right pSTS	Pericalcarine	-.007	-.55	.581
mPFC	Pericalcarine	.014	1.04	.303
PCC	Superior Frontal Gyrus	.013	.89	.37
PCC	Right Insula	.001	.08	.936
PCC	Left Crus 1	.019	1.85	.067

Table 2.S8: Group (L-ASD vs. H-ASD) by age interactions in seed-cluster connectivity z-scores (N = 44)

Seed	Cluster	Interaction Beta Value	t Value	p Value
mPFC	PCC	-.017	-.91	.37
Left pSTS	Pericalcarine	.021	1.67	.10
Left pSTS	Precuneus	-.003	-.16	.87
Right pSTS	Pericalcarine	.018	1.43	.16
mPFC	Pericalcarine	< -.001	-.04	.97
PCC	Superior Frontal Gyrus	.016	.89	.38
PCC	Right Insula	-.007	-.40	.69
PCC	Left Crus 1	.008	.65	.52

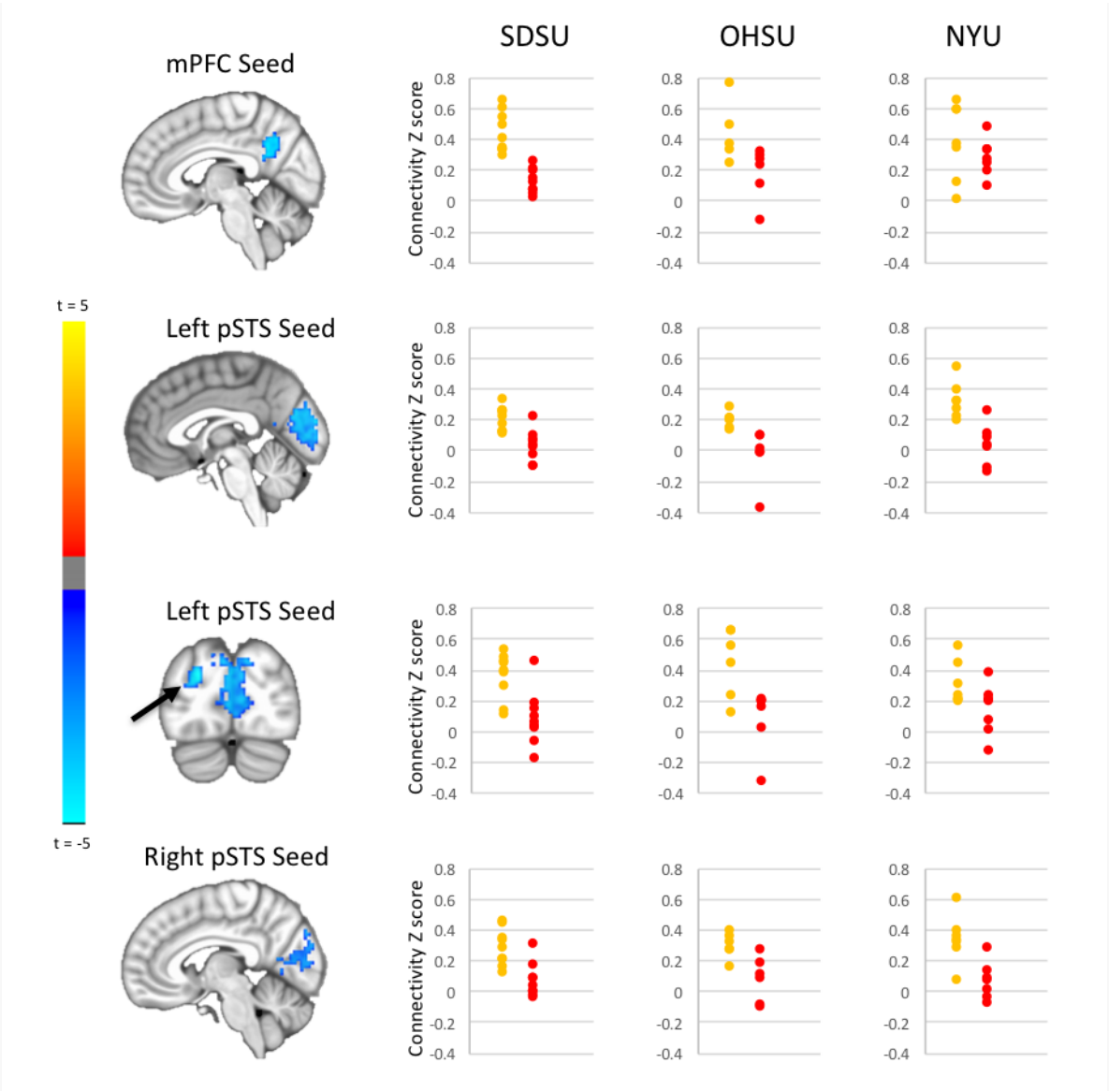

Supplemental Figure 2.S3a: Findings across scanning sites. Plotted are the mean connectivity z scores from each of the significant clusters for each individual across both contrasted groups for each scanning site. Red = L-ASD, Yellow = H-ASD.

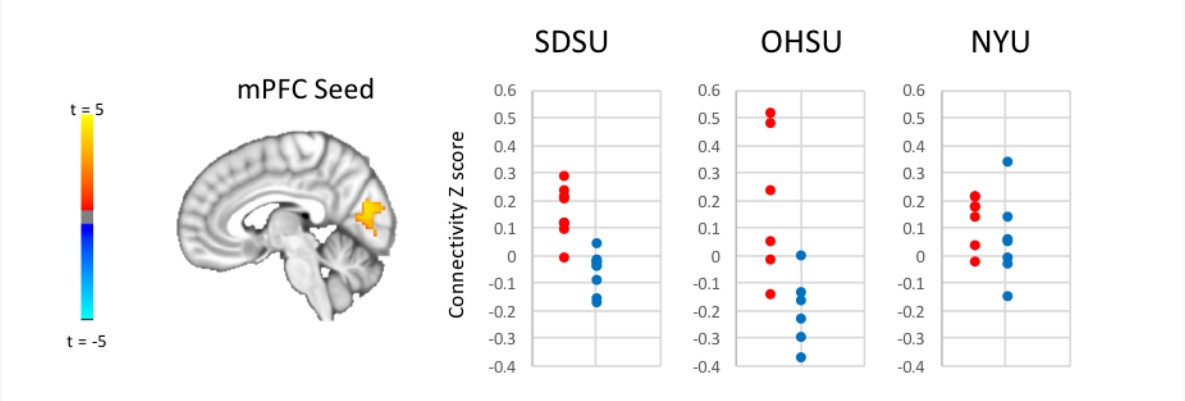

Supplemental Figure 2.S3b: Findings across scanning sites. Plotted are the mean connectivity z scores from each of the significant clusters for each individual across both contrasted groups for each scanning site. Red = L-ASD, Blue = A-TD.

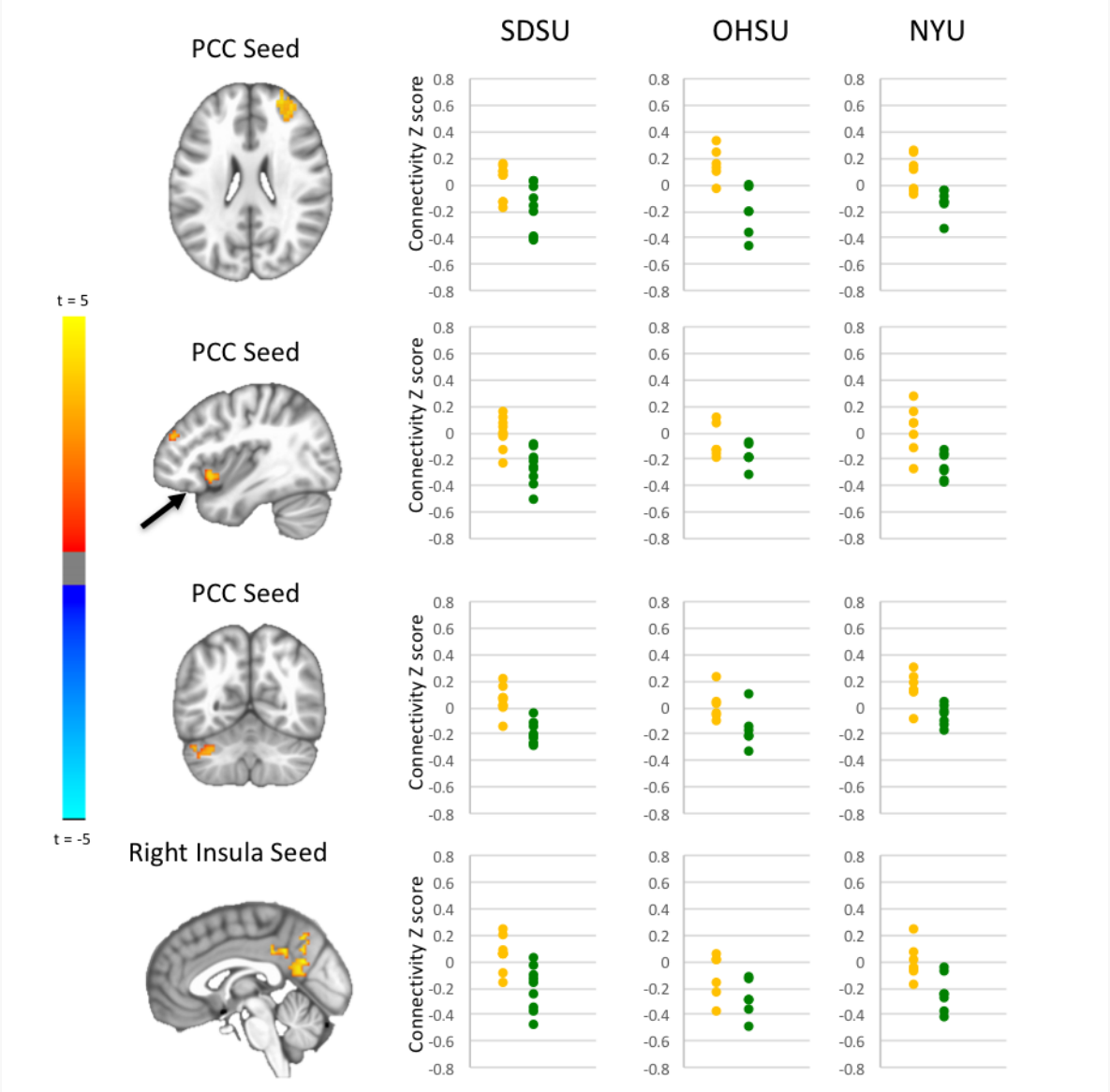

Supplemental Figure 2.S3c: Findings across scanning sites. Plotted are the mean connectivity z scores from each of the significant clusters for each individual across both contrasted groups for each scanning site. Yellow = H-ASD, Green = H-TD.

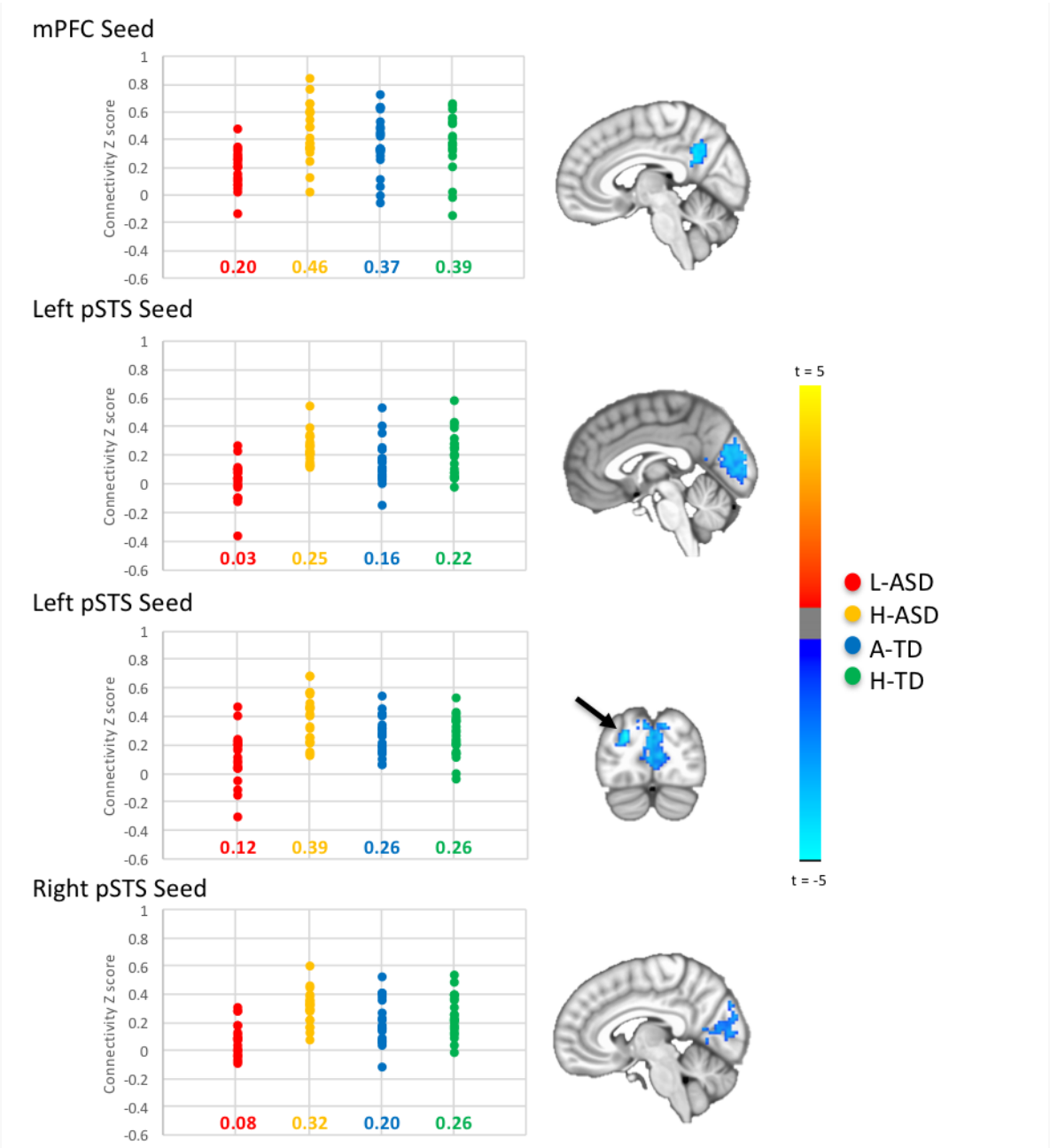

Supplemental Figure 2.S4a: Group clusters from the L-ASD vs. H-ASD contrast. For each of the four groups (H-ASD = yellow; L-ASD = red; H-TD = green; A-TD = blue), scatter plots illustrate connectivity between the seed and significant cluster. Only group differences between the two groups contrasted were tested statistically and corrected for multiple comparisons. Mean z connectivity-scores for all 4 groups (listed under scatter-plots) are provided for illustrative purposes.

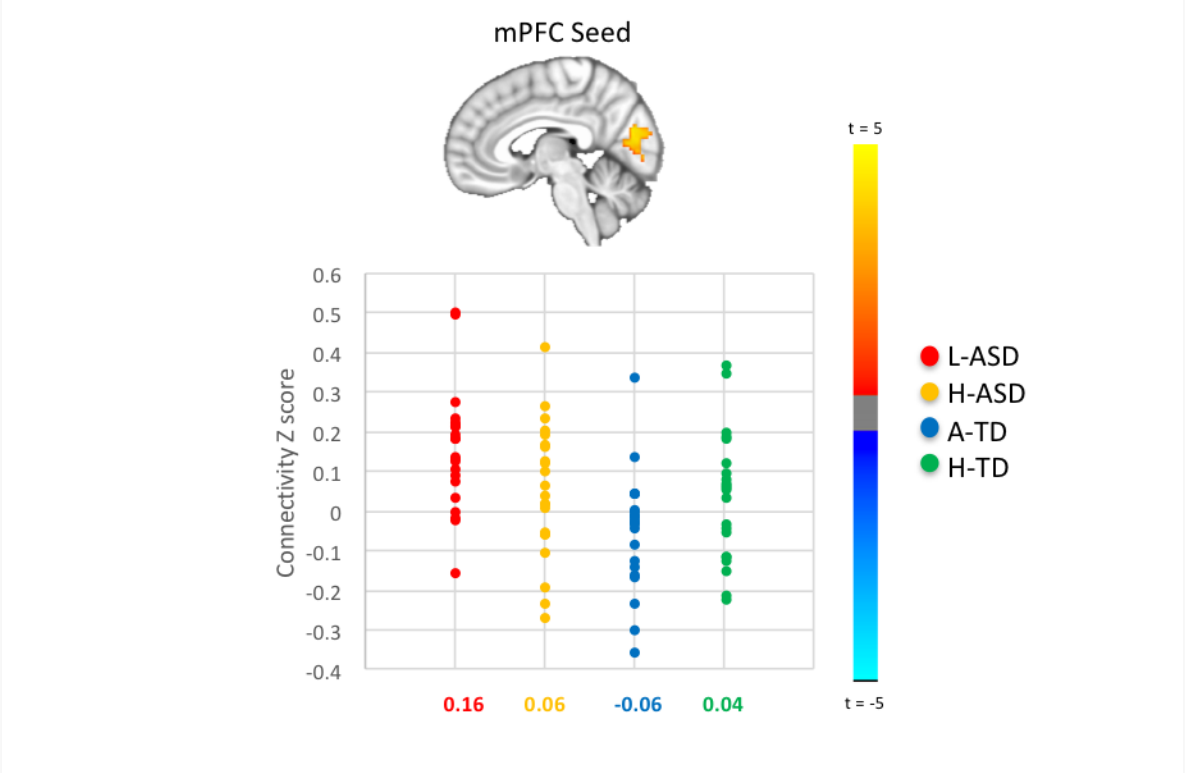

Supplemental Figure 2.S4b: Group clusters from the L-ASD vs. A-TD contrast. For each of the four groups (H-ASD = yellow; L-ASD = red; H-TD = green; A-TD = blue), scatter plots illustrate connectivity between the seed and significant cluster. Only group differences between the two groups contrasted were tested statistically and corrected for multiple comparisons. Mean z connectivity-scores for all 4 groups (listed under scatter-plots) are provided for illustrative purposes.

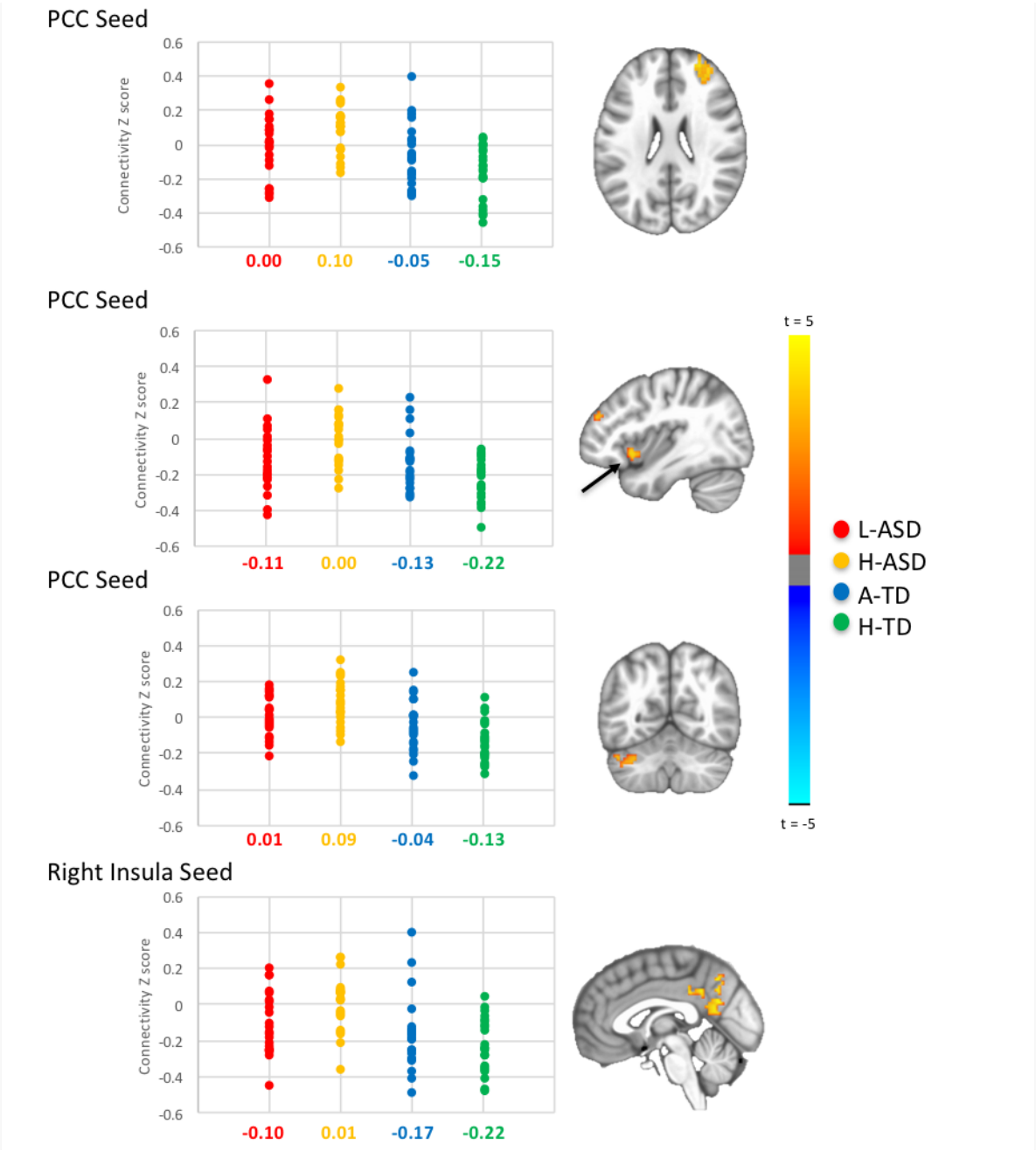

Supplemental Figure 2.S4c: Group clusters from the H-ASD vs. H-TD contrast. For each of the four groups (H-ASD = yellow; L-ASD = red; H-TD = green; A-TD = blue), scatter plots illustrate connectivity between the seed and significant cluster. Only group differences between the two groups contrasted were tested statistically and corrected for multiple comparisons. Mean z connectivity-scores for all 4 groups (listed under scatter-plots) are provided for illustrative purposes.

A. Cluster Thresholds

Contrast	Seed	Cluster Size Threshold (voxels)	Clustering Method	Voxel-wise p-Value Threshold
L-ASD vs. H-ASD	mPFC	67	Faces of adjacent voxels must touch to be included in the same cluster (NN1 bi-sided)	.005
	Left pSTS	67		
	Right pSTS	69		

B. L-ASD vs. H-ASD

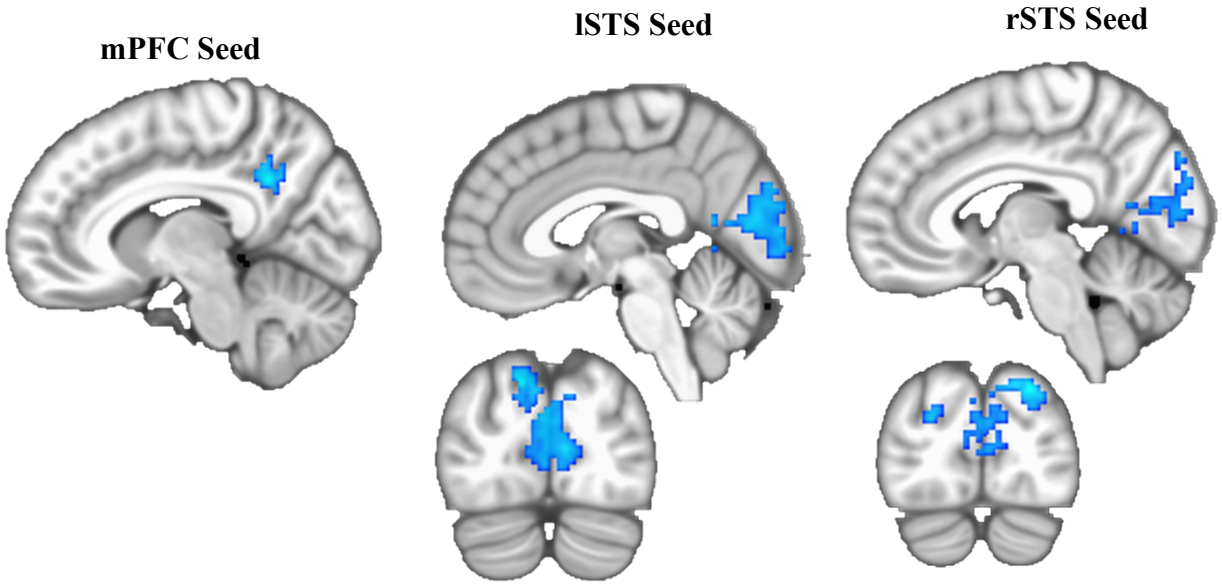

C. Cluster Statistics

Seed	Size	Peak t	Peak β	mm x	mm y	mm z	Peak Regions
mPFC	110	-4.58	-0.26	9	-51	30	Posterior Cingulate Cortex
lSTS	545	-4.46	-0.35	-12	-81	42	Left Cuneus, (other: Pericalcarine Cortex)
rSTS	332	-4.12	-0.26	24	-83	32	Right Cuneus (other: Pericalcarine Cortex)

Supplemental Figure 2.S5: Contrast between the L-ASD vs. H-ASD groups controlling for ASD symptom severity (ADOS-2 Total). Panel A: cluster thresholds used to determine statistical significance. Panel B: spatial maps for the L-ASD vs. H-ASD contrast for connectivity with the mPFC, left pSTS, and right pSTS seeds (presented in neurological orientation, L=L). Panel C shows the cluster statistics, and anatomical labels for the significant cluster. Peak coordinates are given in MNI space.

A. Cluster Thresholds

Contrast	Seed	Cluster Size Threshold (voxels)	Clustering Method	Voxel-wise p-Value Threshold
L-ASD vs. A-TD	mPFC	67	Faces of adjacent voxels must touch to be included in the same cluster (NN1 bi-sided)	.005

B. L-ASD vs. A-TD

mPFC Seed

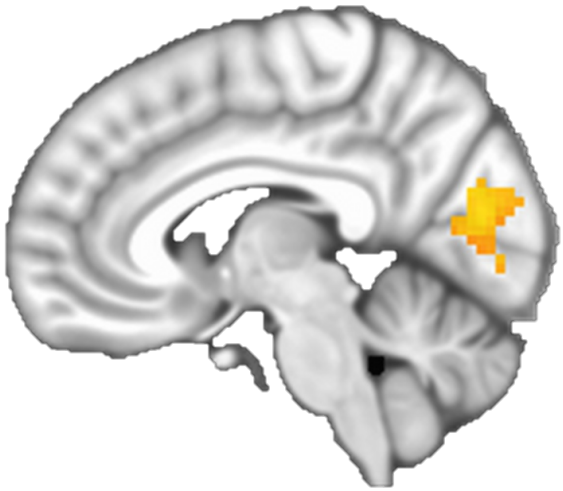

C. Cluster Statistics

Seed	Size	Peak t	Peak β	mm x	mm y	mm z	Peak Regions
mPFC	160	4.29	0.29	9	-78	15	Pericalcarine Cortex

Supplemental Figure 2.S6: Contrast between the L-ASD vs. A-TD groups controlling for FIQ. Panel A: cluster thresholds used to determine statistical significance. Panel B: spatial maps for the L-ASD vs. A-TD contrast for connectivity with the mPFC seed (presented in neurological orientation, L=L). Panel C shows the cluster statistics, and anatomical labels for the significant cluster. Peak coordinates are given in MNI space.

A. Cluster Thresholds

Contrast	Seed	Cluster Size Threshold (voxels)	Clustering Method	Voxel-wise p-Value Threshold
H-ASD vs. A-TD	mPFC	67	Faces of adjacent voxels must touch to be included in the same cluster (NN1 bi-sided)	.005

B. H-ASD vs. A-TD

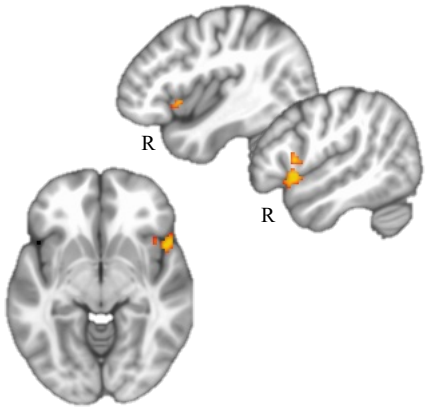

C. All Groups Scatter Plots

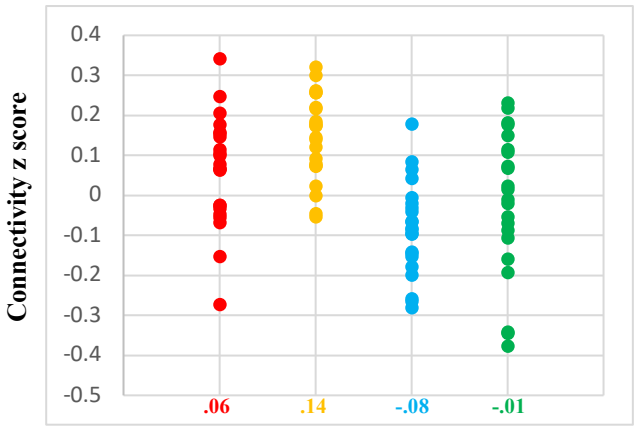

D. Cluster Statistics

Seed	Size	Peak β	mm x	mm y	mm z	Mean z (sd) H-ASD	Mean z (sd) A-TD	Cohen's d	Peak Regions
mPFC	76	.32	57	18	-3	.14 (.11)	-.08 (.12)	1.91	Right Inferior Frontal Gyrus (other: Right Insula)

Supplemental Figure 2.S7: Contrast between the H-ASD and A-TD group. The H-ASD group showed significantly increased connectivity between mPFC seed and the right inferior frontal gyrus/anterior insula compared to the A-TD group. Panel A: cluster thresholds used to determine statistical significance. Panel B: spatial maps for the H-ASD vs. A-TD contrast for connectivity with the mPFC seed (presented in neurological orientation, L=L). Panel C: scatter plots depicting connectivity between the mPFC and the cluster presented in panel b in each of the four groups, provided for illustrative purposes (L-ASD = red, H-ASD = yellow, A-TD = light blue, H-TD = green). Panel D shows the cluster statistics, parameter estimates, and anatomical labels for the significant cluster. Peak coordinates are given in MNI space.

Chapter 3 (Study 2): Atypical functional connectivity of visual cortex relates to symptom severity and cognitive developmental skills in toddlers and preschoolers with autism

Abstract

Despite accumulating evidence of altered development of visual cortex in autism, including in early childhood, it remains unknown how its connectivity relates to the emerging developmental skills in young children with autism spectrum disorders (ASD). This study examines the links between functional connectivity of visual cortex and acquisition of early developmental skills in a cohort of 84 toddlers and preschoolers between the ages 1.5 and 5 years (48 children with ASD and 36 typically developing children), using resting-state fMRI data acquired during natural sleep. Resting-state fMRI data were submitted to independent component analysis to identify visual networks in order to generate bias-free visual cortex seeds for whole-brain functional connectivity analyses. Ordinary Least Squares regression models implemented in AFNI were used to estimate the main effects of diagnosis and developmental skills, and their interaction on visual cortex functional connectivity, while controlling for head motion and age. A significant diagnostic group by general developmental abilities interaction effect on functional connectivity between right inferior lateral occipital cortex and left posterior superior temporal sulcus was observed, with greater connectivity between these visual regions strongly associated with more advanced developmental skills in typically developing children, but not so in children with ASD. Among children with ASD, lower connectivity between the left lingual gyrus and pericalcarine cortex was significantly associated with higher autism symptom severity. Age related changes in connectivity between visual cortex and sensorimotor regions were also atypical in ASD. These findings suggest that atypical functional connectivity of visual cortex may play a role in early autism symptomatology and cognitive development.

Introduction

Autism spectrum disorder (ASD) is a neurodevelopmental disorder with a current prevalence rate of 2% (Maenner et al., 2020), characterized by early-appearing deficits in social communication and restricted and repetitive behaviors and interests (American Psychiatric Association, 2013). ASD has a significant impact on affected individuals and families, with most people with ASD requiring some form of lifelong support by family, public services, healthcare systems, etc. (Lord et al., 2018). Much is unknown regarding factors contributing to the remarkable heterogeneity in lifespan outcomes, including independent living skills, occupational and social attainment in adulthood, and mental and physical health (Hand, Angell, Harris, & Carpenter, 2020; Steinhausen, Jensen, & Lauritsen, 2016). However, recently emerging longitudinal studies following people on the autism spectrum from early childhood to adulthood suggest that general cognitive abilities (including early developmental skills measured in preschool age) predict later adaptive functioning, independence, and overall quality of life and well-being in ASD (Ben-Itzchak & Zachor, 2020; Lord, McCauley, et al., 2020).

About one third of children with autism are estimated to have intellectual disability (ID), with a further ~25% exhibiting intellectual abilities in the borderline range, referred to hereafter as lower cognitive abilities (LCA) (Maenner et al., 2020). However, children and adults with ASD *and* ID or LCA are underrepresented in neuroimaging studies, due to practical challenges associated with obtaining low-motion MRI data from this population. Thus, very little is known about brain functioning or connectivity patterns related to ID or LCA in ASD, or about neural substrates of early developmental skills foreshadowing cognitive abilities in autism in general. This is critical because no specific genetic markers or molecular pathways have been identified to date that confer unique risk for ASD without co-occurring ID, despite significant advances in

research into genomics (Iakoucheva, Muotri, & Sebat, 2019; Myers et al., 2020). Similarly, despite decades-long extensive efforts, no fully-replicated neural markers of ASD have been identified amidst high rates of mixed findings that have been largely attributed to heterogeneous cohorts with regard to participants' age (Uddin et al., 2013), sex (L. A. Olson et al., 2020), autism symptom severity (Reiter et al., 2021), or treatment history (Linke, Olson, Gao, Fishman, & Müller, 2017). Importantly, variability along the full spectrum of cognitive and intellectual abilities among people with ASD – often insufficiently considered or represented in research cohorts – has also been identified as contributing to variability in functional connectivity patterns in school-age children and adolescents with ASD (Gabrielsen et al., 2018; Reiter et al., 2018). However, similar links between developmental skills in early childhood and brain connectivity patterns in ASD have yet to be investigated.

Although still scarce, existing research on functional connectivity in ASD cohorts characterized by lower intellectual abilities suggests atypical development and functioning of brain visual systems. Specifically, our group previously reported weaker connectivity between visual cortex (VC) within the ventral visual stream and midline hubs of the default mode network (DMN) in school-age children and adolescents with ASD and LCA when compared to age-matched peers with ASD and average or higher cognitive abilities (HCA), but atypically increased connectivity between the pericalcarine VC and one of the DMN hubs, medial prefrontal cortex, when compared to typically developing (TD) peers (Reiter et al., 2018). Additionally, Gabrielsen et al. (2018) identified reduced interhemispheric homotopic connectivity across the brain in youth with ASD and LCA (with minimal spontaneous language) when compared to those with ASD and HCA, and overconnectivity between DMN and temporo-occipital VC when compared to TD peers. Although to date no published studies investigated links between functional connectivity and emerging

developmental skills in toddlers and preschoolers with ASD, one structural MRI study in 3-6 year-old children found cortical thickness of the right inferior occipital gyrus (part of the VC) to be the most prominent feature distinguishing participants with ASD and LCA/ID from typically developing controls (Kim et al., 2022). Increased VC activation (Samson et al., 2012) and connectivity (Keehn et al. 2013) have also been reported in ASD cohorts of children with mostly average or above average intellectual abilities and linked with poorer cognitive task performance. Furthermore, atypical recruitment of VC during functionally-independent auditory processing has been observed in children and adolescents with ASD and HCA, and was associated with greater ASD symptom severity (Keehn et al., 2017), while increased connectivity between VC and the extended language network was observed in youth with ASD with lower language abilities (Y. Gao et al., 2019). Together, these findings suggest that, at least by school age, atypical development of visual systems and cognitive abilities in ASD may be inter-linked.

Along with other primary sensory circuits, VC is one of the earliest to mature (W. Gao, Alcauter, Smith, Gilmore, & Lin, 2015; Gilmore et al., 2012). Thus, investigations in *early* childhood cohorts are critical to improved understanding of the links between visual circuitry and cognitive abilities in ASD. Behavioral and neuroimaging evidence in young children with ASD studied in the first years of life suggests that atypical development of visual attention may have cascading effects on the child's emerging developmental skills, giving rise to sociocommunicative impairments associated with ASD. For example, infants at high familial risk for ASD (i.e., with older siblings with ASD) show reduced dyadic synchrony in gaze, linked with poorer developmental abilities two years later (Kellerman et al., 2020). Initiation of joint attention (IJA), which involves coordinating visual attention between two people (typically a child and a caregiver in early life) is often impaired in ASD (Korhonen, Kärnä, & Räty, 2014) and commonly persists

into adolescence and beyond (Mundy, Sullivan, & Mastergeorge, 2009). In infants at high risk for ASD, increased functional connectivity between visual and dorsal attention networks is associated with impaired IJA (Eggebrecht et al. (2017). In toddlers and preschoolers with ASD, VC connectivity patterns have been linked to autism symptom severity, with weaker connectivity between occipito-temporal VC and the DMN associated with higher autism symptom severity in a subgroup of toddlers with ASD and social visual engagement difficulties (Lombardo, Eyler, et al. (2019)), and greater connectivity between visual and sensorimotor networks associated with higher autism symptom severity in a cohort of young preschoolers with ASD (Chen et al. (2021)).

Despite accumulating evidence of the altered development of VC in ASD, including in early childhood, it remains unknown how its connectivity relates to emerging developmental skills that are recognized as foundational precursors of longer-term cognitive abilities (Girault et al., 2018), in young children with ASD. Therefore, the current study's primary objective was to examine the links between functional connectivity of VC and emerging early developmental skills in a cohort of toddlers and preschoolers with ASD, using resting-state fMRI data acquired during natural sleep. A secondary aim was to examine whether connectivity of the VC was associated with ASD symptom severity.

Methods

Participants. Cross-sectional data from eighty-four toddlers and preschoolers, ages 1.5 – 5 years (ASD: n = 48, TD: n = 36), participating in the San Diego State University (SDSU) Toddler MRI Project were included in the study. Children with early diagnoses of ASD (or behavioral concerns consistent with ASD symptoms) were referred to the longitudinal Toddler MRI Project from specialty autism clinics, state-funded early education and developmental evaluation programs, and local health care providers and clinics in the community, and were followed up

through age 5 years. Typically developing (TD) children were recruited from the community, including early head start programs, and via print and social media advertisements. All participants were screened and excluded for any co-occurring neurological disorders (e.g., cerebral palsy), history of perinatal central nervous system (CNS) infection or gross CNS injury, non-febrile seizures, and contraindications for MRI, as well as for known syndromic forms of ASD (e.g., fragile X or Rett syndrome). To limit known risk factors for developmental delays among children enrolled in the TD group, TD participants were also screened and excluded for prematurity (<36 weeks of gestation) and family history (in first-degree relatives) of ASD, intellectual disability, or other heritable neurological or neuropsychiatric disorders. Informed written consent was obtained from caregivers under protocols approved by the SDSU and UCSD Institutional Review Boards, and by the County of San Diego Health and Human Services Agency. This report includes cross-sectional data only from one of the study visits, determined by the availability of fMRI data (as described below).

Diagnostic and developmental assessment. Upon enrollment, all participants with ASD, or suspected to have ASD, underwent full diagnostic evaluation, using standardized measures in combination with clinical judgment, in accordance with the current recommendations by the American Academy of Pediatrics and Society for Developmental and Behavioral Pediatrics (Weitzman & Wegner, 2015). Only participants who met the DSM-5 (APA, 2013) diagnostic criteria for ASD, or clinical best estimate in children younger than age three (Ozonoff et al., 2015), were included in the ASD group. The diagnoses were supported by the Autism Diagnostic Observation Schedule-2nd edition (Lord et al., 2012) administered by research-reliable clinicians, the Social Communication Questionnaire (SCQ, Current form (Rutter, Bailey, & Lord, 2003)) or the Autism Diagnostic Interview-Revised (Lord et al., 1994) administered to caregivers of children

36 month-old and older, and expert clinical judgment (by the senior author). Only children with confirmed diagnosis (at follow-up study visits) were included in the current dataset. Developmental skills were assessed in all (ASD and TD) participants with the Mullen Scales of Early Learning (Mullen, 1995), a clinician-administered assessment of cognitive, language, and motor development, which yields standardized age-normed scores used here as predictor variables. Specifically, the Mullen Early Learning Composite (ELC) standard score was used as an index of overall developmental level. For inclusion in the TD group, children had below clinical cutoff scores on the ASD screener, the SCQ, and demonstrated developmental skills falling no more than 1.5 SD below the normative mean for their age on measures of early learning and development (the Mullen Scales of Early Learning). The Vineland Adaptive Behavior Scales, 2nd edition (Sparrow, Cicchetti, & Balla, 2005), a semi-structured interview, was administered to caregivers to assess the child's adaptive behavior skills demonstrated at home and other settings; the Vineland scores were utilized to support the diagnostic and developmental classification, and were not used as variables of interest in the current analyses.

MRI data acquisition. MRI data were acquired during natural nocturnal sleep on a GE Discovery MR750 3T MRI scanner at the UCSD Center for Functional Magnetic Resonance Imaging, using a Nova Medical 32-channel head coil. A multiband multi-echo planar imaging (EPI) sequence allowing simultaneous acquisition of multiple slices was used to acquire two fMRI runs (400 volumes per each 6-min run) with high spatial resolution and fast acquisition (TR = 800ms, TE = 35ms, flip angle = 52°, 72 slices, multiband acceleration factor = 8, 2mm isotropic voxel size, matrix = 104 x 104, FOV = 20.8cm). Two separate 20s spin echo EPI sequences with opposing phase encoding directions were also acquired using the same matrix size, FOV, and prescription to correct for susceptibility-induced distortions. High-resolution anatomical images

were acquired with a fast 3D spoiled gradient recalled (FSPGR) T1-weighted sequence (0.8mm isotropic voxel size, NEX = 1, TE/TI = min full/1,060 ms, flip angle = 8°, FOV = 25.6cm, matrix = 320 x 320, receiver bandwidth 31.25 Hz). Motion during T1 (anatomical) scans was corrected in real-time using three navigator scans and prospective motion correction (White et al., 2010), and images were bias-corrected using the GE PURE option. Protocols for the successful acquisition of MRI data in sleeping toddlers and preschoolers have been described elsewhere (Chen, Linke, Olson, Ibarra, Kinnear, et al., 2021).

MRI data preprocessing. Data from one resting-state fMRI scan (to maximize sample size and motion matching across groups) were included per participant. MRI data were preprocessed with FMRIB's Software Libraries (FSL v5.0.10; (Smith et al., 2004)), MATLAB 2015b (Mathworks Inc., Natick, MA) using SPM12, and the CONN toolbox v17f ((Whitfield-Gabrieli & Nieto-Castanon, 2012); http://www.nitrc.org/projects/conn). Data were corrected for susceptibility-induced distortions using two spin-echo EPI acquisitions with opposite phase encoding directions and FSL's TOPUP tools, and motion corrected using rigid-body realignment, implemented in SPM12. Following spatial smoothing using a 6mm Gaussian kernel at full-width half maximum, outlier volumes (with frame-wise displacement (FD) >0.5 mm and/or changes in signal intensity >3 standard deviations) were identified using the CONN v17f Artifact Detection Toolbox (ART; https://www.nitrc.org/projects/artifact_detect), and nuisance regression (including censoring of ART-detected outliers, regression of the 6 rigid-body motion parameters and their derivatives, and the first five PCA components derived from the CSF and white matter compartments using aCompCor (Behzadi, Restom, Liau, & Liu, 2007)) and band-pass temporal filtering (0.008–0.08 Hz) were applied.

The structural images were spatially aligned to the mean functional image, segmented and normalized to the Montreal Neurological Institute (MNI) atlas space using nonlinear registration, and the default tissue probability maps included with SPM12 (for a detailed discussion on spatial normalization see (Chen, Linke, Olson, Ibarra, Kinnear, et al., 2021)). The white matter (WM) and CSF probability maps obtained from segmentation of the structural image for each subject were thresholded at 0.95, eroded by 1 voxel, and applied to functional images to extract WM and CSF time courses, which were submitted to a principal component analysis with aCompCor (Behzadi et al., 2007) for subsequent nuisance regression. Functional images were directly registered to MNI space with the same nonlinear registration used for the structural images. To ensure that the findings were not due to group differences in motion, ASD and TD groups were matched, at the group level, on mean head motion indexed by root mean square of displacement (RMSD), calculated from rigid-body realignment of the raw data prior to TOPUP correction (see Table 3.1). RMSD was also included as a covariate in all imaging analyses.

Analytic strategy and functional connectivity analyses. In order to identify bias-free VC seeds for whole-brain functional connectivity analyses, an independent component analysis (ICA) was conducted to extract visual resting-state functional networks as follows. Preprocessed fMRI data (400 volumes per participant) from all participants (ASD and TD) were entered into group ICA using FSL's MELODIC (6.0), in order to generate maximally independent intrinsic functional networks. Twenty independent components were extracted, and each component's spatial distribution and time course were visually inspected by two raters. ICs were compared to the 20 canonical components generated by Smith et al. (2009) in an adult dataset, as well as to published pediatric templates (Manning, Courchesne, & Fox, 2013; Thornburgh et al., 2017; Chen et al., 2021). Four visual networks were identified and used here as primary networks of interest for VC

seed generation. FSL cluster was used to extract coordinates from peaks of the four visual networks, with a total of nine such peaks identified and used to generate nine 5mm-radius spherical seeds, which were anatomically labeled using the Harvard Oxford Cortical Atlas (Desikan et al., 2006) as following: pericalcarine cortex, bilateral lingual gyri, bilateral occipital poles, bilateral inferior lateral occipital cortices, and bilateral superior lateral occipital cortices (see Figure 3.1).

Mean timeseries extracted from each of the nine VC seeds were Pearson correlated with time series of all the voxels in the brain, and converted to z' connectivity maps using Fisher-z transform. These individual connectivity maps were entered into AFNI 3dttest++ analysis (R. W. Cox, 1996) as dependent variables to test (using Ordinary Least Squares [OLS]) for the diagnosis by developmental skills (Mullen ELC) interaction effect on VC functional connectivity, while controlling for in-scanner head motion (RMSD) and age. Given that the Mullen scores were left-censored (due to floor effects in the ASD group), tobit regression (designed to estimate linear relationships between variables when a dependent variable is censored) was used to test the robustness of significant clusters identified using AFNI3dttest++. To test whether VC connectivity was associated with autism symptoms among children with ASD, AFNI 3dttest++ analysis was repeated with ADOS-2 Calibrated Severity Score as an independent variable, while controlling for in-scanner head motion (RMSD) and age (ADOS-2 Calibrated Severity Score allows comparison of autism symptoms across different ADOS-2 Modules administered to children of different ages and with different levels of verbal abilities). A voxel-wise threshold for significance was set at $p < .005$, and the additional cluster-size thresholds (number of contiguous significant voxels) were determined using permutation testing with AFNI's 3dttest++ function and the "Clustsim" flag (R. W. Cox et al., 2017), for an overall False Discovery Rate (FDR) corrected clusterwise α of 0.05, per each seed-based analysis.

Results

Participant demographic, diagnostic, and behavioral characteristics are presented in Table 3.1. As expected, children in the ASD group had significantly lower developmental skills as measured with MSEL. No TD participants had a MSEL Early Learning Composite (ELC) score < 80, which is equivalent to no more than 1.3 SD below the normative mean. Floor effects were observed in the Mullen scores in some children with ASD (ELC = 49 in 10 children with ASD, see Supplemental Figure 3.S1).

Relationships between VC functional connectivity and early developmental skills: A significant diagnostic group by general developmental abilities (as measured by the Mullen ELC) interaction effect on functional connectivity was observed (see Table 3.2, Model A). Namely, diagnosis moderated the relationship between functional connectivity of the right inferior LOC and the left posterior superior temporal sulcus (pSTS) and general developmental abilities (Mullen ELC), independent of age, head motion, race, ethnicity, gestational age, and birthweight. As seen in Figure 3.2A, greater connectivity between these regions was associated with greater developmental abilities in the TD group (simple effect: $r = 0.65$; $p_{FDR} < 0.03$), while this relationship was absent in the ASD group. Sensitivity analyses using tobit regression parameter estimation (robust to left-centered data, to account for floor effects on Mullen scores in the ASD group) revealed that observed interaction effects remained statistically significant when tested using censored regression (diagnostic group by ELC interaction t-statistic = -4.57, $p < 0.001$).

Links between VC functional connectivity and ASD symptom severity: Results revealed that decreased functional connectivity between the left lingual gyrus and the pericalcarine cortex was significantly associated with higher ADOS-2 severity scores (or greater ASD

symptoms), independent of age, race, ethnicity, and head motion (see Table 3.2, Model B and Figure 3.2C).

Age-related effects and VC connectivity: A post-hoc analysis examining associations between VC connectivity and age revealed a significant diagnostic group by age interaction effect on VC functional connectivity, after correction for multiple comparisons using the same procedures as described above, and independent of race, ethnicity, gestational age, birthweight, and head motion (see Table 3.2, Model C). Namely, diagnosis moderated the relationship between age and connectivity of the right lingual gyrus and the right postcentral gyrus / somatosensory cortex, such that connectivity between these regions increased with age in the TD but not in the ASD group (see Figure 3.2b).

Discussion

To examine whether evidence of altered relationships between brain visual systems and cognitive abilities in ASD extends into early childhood, we investigated links between VC functional connectivity and developmental abilities in toddlers and preschoolers with ASD compared to age-matched TD children. We observed atypical relationships between connectivity of VC and developmental skills in young children with ASD. Most notably, stronger connectivity between right inferior lateral occipital cortex (LOC) and left posterior superior temporal sulcus (pSTS) was associated with more advanced developmental skills in TD toddlers and preschoolers (large effect size: r = 0.65), but not in children with ASD. Furthermore, weaker functional connectivity between two additional VC regions, lingual gyrus and pericalcarine cortex, was associated with greater autism symptoms among children with ASD.

Disrupted VC connectivity in the first years of life may be linked to atypical cognitive development in ASD. Our finding of the robust link between VC connectivity and more advanced

early cognitive developmental skills in the TD group highlights the critical role that the inferior LOC and pSTS cortices play in early child development. The pSTS plays a critical role in multisensory integration and biological motion perception, including perception of body and face motion (Beauchamp, Lee, Haxby, & Martin, 2003; Pelphrey, Morris, Michelich, Allison, & McCarthy, 2005; Redcay, 2008; Redcay et al., 2008; Saygin, Wilson, Hagler, Bates, & Sereno, 2004), all of which are key components of social perception and cognition (Yang, Rosenblau, Keifer, & Pelphrey, 2015). Given the central role that multisensory integration plays in cognitive development in the first years of life (Dionne-Dostie, Paquette, Lassonde, & Gallagher, 2015), the positive association between VC-pSTS connectivity and early developmental abilities observed among TD children is particularly informative.

In stark contrast, such relationship between VC-pSTS connectivity and early developmental skills was absent among young children with ASD. Atypical processing of visual information (including orienting, gaze, and joint attention) is evident as early as the first year of life in ASD [e.g., see (Apicella, Costanzo, & Purpura, 2020; Gammer et al., 2015; Gangi, Ibanez, & Messinger, 2014; Gangi et al., 2018; Tanner & Dounavi, 2021)] and is longitudinally predictive of poorer developmental abilities in later years (Kellerman et al., 2020; Thurm, Lord, Lee, & Newschaffer, 2007; Toth, Munson, Meltzoff, & Dawson, 2006). Atypical development of multisensory integration, including audio-visual integration, has also been associated with poorer language outcomes in children with ASD (Kissine, Bertels, Deconinck, Passeri, & Deliens, 2021; R. A. Stevenson et al., 2018; R. A. Stevenson et al., 2014). Thus, current findings suggest that the circuitry involved in multisensory integration may be disrupted in ASD, with potential impact on cognitive development in autism (given the robust link between the two in typical neurodevelopment).

Atypical connectivity involving pSTS has been reported in older, school-age children with ASD (Fishman, Keown, Lincoln, Pineda, & Müller, 2014; Hull, Jacokes, Torgerson, Irimia, & Van Horn, 2017) as well as in adults with ASD (Alaerts et al., 2015). Thus, our results extending this evidence of disrupted pSTS connectivity into early childhood contribute to our understanding of the lifespan trajectory of atypical neurodevelopment in ASD. Earlier findings by our group have provided evidence for a direct association between lower cognitive abilities (LCA) among adolescents with ASD and underconnectivity of pericalcarine VC and pSTS (Reiter et al., 2018). Since early developmental skills measured in the present study are known precursors of intellectual abilities (Girault et al., 2018), which are in turn predictive of broad life outcomes in ASD (Ben-Itzchak & Zachor, 2020), current results help delineate early atypical neurodevelopmental patterns in ASD that are likely involved in shaping long-lasting cognitive function, including LCA, related to long-term quality of life in people with autism. Furthermore, the links between weaker visual cortex connectivity (between the left lingual gyrus and pericalcarine cortex) and greater autism symptom severity observed in children with ASD suggest that the within-network integration in visual circuitry may be related to the emergence of autism symptoms early in life.

Finally, age-related effects on connectivity between visual cortex and sensorimotor regions were also atypical in this cohort of young children with ASD. Consistent with the results reported by Bruchhage et al. (2020), connectivity between right lingual gyrus and right somatosensory cortex increased with age in the TD group. However, this relationship was not observed in the ASD group. Somatosensory cortex integrates multisensory signals necessary for skilled coordinated movement (Borich, Brodie, Gray, Ionta, & Boyd, 2015), a developing skill which is being progressively mastered within this age-range. Absence of neurotypical increases in connectivity between visual and somatosensory cortex in preschoolers with ASD could underlie

commonly observed deficits in somatosensory (Cascio, 2010) and motor functions in ASD (Cascio, 2010; Mohd Nordin, Ismail, & Kamal Nor, 2021; Thompson et al., 2017). Thus, disruptions in circuitry involved in multisensory integration of visual input in ASD (i.e., atypical connectivity between visual and somatosensory cortices as well as between visual cortex and the pSTS) could impact development across multiple domains of functioning in ASD.

Limitations. A modest sample size, secondary to the known challenges associated with acquiring quality fMRI data in young children (Turesky, Vanderauwera, & Gaab, 2021), warrants that the current findings be interpreted with caution, pending future replication. Additionally, we note that the current study incorporated cross-sectional data, and that although results provide evidence for associations between age and development and VC connectivity, future research should attempt to test these hypotheses in longitudinal datasets. We also acknowledge that many socioeconomic variables, known to shape social and cognitive development and related to brain structure and functioning during the first 5 years of life (L. Olson, Chen, & Fishman, 2021), were not comprehensively modeled in the current study, and likely influence brain-behavior relationships identified in this study.

Conclusions. We found atypical associations of VC functional connectivity (with regions involved in multisensory integration) with both developmental abilities and age in toddlers and preschoolers with ASD. Furthermore, decreased VC functional connectivity was related to higher symptoms severity in this age range. We propose that a potential mechanism supporting cognitive development involving connectivity between lower-order visual regions and other sensory and multisensory circuits, which may be disrupted in ASD, could hinder the integration and processing of instrumental visual information such as (but not limited to) caregiver facial expressions, and contribute to developmental delays in ASD.

Table 3.1: Participant Characteristics

	ASD (n = 48)		TD (n = 36)		ASD vs. TD
	mean ± SD	**range**	**mean ± SD**	**range**	***p*-value**
Age (months)	40.3 ± 14.4	18 - 67	40.8 ± 15.5	16 - 65	0.88
Gestational Age* (weeks)	38.5 ± 2.2	31 - 43	39.6 ± 1.1	37 - 42	0.01
Birth Weight* (grams)	3237 ± 742	1755 - 5160	3504 ± 338	2863 - 4082	0.06
Ethnicity (Hispanic / Not Hispanic / Unknown)	20 / 14 / 14		8 / 26 / 2		
Race (White/ Black / Asian / Mixed or Multiple / Unknown)	23 / 1 / 2 / 11 / 11		25 / 3 / 2 / 5 / 2		
Gender M:F (Females %)	35:13 (27%)	--	22:14 (39%)	--	0.25
MSEL ELC	73.5 ± 20.3	49 - 112	104.8 ± 15.6	80 - 143	0.001
ADOS-2 CCS**	6.3 ± 2.2	2 - 10	N/A	N/A	--
Head motion (RMSD)	0.113 ± 0.035	0.046 - 0.197	0.107 ± 0.036	0.050 - 0.199	0.47

MSEL ELC = Mullen Scales of Early Learning Early Learning Composite (Standard Score); ADOS-2 CCS = Autism Diagnostic Observation Schedule, 2nd Edition, Calibrated Comparison Score; RMSD = root mean square displacement.

*Information on gestational age and birth weight was not available for 8 children with ASD and 2 TD children. Five children with ASD were born before 36 weeks of gestation (one at 31 weeks and four at 35 weeks).

**The ADOS-2 was administered only to participants in the ASD group.

Table 3.2: Effects of Diagnosis, Developmental Skills, and Autism Symptoms on Visual Cortex Functional Connectivity

Model A	**VC Seed**	**Cluster Size**	**MNI (x, y, z) Coordinates**	**p-value (cluster)**	**Peak Region**
Diagnostic Group by Mullen ELC Interaction	Right inferior LOC	1106	(-44, -66, 18)	***p* < 0.01***	Left posterior superior temporal sulcus (pSTS)

Regression Results: Right Inferior LOC – pSTS

Coefficient	**β Estimates**	**CI (95%)**	**T-Statistic**	**p-value**
Intercept	-0.11	-0.305 – 0.077	0.24	0.239
Dx	-0.06	-0.133 – 0.003	-1.91	0.060
ELC	0.002	0.001 – 0.004	3.78	<0.001
Dx by ELC (interaction)	1.115	0.920 – 1.311	11.37	**<0.001***
Age	-0.002	-0.004 – -0.0004	-2.49	0.015
RMSD	0.44	-0.271 – 1.168	1.24	0.219
Observations:	84			
R^2 / R^2 adjusted:	0.63 / 0.61			
F-statistic (*p*-value):	26.91 (< 0.0000)			

Model B	**VC Seed**	**Cluster Size**	**MNI (x, y, z) Coordinates**	**p-value (cluster)**	**Peak Region**
Autism symptoms (*ASD group only*)	Left lingual gyrus	683	(-2, -70, 6)	***p* < 0.03**	Pericalcarine cortex

Regression Results: Left lingual gyrus – Pericalcarine cortex

Coefficient	**β Estimates**	**CI (95%)**	**T-Statistic**	**p-value**
Intercept	0.52	0.199 – 0.842	3.27	0.002
ADOS-2	-0.49	-0.075 – -0.022	-3.67	**<0.001***
Age	0.001	-0.003 – 0.004	0.22	0.830
RMSD	0.14	-1.516 – 1.795	0.17	0.866
Observations:	48			
R^2 / R^2 adjusted:	0.25 / 0.20			
F-statistic (*p*-value):	4.88 (0.0052)			

Table 3.2: Effects of Diagnosis, Developmental Skills, and Autism Symptoms on Visual Cortex Functional Connectivity, continued

Model C	VC Seed	Cluster Size	MNI (x, y, z) Coordinates	p-value (cluster)	Peak Region
Diagnostic Group by Age Interaction	Right lingual gyrus	681	(62, -8, 12)	***p* < 0.03**	Right somatosensory cortex

Regression Table: Right lingual gyrus – Right Postcentral Gyrus

Coefficient	β Estimates	CI (95%)	T-Statistic	p-value
Intercept	-0.130	-0.2670 – -.0069	-1.89	0.062
Age	0.004	0.0015 – 0.0068	3.18	0.002
Dx	0.389	0.2334 – 0.5440	4.98	<0.000
Age by Dx (interaction)	-0.009	-0.0126 – 0.0054	-5.02	**<0.001***
RMSD	0.206	-0.5436 – 0.9561	0.55	0.586

Observations:	84
R^2 / R^2 adjusted:	0.25/0.21
F-statistic (*p*-value):	6.64 (0.0001)

All reported clusters were significant at the criterion threshold of alpha = .05 (p < .005, voxel-wise). Cluster size is reported in voxels (2-mm isotropic resolution). Peak regions were labeled using the Talairach and Harvard-Oxford cortical and subcortical atlases. VC = visual cortex, ELC = Early Learning Composite, ADOS-2 = Autism Diagnostic Observation Schedule, 2nd Edition, LOC = lateral occipital cortex. Effects reported were also significant after controlling for self-identified race, ethnicity, as well as gestational age and birthweight.

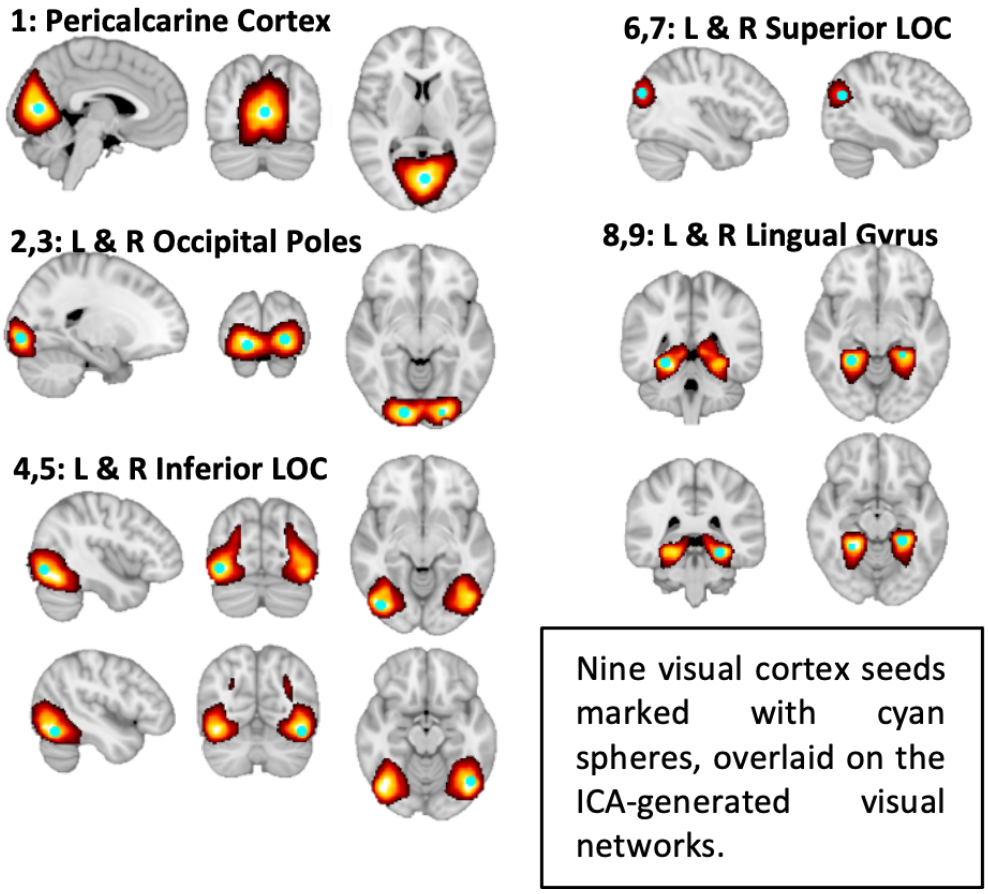

Figure 3.1: Visual cortex seeds (indicated with cyan spheres) overlaid on the ICA-generated visual networks. Images are *z* statistics thresholded at $z > 5.5$. Images are presented in the Montreal Neurological Institute (MNI) space, in neurological convention (with the left side of the brain represented on the left). MNI coordinates for the 9 visual cortex seeds are: **(1)** pericalcarine cortex (x = 2, y = –72, z = 8), **(2-3)** bilateral occipital poles (left: x = –16, y = –90, z = –10; right: x = 20, y = –90, z = –4), **(4-5)** bilateral inferior lateral occipital cortices (left: x = –42, y = –76, z = –8; right: x = 44, y = –64, z = –16), **(6-7)** bilateral superior lateral occipital cortices (left: x = –36, y = –80, z = 26; right: x = 44, y = –70, z = 24), and **(8-9)** bilateral lingual gyri (left: x = –26, y = –44, z = –10; right: x = 24, y = –38, z = –14)**.**

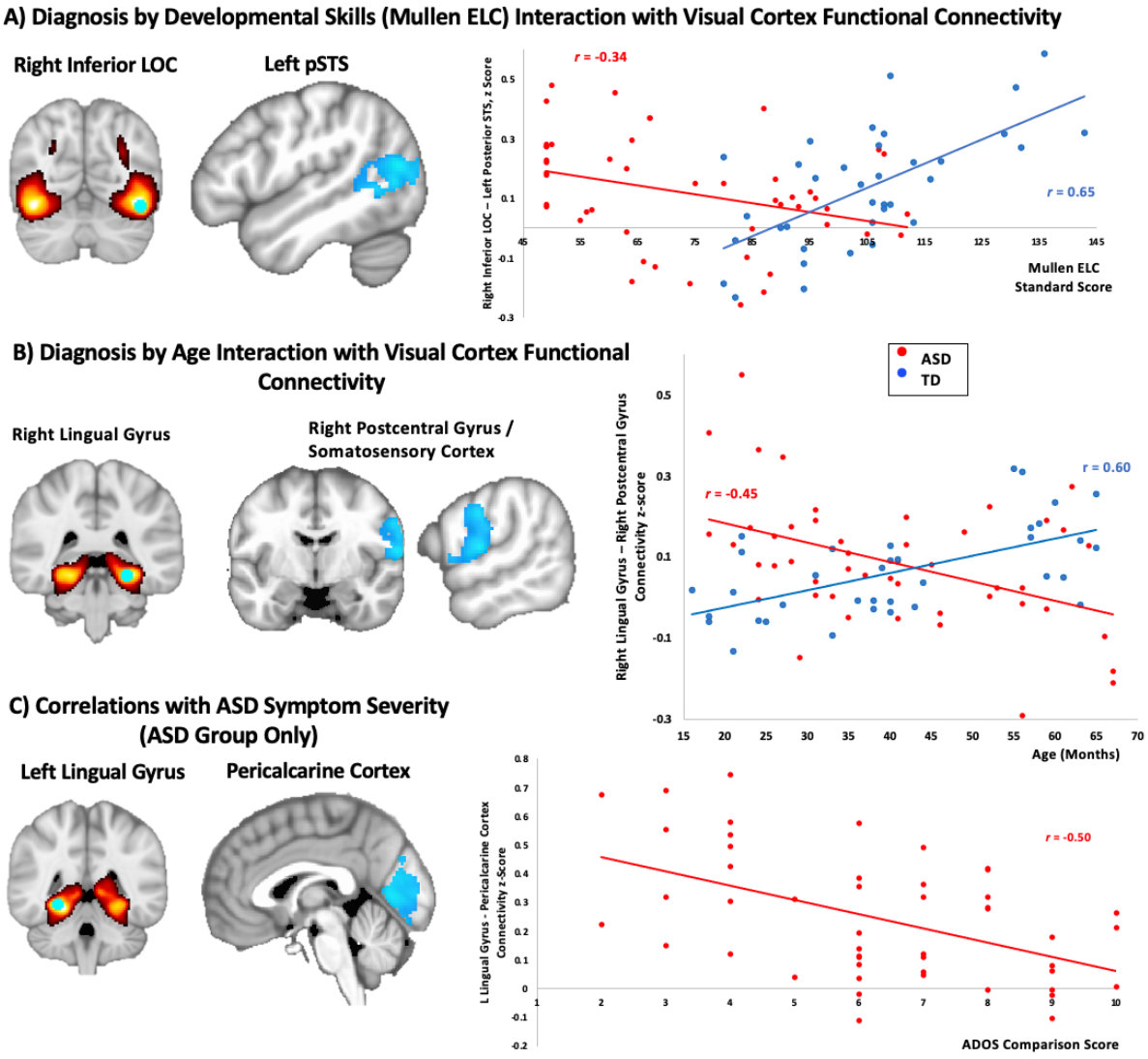

Figure 3.2: (A) Diagnosis by developmental skills interaction effect with visual cortex functional connectivity. (B) Diagnosis by age interaction effect with visual cortex functional connectivity. (C) Links between visual cortex functional connectivity and autism symptoms. In all panels, images are presented in neurological orientation (Left = Left), and VC seeds used in each analysis are indicated with cyan spheres.

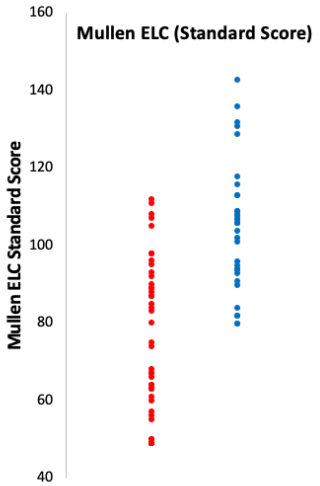

Supplemental Figure 3.S1: Developmental skills as measured by the Mullen Scales of Early Learning, in children with and without ASD. ASD = red; TD = blue; ELC = early learning composite.

Chapter 4 (Study 3): Relationships of cognitive abilities with visual cortex surface area and cortical thickness are atypical in children with autism spectrum disorder

Abstract

Autism Spectrum Disorder (ASD) is associated with a higher prevalence of intellectual disability and/or cognitive impairment, with over 50% of individuals exhibiting lower cognitive abilities (LCA). However, the neural substrates of general, verbal, and visuospatial cognitive abilities (CA) are poorly understood due to difficulties scanning individuals with ASD and LCA. Evidence from functional MRI studies suggests that connectivity of occipital visual cortex (VC) is atypically related to CA assessed with IQ measures in ASD. However, limited research has examined relationships between VC morphology (surface area [SA], cortical thickness [CT], and local gyrification index [LGI]) and CA in ASD. In particular, little is known about how visuospatial compared to verbal CA may relate to VC morphology. The current study compared SA, CT, and LGI of VC in 87 children and adolescents with ASD to a group of 87 age-, handedness-, gender-, and IQ-matched TD peers, and also tested for differences in the relationships between VC morphology and IQ measures across groups (age range 7-18 years, mean 12.7 years). Data (T1 anatomical scans) were collected at two different sites, inspected for quality, and harmonized to account for scanner-related noise. SA, CT, and LGI were calculated within occipital lobe VC regions of interest (ROIs; derived from Freesurfer), including left and right pericalcarine cortices, lingual gyri, lateral occipital cortices, and cuneus cortices. All analyses were carried out using regression (corrected for multiple comparisons), and controlled for age, scanning site, and (for SA analyses only) whole-brain SA. In the ASD group, a pattern of reduced SA and increased CT in VC ROIs was observed and was much more pronounced in the participants with ASD and lower FSIQ. We also observed a diagnosis by left lingual gyrus CT interaction effect on full scale IQ, which appeared to be primarily driven by verbal over non-verbal IQ scores in the ASD group.

In the TD group, relationships between CA and VC morphology were observed only in left lingual gyrus SA and CT. In contrast, the ASD group showed atypical relationships between SA and CT morphology across left lingual gyrus, left pericalcarine cortex, and left lateral occipital cortex. Results suggest that ASD with LCA may distinctly be associated with atypical morphology of occipital VC. Atypicalities in VC morphology may be more strongly related to verbal over visuospatial CA.

Introduction

There are large individual differences in general cognitive abilities (CA) among individuals diagnosed with Autism Spectrum Disorder (ASD). Approximately 30% of people with ASD are diagnosed with Intellectual disability (ID), with another 25% having intellectual functioning in the borderline range, and the remaining 45% having average or above average CA (HCA) (Maenner et al., 2020). General CA are important predictors of quality of life (QoL) in ASD (Lord, Brugha, et al., 2020), with higher CA associated with better QoL outcomes (Ben-Itzchak & Zachor, 2020; Lord, Brugha, et al., 2020), notwithstanding some exceptions in the realm of mental health (Edirisooriya, Dykiert, & Auyeung, 2021). Genetic markers and/or determinants of ID (in individuals with or without ASD) are not well understood (Chiurazzi et al., 2020; Rylaarsdam & Guemez-Gamboa, 2019), with only 7% of cases of ID being attributable to a single gene etiology and 60% of cases undergoing genomic sequencing showing an unresolved/unknown genetic etiology (Srivastava & Schwartz, 2014). Additionally, despite advances in genomics, specific genetic markers or molecular pathways that confer unique risk for ASD without co-occurring ID have not been identified (Iakoucheva et al., 2019; Myers et al., 2020).

Neuroimaging research on ASD from infancy through old age, has shown that autism is associated with atypical brain structure, functioning, and development (Girault & Piven, 2020; Hull, Jacokes, Torgerson, Irimia, & Van Horn, 2017; Molnar-Szakacs, Kupis, & Uddin, 2021; Song, Topriceanu, Ilie-Ablachim, Kinali, & Bisdas, 2021). However, conflicting findings and a lack of well-replicated neural biomarker/s of ASD are currently attributed predominantly to sample heterogeneity [e.g., in age (Uddin et al., 2013), sex (L. A. Olson et al., 2020), autism symptom severity (Reiter et al., 2021), or treatment history (Linke et al., 2017)], including heterogeneity in CA (Reiter et al., 2018). Considering that CA are likely a major source of heterogeneity in ASD,

the neural underpinnings (and developmental trajectories) of CA (and especially LCA) are remarkably understudied in neuroimaging research (Jack & Pelphrey, 2017). In most studies, mean sample IQ scores are skewed far above the ASD population average, with CA most commonly treated as a matching/nuisance variable in neuroimaging studies [as pointed out by S. A. Bedford et al. (2020)].

Several core impairments associated with ASD [e.g., deficits in face processing and atypical eye contact and gaze (American Psychiatric Association, 2013)] are related to atypical processing of visual information (Behrmann, Thomas, & Humphreys, 2006). Atypical functional activity and connectivity of visual cortex (VC) has been frequently reported in ASD (Chung & Son, 2020), with hyperactivity of VC suggested over a decade ago as a theory to explain behaviorally distinct cognitive profiles of ASD (Mottron, Dawson, Soulieres, Hubert, & Burack, 2006) (Gaffrey et al., 2007; Samson et al., 2012; Soulieres et al., 2009). However, this theory had until recently never been explored in LCA populations or in early childhood when VC function is established, significantly limiting its ecological validity. To address this gap, our group examined resting-state functional connectivity across sub-groups of children (ages 6-15 years) with ASD stratified by CA (including LCA and HCA sub-groups), finding that children with ASD+LCA exhibited under-connectivity of pericalcarine visual cortex with the posterior Superior Temporal Sulcus [pSTS, (Reiter et al., 2018)]. We then examined associations between resting-state functional connectivity of VC during natural nocturnal sleep and cognitive developmental abilities (precursors to IQ) in toddlers and preschoolers with ASD (ages 16-67 months), and found that a strong association between VC-pSTS connectivity and general developmental abilities observed in TD young children was absent in ASD peers (Reiter et. al, in progress). These studies provide evidence for a developmental hypothesis that LCA in ASD may be related to atypical connectivity

of visual circuitry that develops early in life and persists into childhood and adolescence [specifically involving connections between occipital visual cortex and higher-order processing regions involved in multisensory integration (Reiter et al., 2018; Reiter et al., in preparation]. Given these findings, it is likely that evidence of VC involvement in CA in ASD may also be found in neuroanatomy and brain morphology.

Individuals with ASD show widespread abnormalities in MRI-derived measures of neuroanatomy, including cortical thickness (CT), surface area (SA), and local gyrification index (LGI) [for example, see (Kohli et al., 2019; Laidi et al., 2019; Mensen et al., 2017; van Rooij et al., 2018)], with mixed findings in regards to regional patterns of differences (Pagnozzi et al., 2018). Research using machine learning suggests that VC CT (including right lingual gyrus, right pericalcarine and cuneus visual cortices) may be an important predictor of ASD symptom severity (Moradi, Khundrakpam, Lewis, Evans, & Tohka, 2017). Furthermore, a machine learning study (incorporating T1 weighted MRI and diffusion weighted imaging scans collected from preschoolers with and without ASD+LCA) reported that CT of right inferior occipital gyrus was the most prominent feature differentiating the two groups (Kim et al., 2022). However, relationships between morphology and CA may be atypical in ASD. Misaki, Wallace, Dankner, Martin, and Bandettini (2012) found diagnosis by CA (measured with full scale IQ) interactions on CT in adolescents with ASD, with higher CA related to higher CT in postcentral, superior temporal, and orbitofrontal regions in TD participants, and absence/reversal of this relationship in the ASD group. Notably, S. A. Bedford et al. (2020) also found significant diagnosis by CA interactions on CT in superior temporal, medial frontal, and occipital regions (in a large sample of individuals between the ages of 2-65 years), supporting the hypothesis that anatomical organization of VC may be atypically related to CA in ASD.

To our knowledge, no studies have investigated whether individuals with ASD show atypical relationships between neuroanatomy and morphology of VC and verbal and non-verbal CA, which may be especially important given the common gap between these two aspects of CA in individuals with ASD (Joseph, Tager-Flusberg, & Lord, 2002). As such, we aimed to investigate VC morphology (SA, CT, and LGI) in children and adolescents with autism, and the relation of these neural markers with general, verbal, and non-verbal CA in ASD, compared to typically developing peers. Broadly, we hypothesized that VC morphology (CT, SA, and LGI) would be atypical in ASD. Based on prior findings [e.g., see (S. A. Bedford et al., 2020; Misaki et al., 2012)], we further hypothesized that CT in VC would be greater in the ASD group. Due to dearth of prior research, specific a-priori hypotheses around expected interactions with CA could not be generated. In typical development, VC CT is associated with CA during childhood and adolescence, although the directionality of this relationship was appeared inconsistent across two major studies (Brouwer et al., 2014; Schmitt et al., 2019). The possibility that in the ASD group verbal CA would show an atypical association with VC CT compared to the TD group was also plausible. We note here that Kohli et al. (2019) also examined SA, CT, and LGI in a predominantly overlapping multi-site cohort of children with and without ASD and found lower LGI in left lingual gyrus in children with ASD (in a single-site cohort), as well a diagnosis by age interaction effects on VC LGI (albeit in different regions across two cohorts scanned at different research sites). However, Kohli et al. (2019) did not focus specifically on visual cortex (but took a whole-cerebrum vertex-wise approach), nor examined associations between SA, CT, and LGI and CA, which were the driving motivations of the current study.

Methods

Participants and clinical phenotyping: 174 children and adolescents (87 ASD, 87 TD), ages 7-18 years, were included in the current study. Data were drawn from a cohort participating in research at the Brain Development Imaging Laboratories at San Diego State University (SDSU), and from data collected at New York University (NYU), downloaded from the publicly available Autism Brain Imaging Data Exchange (ABIDE) dataset (Di Martino et al., 2017a; Di Martino et al., 2014). As noted, the combined dataset predominantly overlapped with the sample utilized in Kohli et al. (2019), with additional 10 female participants (5 ASD, 5 TD) added from the NYU dataset to improve matching on gender across scanning sites. However, while Kohli et al. (2019) analyzed data from two research sites separately, the current study combined data collected across the two scanning sites in order to increase statistical power so that we could better test for diagnosis by morphology interactions on cognitive abilities. Protocols were approved by the Institutional Review Boards governing each scanning site. In addition to informed assent provided by the participating minors, informed consent for participation (as well as consent to have the de-identified data shared with the ABIDE consortium) was provided by all caregivers. For the in-house SDSU sample, exclusionary criteria for children with ASD were presence of any known neurological or genetic disorders other than ASD (e.g., epilepsy, tuberous sclerosis, fragile X, Rett syndrome), and inclusion in the TD group further required a negative family history for ASD and/or other neuropsychiatric conditions. Inclusionary criteria for participants scanned at NYU, per the ABIDE website (http://fcon_1000.projects.nitrc.org/indi/abide/), required an absence of current chronic systemic medical conditions (besides ASD for participants with ASD), contraindications to MRI scanning, current pregnancy (confirmed by negative pregnancy test in female participants), and use of antipsychotic medication. TD participants were excluded if they

had a current psychiatric disorder as assessed with a clinician-administered semi-structured caregiver interviews. Clinical diagnosis of ASD was assigned using the Autism Diagnostic Observation Schedule-2nd edition (Lord et al., 2012), as well as the Autism Diagnostic Interview-Revised (Lord et al., 1994), supported by expert clinical judgement at each scanning site. CA were measured using the Wechsler Abbreviated Scale of Intelligence, Second Edition [WASI-II, (Wechsler, 1999)]. The ASD and TD groups were matched on age, sex, handedness, whole brain SA, total brain volume, and performance IQ, both across the full sample (Table 4.1) and across each individual scanning site (Tables 4.2-4.3).

MRI Data collection and image processing: High quality T1 MRI scans were collected from each participant at their respective scanning site. MRI scanning parameters and procedures are depicted in Supplemental Table 4.S1 for each scanning site. FreeSurfer version 5.3.0 was used to conduct a semi-automated cortical reconstruction on MRI images (Dale, Fischl, & Sereno, 1999; Fischl, Sereno, & Dale, 1999). Output from FreeSurfer was visually inspected slice-by-slice to identify inaccuracies in surface reconstruction as a part of quality assurance. T1 anatomical MRI scans with excessive artifacts (e.g., ghosting or ringing) were excluded. When inaccuracies were identified during quality control, they were corrected with white matter control points, reprocessed, subsequentially re-examined for accuracy, and only included in the analysis if they met standards for sufficient quality. After quality assessment, SA and CT measures were extracted [using methods also reported in (Kohli et al., 2019)] for 8 VC regions of interest (ROIs): bilateral pericalcarine cortex, lingual gyrus, lateral occipital cortex, and cuneus cortex (Desikan et al., 2006). LGI was derived for these ROIs using a FreeSurfer add-on (Schaer et al., 2008), that uses a 3D surface-based method to calculate the ratio of the pial surface (the cortical SA within the sulcal folds) relative to the amount of cortex on the cortical hull (the outer visible cortex). LGI was

calculated within a sphere of 25 mm radius around the pial surface vertex, for each vertex on the mesh. LGI has been previously validated as a reliable measure of local cortical gyrification compared to manual measurement (Schaer et al., 2012). In order to regress out potential systematic scanner differences, measures of SA, CT, and LGI within the 8 aforementioned VC ROIs were harmonized across the two scanning sites using ComBat (Fortin et al., 2018). Age-related signal was preserved during harmonization, as demonstrated by Fortin et al. (2018), due to the difference in mean age across the two scanning sites, with NYU participants being younger on average than SDSU participants (see Supplemental tables 1-2).

Analytic Strategy: We used linear regression to examine ASD v. TD group-level differences in anatomical measures and relationships (including IQ x diagnosis interactions) between CA and VC SA, CT, and LGI. We controlled for scanning site and age in all primary analyses. For SA models, whole-brain SA was also covaried.

Sensitivity analyses involving age, gender, race/ethnicity: To bolster confidence in inferences drawn based on tests for group differences and group by IQ interaction effects, we additionally tested for effects of age, gender, and race/ethnicity. A step-wise regression approach with backward elimination was implemented to test for age and gender effects. Regression models were initially tested with higher-order predictor terms (for gender: diagnosis by gender effects; for age: diagnosis by age effects, quadratic effects of age, and diagnosis by age^2 effects), and then re-tested with higher-order predictor terms that weren't statistically significant eliminated one at a time. Gender was coded as a binary categorical variable (female, male) due to the format of available data which were based on participant and/or caregiver self-report. Given the known bias of IQ tests, which in the United States unfairly advantage white individuals (Gould, 2008), we tested for race/ethnicity related bias in IQ scores and for relationships between race/ethnicity and

VC SA, CT, and LGI. Because self-reported data on race/ethnicity were not available in ABIDE (i.e., for the NYU data), race/ethnicity analyses were limited to the in-house (SDSU) cohort, with. race/ethnicity coded as a binary categorical variable (0 = Hispanic or Latino and/or any race except Caucasian/White; 1 = Caucasian/White and not Hispanic or Latino).

Type 1 error control: Correction for multiple comparisons was carried out using the Benjamini-Hochberg method, with a family-wise false discovery rate (FDR) threshold of 0.05, applied to two sets of analyses: one testing for group differences in SA, CT, and LGI, and the other testing for diagnosis by FSIQ interaction effects on these measures. Each family included 24 regression models: 8 VC ROIs x 3 anatomical measures, SA, CT, and LGI. We applied the same correction method to models establishing divergent validity (with age, gender, and race/ethnicity, counted as distinct families) and to follow-up analyses examining diagnosis by VIQ and PIQ interaction effects on VC morphology (with VIQ and PIQ models counted as distinct families) .

Results

Group differences in SA, CT, and LGI: As shown in Figure 4.1 and Table 4.4, decreased SA was detected in participants with ASD in comparison to the TD group for left pericalcarine cortex (p = 0.007, Cohen's d = -0.36) as well as for left lingual gyrus (p = 0.02, Cohen's d = -0.28). Additionally, the ASD group had greater CT in the bilateral lingual gyrus (left: p = 0.015, Cohen's d = 0.334; right: p = 0.024, Cohen's d = 0.318), as well as in the right pericalcarine cortex (p = 0.021, Cohen's d = 0.33; see Figure 4.2). These effects were not statistically significant after FDR correction. No significant differences in LGI were found for any of the VC ROIs. (Kohli et al., 2019)Effect sizes for group differences (ASD vs. TD) in SA, CT, and LGI are shown in Supplemental table S4.

Diagnosis by FSIQ interactions on SA, CT, and LGI: As shown in Figure 4.3 and Table 4.5, the relationship between FSIQ and left lingual gyrus CT differed significantly (after FDR correction) in the ASD group compared to the TD group ($p = 0.002$). Greater CT in left lingual gyrus was associated with higher FSIQ scores, independently of age, in the TD group ($r = 0.38$, $\beta = 0.003$, $p = 0.005$; see Supplemental table S8), whereas this relationship was absent in the ASD group. Diagnostic status also moderated the relationship between left pericalcarine cortex SA and FSIQ ($p = 0.047$, not significant after FDR correction). In this case, the TD group exhibited a negative relationship between SA and FSIQ, which was reversed in ASD (slope tests can be found in Supplemental tables S7 and S8). No diagnosis by FSIQ interaction effects on VC LGI were observed.

Follow-up analyses of interaction effects involving VIQ and PIQ: Left lingual gyrus CT was negatively associated with VIQ as well as PIQ in the ASD group, whereas the TD group showed positive associations between left lingual gyrus CT and VIQ as well as PIQ (VIQ interaction effect p-value = 0.003; PIQ interaction effect p-value = 0.014; effects were not significant after FDR correction). Additionally, relationships between bilateral pericalcarine cortex SA and VIQ (but not PIQ) differed in the ASD group (left hemisphere interaction effect p-value = 0.023, uncorrected; right hemisphere interaction effect p-value = 0.024, uncorrected). The ASD group exhibited positive relationships between bilateral pericalcarine cortex SA and VIQ, whereas the TD group showed negative relationships.

Divergent validity (effects of gender, age, and race/ethnicity): As shown in Supplemental table S5, there were no significant diagnosis by gender interactions on VC SA, CT, and LGI, even before FDR correction. Once the gender x diagnosis interaction term was omitted, gender predicted only left lingual gyrus LGI, with females showing lower LGI compared to males

(p = .037), and this was not a significant effect after FDR correction [critical p-value was 0.0021]). Supplemental table S6 depicts associations between age and VC morphology. No higher order predictor terms involving age (diagnosis by age, age^2, and diagnosis by age^2) were significantly associated with VC SA, CT, or LGI after FDR correction. Thus, these predictor terms were not modeled by the current study in main analyses. However, uncorrected, right pericalcarine cortex CT was associated with age^2 (p = 0.027; critical p-value threshold = 0.0021), and right lingual gyrus CT was predicted ($p < 0.05$, not significant after FDR correction) by age^2, diagnosis by age, and by diagnosis by age^2. Multiple relationships between age and SA, CT, and LGI (especially for CT) that were significant after FDR correction were observed after dropping higher-order predictor terms involving age. All CT ROIs were significantly predicted by age (with CT decreasing as age increased). Additionally, left lingual gyrus SA, and right lateral occipital cortex LGI were significantly and negatively associated with age. In terms of self-identified race and ethnicity, 87 of 102 participants at SDSU provided self-reported information on race and ethnicity. Of these 87 participants, 51 identified as White and not Hispanic (25 ASD, 26 TD). Thirty-six participants self-identified as Hispanic and/or Not White (19 ASD, 17 TD). Race/ethnicity did not significantly predict FSIQ (p = 0.52), VIQ (p = 0.12) or PIQ (p = 0.572) in the SDSU cohort. Moreover, beta coefficients from regression tests indicated that group averages in IQ scores were similar across groups, with White / non-Hispanic participants scoring 1.98 FSIQ points higher (on the standard score scale), 4.76 VIQ points higher, and 2 PIQ points lower compared to participants identifying as Hispanic and/or not White. Whiteness was also not significantly associated with SA, CT, or LGI, even before correcting for multiple comparisons. At most, whiteness explained 4% of the variance in the SA, CT, and LGI.

Post-hoc exploratory analysis in samples restricted based on FSIQ: As a qualitative illustration for the pattern of interactions observed in the current study, we conducted a post-hoc illustrative examination of effect sizes for differences in ASD and TD group means in VC SA, CT, and LGI in samples differing in IQ. Specifically, we re-calculated all effect size statistics when the full sample was divided into subsamples including only participants with FSIQ scores $\leq$ 100 vs. those with FSIQ scores > 100. The ASD and TD samples with FSIQ $\leq$ 100 included 25 ASD and 21 TD participants, matched on age (p = 0.23), in addition to handedness (p = 0.20), gender (p = 0.68), performance IQ (p = 0.48), and scanning site (p = 0.64). The ASD and TD samples with FSIQ > 100 were larger (57 ASD, 65 TD), and matched on age (p = 0.25), handedness (p = 0.42), gender (p = 0.76), FSIQ (p = 0.79), and scanning site (p = 0.63). Effect sizes (Hedge's g) calculated based on these two subsamples, as well as for the full sample (unrestricted FSIQ), are depicted in Supplemental Table 4.S2 and Figure 4.4. Examination of the effect sizes for group differences in anatomical measures revealed that effect sizes were notably larger when only individuals with FSIQ $\leq$ 100 were included. Specifically, this was observed for pericalcarine cortex SA and CT (bilaterally), lingual gyrus SA and CT (bilaterally), lateral occipital cortex CT (bilaterally), as well as LGI (left), and cuneus cortex SA (right) as well as CT (bilaterally).

Discussion

The current study investigated differences of SA, CT, and LGI in the visual cortex of children and adolescents with ASD as compared to TD peers, as well as relationships between these neural markers and CA as measured with IQ in these groups. (Kohli et al., 2019)A diagnosis by left lingual gyrus CT interaction with FSIQ provided evidence of differing brain-behavior relationships involving CA in ASD. Post-hoc examination of VC morphology in ASD and TD in groups stratified by FSIQ suggested that group-level differences (reduced SA and increased CT in

ASD) may be driven predominantly by individuals with ASD and LCA. Results were largely consistent with those reported in Kohli et al. (2019) which used a largely overlapping data sample but differed in analytic approach and focus. No statistically significant group differences for visual cortex SA or CT were observed after FDR correction in either study. Notably, whereas we found no differences in LGI across groups (when combining the SDSU and NYU samples), Kohli et al. (2019) did find significantly decreased left lingual gyrus LGI in ASD in the SDSU research cohort. However, this finding was not replicated for the NYU cohort in Kohli et al. (2019). As such, the current study's null findings for group differences in LGI when combining the SDSU and NYU data are not contradictory with findings presented in Kohli et al. (2019).

Atypical relationships between morphology of VC and CA in children and adolescents with ASD. After peaking at around the age of two years (following rapid increases in CT that begin prenatally), CT slowly decreases during later childhood and adolescence (Bethlehem et al., 2022). This neurodevelopmental trend was observed in the current study, independently of diagnostic status. Notably, independent of age, a positive correlation (of medium effect-size) between left lingual gyrus CT and CA as measured with FSIQ was observed in the TD but not in the ASD group. The positive association between VC CT and IQ has previously been shown in neurotypical children in this age range, when CT is gradually decreasing with age (Schmitt et al., 2019; Shaw et al., 2006), although negative correlations between these variables within the same age range have also been reported (Brouwer et al., 2014). The observed lack of the relationship between VC CT and CA in the ASD group suggests that the atypical neuroanatomy of visual cortex may be implicated in CA in ASD, at least through late adolescence. CT is thought to be influenced by various neural variables including synaptic density, synaptic pruning, and intracranial myelination (Tahedl, 2020). At the gray/white matter boundary, increases in myelination may

result in artificially lower CT estimates calculated based on T1 weighted MRI scans (Gogtay & Thompson, 2010; Natu et al., 2019)]. The process of myelination is also associated with CA during childhood [e.g., see (Fields, 2010; Nagy, Westerberg, & Klingberg, 2004)]. As such, it is not possible to determine which specific biological processes may account for the atypical relationships between CA and CT in ASD observed, especially given that increases in myelination of visual cortex may be expected during the age range studied here (Miller et al., 2012). If myelination were the predominant mechanism explaining associations between CT and CA, we would expect a negative, rather than positive, association.

Visual cortex neuroanatomy and verbal and non-verbal CA in the TD and ASD groups: Exploratory analyses revealed that the observed diagnosis by CA interaction effect on left lingual gyrus CT was primarily driven by VIQ and not PIQ (as could be expected given the role of occipital cortex in visual processing; see Figure 4.3, bottom panels), as were the subthreshold interaction effects on pericalcarine cortex and left lingual gyrus SA. These results suggest that phenotypic relationships between CA and morphology in ASD may be driven by the verbal rather than visuospatial CA. Although somewhat counterintuitive given analyses centered on VC, these results are consistent with what has been observed in TD children and adolescents by Brouwer et al. (2014), who additionally noted that correlations between VC morphology and CA were more widespread in the left hemisphere, as also observed in the current study. It is also noteworthy that, unlike in the TD group, where relationships between VC morphology and CA were confined to the left lingual gyrus (additionally including a negative correlation between left lingual gyrus SA and FSIQ), in the ASD group relationships were detected in pericalcarine cortex as well as lateral occipital cortex (see Supplemental tables 7-8). While pericalcarine cortex comprises primary or striate visual cortex (Prasad & Galetta, 2011), lateral occipital cortex is involved in visual object

perception and motion processing, and is part of extrastriate cortex (Malikovic et al., 2016). Results suggest that the neural substrates of CA in ASD may be atypical, with both striate and extrastriate visual regions implicated.

It is currently unknown why some individuals with ASD exhibit clinically significant cognitive impairments and others do not. While it is known that genetics confer risk for ASD *and* ID, with some specific mutations identified as determinants of ID in ASD, the majority of variance remains unexplained (Chiurazzi et al., 2020; Rylaarsdam & Guemez-Gamboa, 2019). Previous research has shown that in late childhood and adolescence, strength of relationships between VC (left lingual gyrus, cuneus, and middle occipital gyrus) CT and CA in typical neurodevelopment is mediated by genetic factors (Brouwer et al., 2014; Schmitt et al., 2019). Thus, it is plausible that VC CT could be a biomarker for LCA in ASD. However, much additional research is warranted to disentangle such complex relationships.

More pronounced effects of diagnosis on VC SA and CT in participants with ASD and lower IQ. Diagnosis by IQ interactions with VC morphology emerged as the most striking findings of the current study. Although group differences or main effects of diagnosis on VC SA and CT were originally hypothesized, the results revealed no significant group differences after FDR correction, although an overall pattern of reduced VC SA and increased VC CT (uncorrected effects) was observed in ASD. There are several potential explanations for this result, the simplest one being that there may truly be no significant differences between VC SA and CT in ASD during late childhood and adolescence. However, observed atypical relationships between CA and VC SA and CT in ASD (even those not meeting corrected statistical significance thresholds) suggests that heterogeneity in CA in ASD could mask group differences when samples include individuals with a broad range of CA. Indeed, when participants were separated into higher and lower CA

subgroups, effect sizes for differences in means across ASD and TD were much more pronounced in the ASD subgroup with FSIQ ≤ 100 (as shown in Figure 4.4), while between-group differences for most VC ROIs were smallest in in the ASD subgroup with FSIQ > 100. This is noteworthy because many participants with ASD in neuroimaging studies have IQ scores > 100. Current results suggest that this may lead to higher likelihood of type 2 errors in studies of HCA individuals with ASD. In view of the high levels of variability in the ASD population (including in CA), even larger samples than available for the current study may be necessary to detect differences from TD comparison samples, as well as differences amongst subgroups within the ASD population.

A need for more research in individuals with ASD and LCA. Deliberate efforts to include ASD participants with LCA are critical despite inherent challenges in collecting data from this population, as results suggest that differences in morphology related to CA in ASD may be masked if the majority of the sample consists of those with average or above-average CA. The expense and challenges associated with collecting MRI data mean that neuroimaging studies of ASD are inherently underpowered, especially given the very high dimensionality of MRI data and the complexity of neural development and functioning. Thus, a potentially effective strategy may be to tailor experimental designs to including more homogeneous ASD cohorts with respect to CA, with deliberate efforts made to represent the full range of the IQ spectrum in autism research. While stratifying the ASD group based on the FSIQ of below or above 100 was suboptimal and not directly capturing the LCA range of CA, it enabled detection of certain patterns not evident when viewing the unstratified full sample. Compromises such as this may be necessary as a first step, while methods enabling easier data collection from LCA participants [e.g., see (Nordahl et al., 2016)] continue to be refined. Multi-site cohorts, use of data harmonization across different sites, and increased cross-group collaboration may also be necessary.

Future research directions. Prior studies have shown that dynamics of changes in brain structure (e.g., longitudinal changes) may be more related to CA than cross-sectional point-estimates of SA, CT, and LGI (Burgaleta, Johnson, Waber, Colom, & Karama, 2014; Schnack et al., 2015; Shaw et al., 2006). Thus, it is possible that atypical relationships between VC morphology and CA would be even better observed longitudinally using within-subjects experimental designs capturing the rate of change in cortical thickness and folding. Furthermore, some have postulated that differences in visual abilities in ASD may arise from atypical function and structure of higher-level cognitive areas and functions, that lead to altered top-down processes (Hadjikhani et al., 2004). Indeed, we reported (Reiter et al., 2018; Reiter et al., in preparation) that connectivity between VC and pSTS was atypically associated with CA in ASD. Additionally, much of the research published on TD populations suggests that relationships between CA and morphology involve higher order and frontal regions (Brouwer et al., 2014; Burgaleta et al., 2014; Narr et al., 2007; Schmitt et al., 2019; Shaw et al., 2006). Thus, future research should incorporate longitudinal designs and consider investigating morphology of higher-order processing regions as well as other sensory-related (e.g., auditory) cortices.

Limitations: Many underlying developmental mechanisms [see (Stiles & Jernigan, 2010)] influence neuroanatomy (Lerch et al., 2017), thus, specific neurobiological processes implicated in the observed atypical relationships between CT and CA in ASD remain unclear. Secondly, although the current study provided evidence that relationships between VC morphology and CA may differ in children with ASD compared to TD peers, such relationships may vary within the heterogeneous ASD population. Indeed, research by Balardin et al. (2015) has shown that adults with ASD exhibited different relationships between lingual gyrus CT and Verbal IQ depending on childhood history of language delay. We acknowledge as a limitation that we were unable (due to

data availability) to adequately examine differences related to treatment history, socioeconomic status, and history of developmental delays. Furthermore, data on self-identified race and ethnicity were not available for participants scanned at NYU. Importantly, although we made a deliberate effort to include as many participants as possible with ASD and LCA, the IQ distribution included in the current study still was not representative of the broader ASD population as a whole, and was skewed towards those with average or above-average FSIQ. Due to practical constraints of sample size, it was impossible to contrast a group of participants with FSIQ < 85, or < 70 with a comparison group. Although results suggest that atypicalities in VC SA and CT may be more pronounced at lower ranges of the IQ spectrum in ASD, future research is needed. Additionally, we acknowledge the wide age range included in the current study as a potential limitation given that VC cortical morphology does change during these ages.

Conclusions: Children and adolescents with ASD show atypical relationships between VC CT and CA. Differences in VC SA and CT in ASD may be more pronounced in individuals with lower CA, and may even be a distinct neural difference characterizing this group. Stratification by CA and inclusion of more participants with ASD and LCA in neuroimaging research may be critical to understanding potential atypical roles of VC in cognitive functioning in ASD. Experimental designs that deliberately focus on more homogeneous samples of participants with ASD, but with cognitive ability profiles that represent those exhibited by individuals in the broader ASD population (e.g., groups with lower and higher cognitive abilities) may be an effective strategy for revealing the neural substrates of CA in autism.

Acknowledgements: Chapter 4, in full, is currently being prepared for publication. Reiter, Maya Anne; Kohli, Jiwandeep; Martindale, Ian; Hau, Janice; Fishman, Inna; Carper, Ruth; Müller, Ralph-Axel. “Relationships of cognitive abilities with visual cortex surface area and cortical

thickness are atypical in children with autism spectrum disorder". The dissertation author was the primary investigator and author of this paper.

Table 4.1: Demographics and Matching for Total Sample

	ASD (n = 87)				TD (n = 87)				
	Mean	SD	Min	Max	Mean	SD	Min	Max	p *
Age	12.68	2.83	7.00	18.58	12.73	2.80	6.90	17.7	0.910
FSIQ	104.70	15.15	66	141	107.75	12.04	79	136	0.146
VIQ	101.66	15.49	56	147	107.98	11.34	80	132	0.003
PIQ	106.68	16.82	53	140	106.26	13.69	62	137	0.860
Males	n = 71; 81.6%				n = 74; 85%				0.541
Right Handed	n = 70; 80%				n = 67; 81.6%				0.578

*t-tests were used to calculate and report statistical differences across groups for age and IQ; Chi-squared tests were used to compare groups for matching on gender and handedness.

Table 4.2: Demographics and Matching from In-House Sample (SDSU)

	ASD (n = 51)				TD (n = 51)				
	Mean	SD	Min	Max	Mean	SD	Min	Max	p
Age	13.39	2.67	7.00	17.80	13.50	2.75	6.90	17.70	0.36
FSIQ	105.96	16.89	66.00	141.00	105.92	10.74	79.00	130.0	0.95
VIQ	102.69	17.65	56.00	147.00	105.80	8.78	87.00	126.0	0.23
PIQ	107.63	18.14	53.00	140.00	105.37	13.98	62.00	134.0	0.52
Males	n = 40; 78%				n = 43; 84%				0.44
Right Handed	n = 45; 88%				n = 44; 86%				0.76

t-tests were used to calculate and report statistical differences across groups for age and IQ. Chi-squared tests were used to compare groups for matching on gender and handedness.

Table 4.3: Demographics and Matching from NYU Sample

	ASD (n = 36)				TD (n = 36)				
	Mean	SD	Min	Max	Mean	SD	Min	Max	p
Age	11.67	2.74	7.15	18.58	11.63	2.47	7.26	16.31	0.94
FSIQ	102.92	12.04	76.00	132.00	110.33	13.23	80.00	136.00	0.02
VIQ	100.19	11.60	79.00	139.00	111.06	13.61	80.00	132.00	**< 0.001***
PIQ	105.33	14.64	72.00	129.00	107.53	13.17	79.00	133.00	0.51
Males	n = 31; % = 86				n = 31; % = 86				1.00
Right Handed	n = 25; 69%				n = 27; 75%				0.60

t-tests were used to calculate and report statistical differences across groups for age and IQ
Chi-squared tests were used to compare groups for matching on gender and handedness.
***Effects for which $p < 0.05$ are depicted in **bold**.

Table 4.4: ASD vs. TD Group Differences in SA, CT, and LGI (controlling for age)

ROI	Beta	SE	t	p	ASD (M)	ASD (SD)	TD (M)	TD (SD)	d	95% CI	
Pericalcarine Left (SA)	-91.90	33.37	-2.75	**0.007***	1374.2	248.2	1464.8	245.9	0.37	-157.769	-26.031
Pericalcarine Right (SA)	-39.07	35.70	-1.09	0.275	1565.4	297.9	1603.3	249.0	0.14	-109.534	31.404
Pericalcarine Left (CT)	0.05	0.03	1.85	0.066	1.9	0.2	1.8	0.2	0.28	-0.003	0.106
Pericalcarine Right (CT)	0.06	0.03	2.33	**0.021***	1.8	0.2	1.8	0.2	0.34	0.009	0.108
Pericalcarine Left (LGI)	0.01	0.03	0.45	0.653	3.0	0.2	3.0	0.2	0.07	-0.049	0.078
Pericalcarine Right (LGI)	0.01	0.03	0.30	0.761	3.1	0.2	3.1	0.2	0.05	-0.055	0.074
Lingual Left (SA)	-130.07	54.77	-2.38	**0.019***	3169.5	459.2	3294.6	435.1	0.28	-238.187	-21.956
Lingual Right (SA)	-75.32	49.85	-1.51	0.133	3233.2	437.8	3304.6	409.9	0.17	-173.723	23.082
Lingual Left (CT)	0.05	0.02	2.46	**0.015***	2.3	0.1	2.2	0.2	0.34	0.010	0.087
Lingual Right (CT)	0.05	0.02	2.28	**0.024***	2.3	0.2	2.2	0.2	0.32	0.007	0.097
Lingual Left (LGI)	0.00	0.03	-0.07	0.946	2.9	0.2	2.9	0.2	0.01	-0.054	0.050
Lingual Right (LGI)	0.00	0.03	0.08	0.935	3.0	0.2	3.0	0.2	0.01	-0.052	0.056
Lateral Occipital Left (SA)	12.46	70.16	0.18	0.859	5265.4	670.8	5247.6	594.9	0.03	-126.044	150.958
Lateral Occipital Right (SA)	-74.22	78.37	-0.95	0.345	5064.3	687.4	5132.6	615.4	0.11	-228.934	80.499
Lateral Occipital Left (CT)	0.04	0.02	1.87	0.064	2.3	0.1	2.3	0.1	0.27	-0.002	0.076
Lateral Occipital Right (CT)	0.04	0.02	1.42	0.156	2.4	0.2	2.4	0.2	0.21	-0.013	0.082
Lateral Occipital Left (LGI)	0.02	0.02	0.75	0.453	2.8	0.1	2.8	0.1	0.12	-0.024	0.053
Lateral Occipital Right (LGI)	0.01	0.02	0.50	0.620	2.8	0.1	2.7	0.1	0.08	-0.030	0.051
Cuneus Left (SA)	-40.67	29.06	-1.40	0.164	1551.4	231.0	1589.9	240.1	0.16	-98.047	16.703
Cuneus Right (SA)	-42.72	29.40	-1.45	0.148	1641.2	269.4	1681.5	219.7	0.17	-100.757	15.309
Cuneus Left (CT)	0.03	0.03	0.99	0.325	2.1	0.2	2.1	0.2	0.15	-0.026	0.079
Cuneus Right (CT)	0.01	0.03	0.45	0.655	2.1	0.2	2.1	0.2	0.07	-0.041	0.065
Cuneus Left (LGI)	0.00	0.03	0.07	0.947	3.1	0.2	3.1	0.2	0.01	-0.061	0.065
Cuneus Right (LGI)	0.03	0.03	0.83	0.407	3.2	0.2	3.2	0.2	0.13	-0.038	0.093

SA = surface area; CT = cortical thickness; LGI = local gyrification index; SE = standard error of the difference in means; M = mean; SD = standard deviation; d = Cohen's d; CI = confidence interval. *****Effects for which $p < 0.05$ are depicted in **bold**.

Table 4.5: Diagnosis by FSIQ, VIQ, PIQ interactions on VC SA, CT, and LGI

ROI (Analysis)	Hemisphere (SA/CT/LGI)	beta	SE	t	p	95% CI	
Pericalcarine Cortex (Group by FSIQ Interaction)	Left (SA)	5.10	2.60	2.00	**0.047***	0.060	10.100
	Right (SA)	4.60	2.70	1.68	0.095	-0.800	10.000
	Left (CT)	0.00	0.00	-0.95	0.343	-0.010	0.000
	Right (CT)	0.00	0.00	-0.36	0.721	0.000	0.000
	Left (LGI)	0.00	0.00	1.11	0.269	0.000	0.010
	Right (LGI)	0.00	0.00	1.02	0.310	0.000	0.010
Pericalcarine Cortex (Group by VIQ Interaction)	Left (SA)	6.08	2.60	2.30	**0.023***	0.870	11.300
	Right (SA)	6.45	2.80	2.28	**0.024***	0.870	12.000
	Left (CT)	0.00	0.00	-1.64	0.103	-0.010	0.000
	Right (CT)	0.00	0.00	-0.84	0.400	-0.010	0.000
	Left (LGI)	0.00	0.00	1.08	0.284	0.000	0.010
	Right (LGI)	0.00	0.00	0.30	0.762	0.000	0.010
Pericalcarine Cortex (Group by PIQ Interaction)	Left (SA)	2.30	2.30	1.02	0.309	-2.150	6.740
	Right (SA)	1.67	2.40	0.69	0.49	-3.090	6.430
	Left (CT)	0.00	0.00	-0.23	0.816	0.000	0.000
	Right (CT)	0.00	0.00	0.02	0.980	0.000	0.000
	Left (LGI)	0.00	0.00	0.82	0.416	0.000	0.010
	Right (LGI)	0.00	0.00	1.36	0.176	0.000	0.010
Lingual Gyrus (Group by FSIQ Interaction)	Left (SA)	7.98	4.20	1.91	0.057	-0.250	16.200
	Right (SA)	6.73	3.80	1.76	0.08	-0.810	14.300
	Left (CT)	0.00	0.00	-3.17	**0.002**[a]	-0.010	0.000
	Right (CT)	0.00	0.00	-1.38	0.169	-0.010	0.000
	Left (LGI)	0.00	0.00	0.39	0.696	0.000	0.000
	Right (LGI)	0.00	0.00	0.92	0.358	0.000	0.010
Lingual Gyrus (Group by VIQ Interaction)	Left (SA)	7.56	4.40	1.74	0.084	-1.040	16.200
	Right (SA)	5.59	4.00	1.40	0.162	-2.270	13.500
	Left (CT)	0.00	0.00	-3.06	**0.003***	-0.010	0.000
	Right (CT)	0.00	0.00	-1.83	0.069	-0.010	0.000
	Left (LGI)	0.00	0.00	0.52	0.604	0.000	0.010
	Right (LGI)	0.00	0.00	0.16	0.869	0.000	0.000

FSIQ = Full Scale IQ; VIQ = Verbal IQ; PIQ = Performance IQ; SA = surface area; CT = cortical thickness; LGI = local gyrification index; SE = standard error of the coefficient; CI = confidence interval.*Effects for which $p < 0.05$ are depicted in **bold**. [a]Statistically significant effect after FDR correction.

Table 4.5: Diagnosis by FSIQ, VIQ, PIQ interactions on VC SA, CT, and LGI, continued

ROI (Analysis)	Hemisphere (SA/CT/LGI)	beta	SE	t	p	95% CI	
Lingual Gyrus (Group by PIQ Interaction)	Left (SA)	0.00	0.00	0.16	0.869	0.000	0.000
	Right (SA)	5.25	3.30	1.57	0.118	-1.340	11.800
	Left (CT)	0.00	0.00	-2.49	**0.014***	-0.010	0.000
	Right (CT)	0.00	0.00	-0.75	0.454	0.000	0.000
	Left (LGI)	0.00	0.00	0.30	0.761	0.000	0.000
	Right (LGI)	0.00	0.00	1.37	0.172	0.000	0.010
Lateral Occipital Cortex (Group by FSIQ Interaction)	Left (SA)	9.97	5.40	1.86	0.064	-0.600	20.500
	Right (SA)	9.95	6.00	1.66	0.1	-1.920	21.800
	Left (CT)	0.00	0.00	-0.90	0.371	0.000	0.000
	Right (CT)	0.00	0.00	-0.91	0.362	-0.010	0.000
	Left (LGI)	0.00	0.00	-0.03	0.980	0.000	0.000
	Right (LGI)	0.00	0.00	0.62	0.533	0.000	0.000
Lateral Occipital Cortex (Group by VIQ Interaction)	Left (SA)	7.30	5.60	1.30	0.195	-3.770	18.400
	Right (SA)	3.93	6.30	0.62	0.533	-8.480	16.300
	Left (CT)	0.00	0.00	-0.95	0.341	0.000	0.000
	Right (CT)	0.00	0.00	-0.91	0.362	-0.010	0.000
	Left (LGI)	0.00	0.00	-0.08	0.938	0.000	0.000
	Right (LGI)	0.00	0.00	-0.37	0.715	0.000	0.000
Lateral Occipital Cortex (Group by PIQ Interaction)	Left (SA)	9.12	4.70	1.95	0.053	-0.120	18.400
	Right (SA)	8.70	5.20	1.66	0.099	-1.650	19.100
	Left (CT)	0.00	0.00	-0.70	0.485	0.000	0.000
	Right (CT)	0.00	0.00	-0.82	0.416	0.000	0.000
	Left (LGI)	0.00	0.00	-0.04	0.966	0.000	0.000
	Right (LGI)	0.00	0.00	1.29	0.198	0.000	0.000
Cuneus Cortex (Group by FSIQ Interaction)	Left (SA)	1.10	2.20	0.49	0.625	-3.340	5.530
	Right (SA)	1.80	2.30	0.79	0.43	-2.680	6.270
	Left (CT)	0.00	0.00	-0.13	0.900	0.000	0.000
	Right (CT)	0.00	0.00	-0.27	0.791	0.000	0.000
	Left (LGI)	0.00	0.00	1.02	0.308	0.000	0.010
	Right (LGI)	0.00	0.00	1.10	0.271	0.000	0.010

FSIQ = Full Scale IQ; VIQ = Verbal IQ; PIQ = Performance IQ; SA = surface area; CT = cortical thickness; LGI = local gyrification index; SE = standard error of the coefficient; CI = confidence interval.*Effects for which $p < 0.05$ are depicted in **bold**. [a]Statistically significant effect after FDR correction.

Table 4.5: Diagnosis by FSIQ, VIQ, PIQ interactions on VC SA, CT, and LGI, continued

ROI (Analysis)	Hemisphere (SA/CT/LGI)	beta	SE	t	p	95% CI	
Cuneus Cortex (Group by VIQ Interaction)	Left (SA)	1.75	2.30	0.75	0.454	-2.860	6.360
	Right (SA)	2.89	2.40	1.23	0.222	-1.760	7.530
	Left (CT)	0.00	0.00	-0.42	0.676	-0.010	0.000
	Right (CT)	0.00	0.00	-0.23	0.816	0.000	0.000
	Left (LGI)	0.00	0.00	0.91	0.362	0.000	0.010
	Right (LGI)	0.00	0.00	0.61	0.544	0.000	0.010
Cuneus Cortex (Group by PIQ Interaction)	Left (SA)	0.17	2.00	0.09	0.932	-3.710	4.050
	Right (SA)	0.96	2.00	0.48	0.63	-2.960	4.890
	Left (CT)	0.00	0.00	0.26	0.797	0.000	0.000
	Right (CT)	0.00	0.00	-0.36	0.720	0.000	0.000
	Left (LGI)	0.00	0.00	0.65	0.518	0.000	0.010
	Right (LGI)	0.00	0.00	1.10	0.273	0.000	0.010

FSIQ = Full Scale IQ; VIQ = Verbal IQ; PIQ = Performance IQ; SA = surface area; CT = cortical thickness; LGI = local gyrification index; SE = standard error of the coefficient; CI = confidence interval.*****Effects for which $p < 0.05$ are depicted in **bold**. [a]Statistically significant effect after FDR correction.

Supplemental Table 4.S1: Anatomical and resting state scan parameters by site

Parameters	**NYU**	**SDSU**
Scanner	Siemens Allegra 3T	GE MR750 3T
Head coil	8Ch	8Ch
TR (repetition time in ms)	2530	8.136
TE (echo time in ms)	3.25	3.172
Flip Angle	7	8
Field of view (mm)	256x256	256x256
Resolution (mm)	1.3x1x1.3	1x1x1
Slices	128	172
Slice Thickness (mm)	1.33	1.0
Scan Time (min)	8:07	4:54

Supplemental Table 4.S2: Effect Sizes for Difference in Means (ASD vs. TD)

ROI	Hedge's g ASD vs. TD Full Sample	Hedge's g ASD vs. TD (FSIQ > 100)	Hedge's g ASD vs. TD (FSIQ < 101)
Pericalcarine Left (SA)	0.37	0.15	0.59
Pericalcarine Right (SA)	0.14	0.19	0.55
Pericalcarine Left (CT)	0.28	0.15	0.57
Pericalcarine Right (CT)	0.34	0.19	0.68
Pericalcarine Left (LGI)	0.07	0.18	0.07
Pericalcarine Right (LGI)	0.05	0.14	0.07
Lingual Left (SA)	0.28	0.16	0.43
Lingual Right (SA)	0.17	0.01	0.50
Lingual Left (CT)	0.34	0.04	1.21
Lingual Right (CT)	0.32	0.13	0.87
Lingual Left (LGI)	0.01	0.10	0.14
Lingual Right (LGI)	0.01	0.11	0.09
Lateral Occipital Left (SA)	0.03	0.20	0.11
Lateral Occipital Right (SA)	0.10	0.03	0.09
Lateral Occipital Left (CT)	0.27	0.11	0.58
Lateral Occipital Right (CT)	0.21	0.15	0.28
Lateral Occipital Left (LGI)	0.12	0.07	0.27
Lateral Occipital Right (LGI)	0.08	0.06	0.08
Cuneus Left (SA)	0.16	0.07	0.19
Cuneus Right (SA)	0.16	0.03	0.38
Cuneus Left (CT)	0.15	0.01	0.37
Cuneus Right (CT)	0.07	0.01	0.14
Cuneus Left (LGI)	0.01	0.06	0.01
Cuneus Right (LGI)	0.13	0.18	0.07

Supplemental Table 4.S3: Gender (M/F) main effects and diagnosis by gender interactions on VC SA, CT, and LGI

ROI	Analysis	Hemisphere (SA/CT/LGI)	Beta	SE	t	p	95% CI	
Pericalcarine Cortex	Gender	Left (SA)	10.76	49.60	0.22	0.829	-87.160	108.678
		Right (SA)	48.81	53.27	0.92	0.361	-56.345	153.974
		Left (CT)	-0.03	0.04	-0.67	0.506	-0.101	0.050
		Right (CT)	-0.02	0.04	-0.67	0.502	-0.094	0.046
		Left (LGI)	-0.07	0.04	-1.74	0.084	-0.159	0.010
		Right (LGI)	-0.06	0.04	-1.27	0.205	-0.142	0.031
	Diagnosis by Gender Interaction	Left (SA)	-8.68	90.39	-0.10	0.924	-187.125	169.758
		Right (SA)	-118.10	96.64	-1.22	0.223	-308.897	72.692
		Left (CT)	-0.06	0.08	-0.76	0.448	-0.210	0.093
		Right (CT)	-0.06	0.07	-0.77	0.440	-0.196	0.085
		Left (LGI)	-0.09	0.09	-1.04	0.299	-0.258	0.080
		Right (LGI)	-0.08	0.09	-0.91	0.363	-0.253	0.093
Lingual Gyrus	Gender	Left (SA)	46.24	82.65	0.56	0.577	-116.922	209.404
		Right (SA)	36.75	73.97	0.50	0.620	-109.266	182.775
		Left (CT)	-0.02	0.03	-0.78	0.434	-0.082	0.036
		Right (CT)	0.00	0.03	-0.12	0.907	-0.070	0.063
		Left (LGI)	-0.07	0.03	-2.11	**0.037***	-0.143	-0.005
		Right (LGI)	-0.06	0.04	-1.52	0.130	-0.127	0.017
	Diagnosis by Gender Interaction	Left (SA)	-86.50	150.47	-0.57	0.566	-383.553	210.555
		Right (SA)	72.72	134.68	0.54	0.590	-193.156	338.594
		Left (CT)	-0.06	0.06	-0.97	0.335	-0.176	0.060
		Right (CT)	-0.04	0.07	-0.61	0.545	-0.175	0.093
		Left (LGI)	-0.06	0.07	-0.90	0.372	-0.201	0.076
		Right (LGI)	-0.03	0.07	-0.47	0.637	-0.179	0.110
Lateral Occipital Cortex	Gender	Left (SA)	61.01	104.21	0.59	0.559	-144.711	266.726
		Right (SA)	101.51	116.18	0.87	0.383	-127.835	330.862
		Left (CT)	-0.03	0.03	-1.14	0.258	-0.089	0.024
		Right (CT)	-0.01	0.03	-0.30	0.768	-0.079	0.058
		Left (LGI)	-0.05	0.03	-1.77	0.079	-0.098	0.005
		Right (LGI)	-0.05	0.03	-1.64	0.103	-0.101	0.009
	Diagnosis by Gender Interaction	Left (SA)	-298.54	188.50	-1.58	0.115	-670.667	73.594
		Right (SA)	-89.39	211.60	-0.42	0.673	-507.134	328.345
		Left (CT)	0.02	0.06	0.38	0.701	-0.092	0.136
		Right (CT)	0.03	0.07	0.40	0.687	-0.110	0.166
		Left (LGI)	-0.05	0.05	-0.88	0.382	-0.149	0.058
		Right (LGI)	-0.05	0.06	-0.92	0.360	-0.162	0.059

M = male; F = female; SA = surface area; CT = cortical thickness; LGI = local gyrification index; SE = standard error of the coefficient; CI = confidence interval. *Effects for which $p < 0.05$ are depicted in **bold**.

Supplemental Table 4.S3: Gender (M/F) main effects and diagnosis by gender interactions on VC SA, CT, and LGI, continued

ROI	Analysis	Hemisphere (SA/CT/LGI)	Beta	SE	t	p	95% CI	
Cuneus Cortex	Gender	Left (SA)	-19.52	43.24	-0.45	0.652	-104.876	65.842
		Right (SA)	39.73	43.66	0.91	0.364	-46.450	125.916
		Left (CT)	-0.04	0.04	-1.10	0.271	-0.120	0.034
		Right (CT)	-0.05	0.04	-1.26	0.211	-0.125	0.028
		Left (LGI)	-0.08	0.04	-1.84	0.067	-0.163	0.006
		Right (LGI)	-0.03	0.04	-0.73	0.469	-0.121	0.056
	Diagnosis by Gender Interaction	Left (SA)	6.59	78.79	0.08	0.933	-148.960	162.148
		Right (SA)	-54.53	79.44	-0.69	0.493	-211.373	102.304
		Left (CT)	-0.07	0.08	-0.91	0.363	-0.225	0.083
		Right (CT)	-0.08	0.08	-1.00	0.316	-0.231	0.075
		Left (LGI)	-0.03	0.09	-0.40	0.691	-0.204	0.135
		Right (LGI)	-0.07	0.09	-0.75	0.452	-0.245	0.109

M = male; F = female; SA = surface area; CT = cortical thickness; LGI = local gyrification index; SE = standard error of the coefficient; CI = confidence interval. *****Effects for which $p < 0.05$ are depicted in **bold**.

Supplemental Table 4.S4: Age main-effects and diagnosis by age interactions on VC SA, CT, and LGI.

ROI	Hemisphere (SA/CT/LGI)	Beta	SE	t	p	95% CI	
Pericalcarine Cortex (linear effects of age)	Left (SA)	4.69	6.38	0.74	0.463	-7.905	17.288
	Right (SA)	11.11	6.83	1.63	0.106	-2.369	24.583
	Left (CT)	-0.02	0.01	-3.36	[a] **0.001**	-0.028	-0.007
	Right (CT)	-0.10	0.04	-2.73	[a] **0.007**	-0.177	-0.029
	Left (LGI)	0.00	0.01	0.22	0.826	-0.011	0.013
	Right (LGI)	0.00	0.01	-0.45	0.650	-0.015	0.009
Lingual Gyrus (linear effects of age)	Left (SA)	-25.67	10.47	-2.45	0.015	-46.343	-4.993
	Right (SA)	-3.48	9.53	-0.37	0.715	-22.300	15.335
	Left (CT)	-0.03	0.00	-6.94	[a] **0.000**	-0.033	-0.018
	Right (CT)	-0.14	0.05	-2.76	[a] **0.006**	-0.236	-0.039
	Left (LGI)	0.00	0.01	0.53	0.594	-0.007	0.012
	Right (LGI)	0.00	0.01	-0.44	0.660	-0.012	0.008
Lateral Occipital Cortex (linear effects of age)	Left (SA)	9.97	13.42	0.74	0.459	-16.519	36.453
	Right (SA)	-8.22	14.99	-0.55	0.584	-37.805	21.369
	Left (CT)	-0.02	0.00	-5.51	[a] **0.000**	-0.028	-0.013
	Right (CT)	-0.02	0.01	-4.88	[a] **0.000**	-0.031	-0.013
	Left (LGI)	-0.01	0.00	-2.08	[a] **0.039**	-0.015	0.000
	Right (LGI)	-0.01	0.00	-2.90	[a] **0.004**	-0.019	-0.004
Cuneus Cortex (linear effects of age)	Left (SA)	-5.45	5.56	-0.98	0.328	-16.424	5.520
	Right (SA)	-5.56	5.62	-0.99	0.324	-16.658	5.537
	Left (CT)	-0.03	0.01	-5.69	[a] **0.000**	-0.038	-0.019
	Right (CT)	-0.03	0.01	-4.88	[a]**0.000**	-0.035	-0.015
	Left (LGI)	-0.01	0.01	-1.08	0.283	-0.018	0.005
	Right (LGI)	-0.01	0.01	-0.98	0.328	-0.018	0.006

SA = surface area; CT = cortical thickness; LGI = local gyrification index; SE = standard error of the coefficient; CI = confidence interval. [a]**Significant after FDR correction**

Supplemental Table 4.S5: Correlations between VC SA, CT, and LGI and FSIQ, VIQ, and PIQ in the TD group

ROI	Analysis	Hemisphere (SA/CT/LGI)	Beta	SE	t	p	95% CI	
Pericalcarine Cortex	FSIQ	Left (SA)	-3.02	2.07	-1.46	0.147	-7.133	1.086
		Right (SA)	-1.73	2.18	-0.79	0.43	-6.070	2.609
		Left (CT)	0.00	0.00	0.42	0.674	-0.003	0.004
		Right (CT)	0.00	0.00	-0.14	0.888	-0.003	0.003
		Left (LGI)	0.00	0.00	-0.01	0.996	-0.003	0.003
		Right (LGI)	0.00	0.00	-0.55	0.581	-0.006	0.003
	VIQ	Left (SA)	-3.31	2.19	-1.51	0.135	-7.672	1.056
		Right (SA)	-2.83	2.31	-1.23	0.223	-7.418	1.757
		Left (CT)	0.00	0.00	0.56	0.579	-0.003	0.005
		Right (CT)	0.00	0.00	0.05	0.958	-0.003	0.003
		Left (LGI)	0.00	0.00	0.14	0.889	-0.003	0.004
		Right (LGI)	0.00	0.00	-0.09	0.925	-0.005	0.004
	PIQ	Left (SA)	-1.51	1.79	-0.84	0.401	-5.062	2.047
		Right (SA)	-0.43	1.88	-0.23	0.821	-4.161	3.308
		Left (CT)	0.00	0.00	0.23	0.816	-0.003	0.003
		Right (CT)	0.00	0.00	-0.31	0.758	-0.003	0.002
		Left (LGI)	0.00	0.00	-0.08	0.940	-0.003	0.003
		Right (LGI)	0.00	0.00	-0.77	0.445	-0.005	0.002

FSIQ = Full Scale IQ; VIQ = Verbal IQ; PIQ = Performance IQ; SA = surface area; CT = cortical thickness; LGI = local gyrification index; SE = standard error of the coefficient; CI = confidence interval. *Effects significant at $p < 0.05$ (uncorrected) are depicted in **bold** font.

Supplemental Table 4.S5: Correlations between VC SA, CT, and LGI and FSIQ, VIQ, and PIQ in the TD group, continued

ROI	Analysis	Hemisphere (SA/CT/LGI)	Beta	SE	t	p	95% CI	
Lingual Gyrus	FSIQ	Left (SA)	-7.65	3.26	-2.34	***0.022**	-14.142	-1.153
		Right (SA)	-4.52	3.07	-1.47	0.144	-10.626	1.582
		Left (CT)	0.00	0.00	2.86	***0.005**	0.001	0.006
		Right (CT)	0.00	0.00	1.13	0.262	-0.001	0.005
		Left (LGI)	0.00	0.00	0.61	0.546	-0.002	0.004
		Right (LGI)	0.00	0.00	-0.26	0.792	-0.004	0.003
	VIQ	Left (SA)	-6.69	3.51	-1.91	0.06	-13.667	0.285
		Right (SA)	-2.57	3.29	-0.78	0.437	-9.121	3.975
		Left (CT)	0.00	0.00	2.60	***0.011**	0.001	0.006
		Right (CT)	0.00	0.00	1.41	0.162	-0.001	0.005
		Left (LGI)	0.00	0.00	0.50	0.620	-0.002	0.004
		Right (LGI)	0.00	0.00	0.15	0.879	-0.003	0.004
	PIQ	Left (SA)	-5.61	2.82	-1.99	0.05	-11.227	0.012
		Right (SA)	-4.33	2.62	-1.65	0.102	-9.549	0.886
		Left (CT)	0.00	0.00	2.30	***0.024**	0.000	0.004
		Right (CT)	0.00	0.00	0.78	0.440	-0.002	0.004
		Left (LGI)	0.00	0.00	0.28	0.779	-0.002	0.003
		Right (LGI)	0.00	0.00	-0.71	0.477	-0.004	0.002

FSIQ = Full Scale IQ; VIQ = Verbal IQ; PIQ = Performance IQ; SA = surface area; CT = cortical thickness; LGI = local gyrification index; SE = standard error of the coefficient; CI = confidence interval. *Effects significant at $p < 0.05$ (uncorrected) are depicted in **bold** font.

Supplemental Table 4.S5: Correlations between VC SA, CT, and LGI and FSIQ, VIQ, and PIQ in the TD group, continued

ROI	Analysis	Hemisphere (SA/CT/LGI)	Beta	SE	t	p	95% CI	
Lateral Occipital Cortex	FSIQ	Left (SA)	-2.61	4.74	-0.55	0.584	-12.037	6.827
		Right (SA)	-7.68	5.12	-1.50	0.137	-17.857	2.495
		Left (CT)	0.00	0.00	0.54	0.593	-0.002	0.003
		Right (CT)	0.00	0.00	1.60	0.112	-0.001	0.005
		Left (LGI)	0.00	0.00	1.04	0.301	-0.001	0.004
		Right (LGI)	0.00	0.00	0.31	0.754	-0.002	0.003
	VIQ	Left (SA)	-2.05	5.04	-0.41	0.685	-12.082	7.982
		Right (SA)	0.25	5.51	0.05	0.964	-10.710	11.214
		Left (CT)	0.00	0.00	0.00	0.997	-0.002	0.002
		Right (CT)	0.00	0.00	1.03	0.305	-0.001	0.004
		Left (LGI)	0.00	0.00	0.61	0.543	-0.002	0.003
		Right (LGI)	0.00	0.00	1.12	0.267	-0.001	0.004
	PIQ	Left (SA)	-2.55	4.06	-0.63	0.532	-10.632	5.536
		Right (SA)	-8.51	4.35	-1.96	0.054	-17.155	0.136
		Left (CT)	0.00	0.00	0.98	0.331	-0.001	0.003
		Right (CT)	0.00	0.00	1.81	0.074	0.000	0.005
		Left (LGI)	0.00	0.00	1.30	0.197	-0.001	0.003
		Right (LGI)	0.00	0.00	-0.45	0.653	-0.003	0.002

FSIQ = Full Scale IQ; VIQ = Verbal IQ; PIQ = Performance IQ; SA = surface area; CT = cortical thickness; LGI = local gyrification index; SE = standard error of the coefficient; CI = confidence interval. *Effects significant at $p < 0.05$ (uncorrected) are depicted in **bold** font.

Supplemental Table 4.S5: Correlations between VC SA, CT, and LGI and FSIQ, VIQ, and PIQ in the TD group, continued

ROI	Analysis	Hemisphere (SA/CT/LGI)	Beta	SE	t	p	95% CI	
Cuneus Cortex	FSIQ	Left (SA)	-0.99	1.93	-0.51	0.611	-4.836	2.861
		Right (SA)	-0.09	1.73	-0.05	0.96	-3.520	3.346
		Left (CT)	0.00	0.00	0.06	0.954	-0.003	0.003
		Right (CT)	0.00	0.00	0.48	0.636	-0.003	0.004
		Left (LGI)	0.00	0.00	-1.15	0.253	-0.006	0.002
		Right (LGI)	0.00	0.00	-0.53	0.596	-0.005	0.003
	VIQ	Left (SA)	-0.82	2.06	-0.40	0.693	-4.908	3.276
		Right (SA)	-1.28	1.83	-0.70	0.487	-4.915	2.361
		Left (CT)	0.00	0.00	-0.06	0.953	-0.004	0.003
		Right (CT)	0.00	0.00	0.29	0.773	-0.003	0.004
		Left (LGI)	0.00	0.00	-0.89	0.373	-0.006	0.002
		Right (LGI)	0.00	0.00	-0.17	0.866	-0.005	0.004
	PIQ	Left (SA)	-0.71	1.66	-0.42	0.672	-4.006	2.597
		Right (SA)	0.27	1.48	0.18	0.859	-2.679	3.208
		Left (CT)	0.00	0.00	-0.05	0.957	-0.003	0.003
		Right (CT)	0.00	0.00	0.55	0.581	-0.002	0.004
		Left (LGI)	0.00	0.00	-0.71	0.478	-0.004	0.002
		Right (LGI)	0.00	0.00	-0.50	0.622	-0.005	0.003

FSIQ = Full Scale IQ; VIQ = Verbal IQ; PIQ = Performance IQ; SA = surface area; CT = cortical thickness; LGI = local gyrification index; SE = standard error of the coefficient; CI = confidence interval. *Effects significant at $p < 0.05$ (uncorrected) are depicted in **bold** font.

Supplemental Table 4.S6: Correlations between VC SA, CT, and LGI and FSIQ, VIQ, and PIQ in the ASD group

ROI	Analysis	Hemisphere (SA/CT/LGI)	Beta	SE	t	p	95% confidence interval	
Pericalcarine Cortex	FSIQ	Left (SA)	2.23	1.62	1.37	0.173	-1.000	5.462
		Right (SA)	1.84	1.76	1.04	0.300	-1.671	5.348
		Left (CT)	0.00	0.00	-1.02	0.310	-0.004	0.001
		Right (CT)	0.00	0.00	-0.84	0.401	-0.003	0.001
		Left (LGI)	0.00	0.00	1.43	0.156	-0.001	0.006
		Right (LGI)	0.00	0.00	0.88	0.383	-0.002	0.004
	VIQ	Left (SA)	3.20	1.58	2.02	***0.046**	0.055	6.337
		Right (SA)	2.95	1.72	1.71	0.090	-0.474	6.363
		Left (CT)	0.00	0.00	-1.98	0.051	-0.005	0.000
		Right (CT)	0.00	0.00	-1.48	0.142	-0.004	0.001
		Left (LGI)	0.00	0.00	1.52	0.132	-0.001	0.006
		Right (LGI)	0.00	0.00	0.47	0.639	-0.002	0.003
	PIQ	Left (SA)	0.55	1.47	0.37	0.710	-2.383	3.482
		Right (SA)	0.18	1.59	0.11	0.911	-2.993	3.352
		Left (CT)	0.00	0.00	-0.15	0.879	-0.003	0.002
		Right (CT)	0.00	0.00	-0.38	0.704	-0.003	0.002
		Left (LGI)	0.00	0.00	1.03	0.306	-0.001	0.005
		Right (LGI)	0.00	0.00	1.05	0.298	-0.001	0.004

FSIQ = Full Scale IQ; VIQ = Verbal IQ; PIQ = Performance IQ; SA = surface area; CT = cortical thickness; LGI = local gyrification index; SE = standard error of the coefficient; CI = confidence interval. *Statistically significant effect after FDR correction. *Effects significant at $p < 0.05$ (uncorrected) are depicted in **bold** font.

Supplemental Table 4.S6: Correlations between VC SA, CT, and LGI and FSIQ, VIQ, and PIQ in the ASD group, continued

ROI	Analysis	Hemisphere (SA/CT/LGI)	Beta	SE	t	p	95% confidence interval	
Lingual Gyrus	FSIQ	Left (SA)	0.79	2.73	0.29	0.773	-4.637	6.217
		Right (SA)	2.09	2.45	0.85	0.397	-2.784	6.956
		Left (CT)	0.00	0.00	-1.49	0.141	-0.003	0.000
		Right (CT)	0.00	0.00	-0.55	0.581	-0.003	0.001
		Left (LGI)	0.00	0.00	1.31	0.193	-0.001	0.004
		Right (LGI)	0.00	0.00	1.27	0.207	-0.001	0.004
	VIQ	Left (SA)	1.41	2.68	0.53	0.600	-3.926	6.752
		Right (SA)	3.33	2.39	1.39	0.168	-1.436	8.088
		Left (CT)	0.00	0.00	-1.83	0.071	-0.003	0.000
		Right (CT)	0.00	0.00	-1.11	0.270	-0.003	0.001
		Left (LGI)	0.00	0.00	1.36	0.176	-0.001	0.004
		Right (LGI)	0.00	0.00	0.74	0.461	-0.002	0.003
	PIQ	Left (SA)	0.09	2.45	0.04	0.970	-4.783	4.971
		Right (SA)	0.34	2.21	0.15	0.880	-4.058	4.728
		Left (CT)	0.00	0.00	-0.92	0.360	-0.002	0.001
		Right (CT)	0.00	0.00	0.16	0.871	-0.002	0.002
		Left (LGI)	0.00	0.00	0.90	0.370	-0.001	0.003
		Right (LGI)	0.00	0.00	1.31	0.195	-0.001	0.004

FSIQ = Full Scale IQ; VIQ = Verbal IQ; PIQ = Performance IQ; SA = surface area; CT = cortical thickness; LGI = local gyrification index; SE = standard error of the coefficient; CI = confidence interval. *Statistically significant effect after FDR correction. *Effects significant at $p < 0.05$ (uncorrected) are depicted in **bold** font.

Supplemental Table 4.S6: Correlations between VC SA, CT, and LGI and FSIQ, VIQ, and PIQ in the ASD group, continued

ROI	Analysis	Hemisphere (SA/CT/LGI)	Beta	SE	t	p	95% confidence interval	
Lateral Occipital Cortex	FSIQ	Left (SA)	6.19	3.11	1.99	0.050	0.001	12.379
		Right (SA)	1.95	3.66	0.53	0.597	-5.345	9.236
		Left (CT)	0.00	0.00	-0.90	0.371	-0.003	0.001
		Right (CT)	0.00	0.00	0.26	0.792	-0.002	0.003
		Left (LGI)	0.00	0.00	1.43	0.157	0.000	0.003
		Right (LGI)	0.00	0.00	1.40	0.164	-0.001	0.003
	VIQ	Left (SA)	4.00	3.11	1.29	0.202	-2.184	10.174
		Right (SA)	2.87	3.60	0.80	0.428	-4.296	10.034
		Left (CT)	0.00	0.00	-2.00	***0.048**	-0.004	0.000
		Right (CT)	0.00	0.00	-0.41	0.683	-0.003	0.002
		Left (LGI)	0.00	0.00	0.89	0.377	-0.001	0.003
		Right (LGI)	0.00	0.00	1.18	0.242	-0.001	0.003
	PIQ	Left (SA)	5.81	2.79	2.09	***0.040**	0.269	11.360
		Right (SA)	0.39	3.30	0.12	0.907	-6.172	6.945
		Left (CT)	0.00	0.00	0.17	0.866	-0.002	0.002
		Right (CT)	0.00	0.00	0.69	0.492	-0.001	0.003
		Left (LGI)	0.00	0.00	1.66	0.101	0.000	0.003
		Right (LGI)	0.00	0.00	1.26	0.211	-0.001	0.003

FSIQ = Full Scale IQ; VIQ = Verbal IQ; PIQ = Performance IQ; SA = surface area; CT = cortical thickness; LGI = local gyrification index; SE = standard error of the coefficient; CI = confidence interval. *Statistically significant effect after FDR correction. *Effects significant at $p < 0.05$ (uncorrected) are depicted in **bold** font.

Supplemental Table 4.S6: Correlations between VC SA, CT, and LGI and FSIQ, VIQ, and PIQ in the ASD group, continued

ROI	Analysis	Hemisphere (SA/CT/LGI)	Beta	SE	t	p	95% confidence interval	
Cuneus Cortex	FSIQ	Left (SA)	0.17	1.35	0.12	0.901	-2.520	2.857
		Right (SA)	1.15	1.53	0.76	0.452	-1.883	4.189
		Left (CT)	0.00	0.00	-0.10	0.924	-0.003	0.002
		Right (CT)	0.00	0.00	0.41	0.683	-0.002	0.003
		Left (LGI)	0.00	0.00	0.01	0.989	-0.003	0.003
		Right (LGI)	0.00	0.00	0.88	0.382	-0.002	0.004
	VIQ	Left (SA)	1.07	1.33	0.81	0.420	-1.564	3.711
		Right (SA)	1.38	1.50	0.92	0.360	-1.605	4.366
		Left (CT)	0.00	0.00	-0.77	0.445	-0.003	0.002
		Right (CT)	0.00	0.00	-0.09	0.930	-0.003	0.002
		Left (LGI)	0.00	0.00	0.22	0.826	-0.003	0.004
		Right (LGI)	0.00	0.00	0.82	0.413	-0.002	0.004
	PIQ	Left (SA)	-0.63	1.21	-0.52	0.607	-3.036	1.785
		Right (SA)	0.61	1.37	0.44	0.661	-2.128	3.339
		Left (CT)	0.00	0.00	0.40	0.694	-0.002	0.003
		Right (CT)	0.00	0.00	0.60	0.547	-0.002	0.003
		Left (LGI)	0.00	0.00	-0.13	0.894	-0.003	0.003
		Right (LGI)	0.00	0.00	0.73	0.469	-0.002	0.004

FSIQ = Full Scale IQ; VIQ = Verbal IQ; PIQ = Performance IQ; SA = surface area; CT = cortical thickness; LGI = local gyrification index; SE = standard error of the coefficient; CI = confidence interval. *Statistically significant effect after FDR correction. *Effects significant at $p < 0.05$ (uncorrected) are depicted in **bold** font.

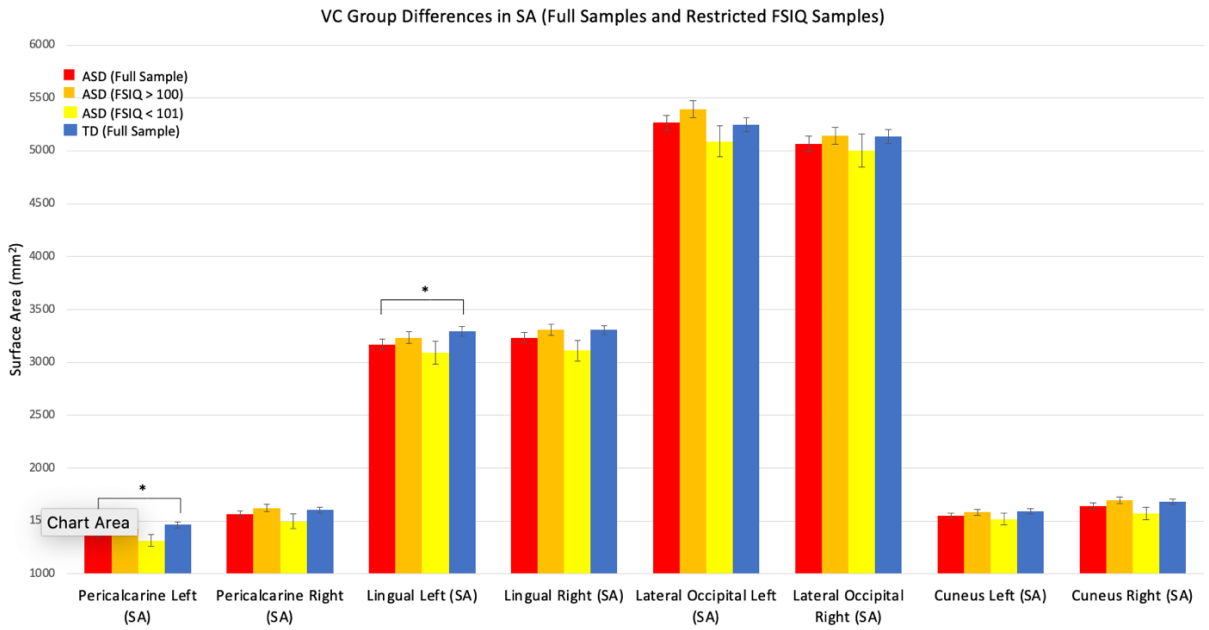

Figure 4.1: ASD vs. TD group differences in mean Visual Cortex (VC) Surface Area (SA). Red = ASD (Full Sample); Orange = ASD (FSIQ > 100); Yellow = ASD (FSIQ $\leq$ 100); Blue = TD (Full Sample). Error bars depict the standard error of the each group mean. *notes a difference in means between the ASD (full sample) and TD (full sample) groups, significant at the threshold of $p < 0.05$, uncorrected.

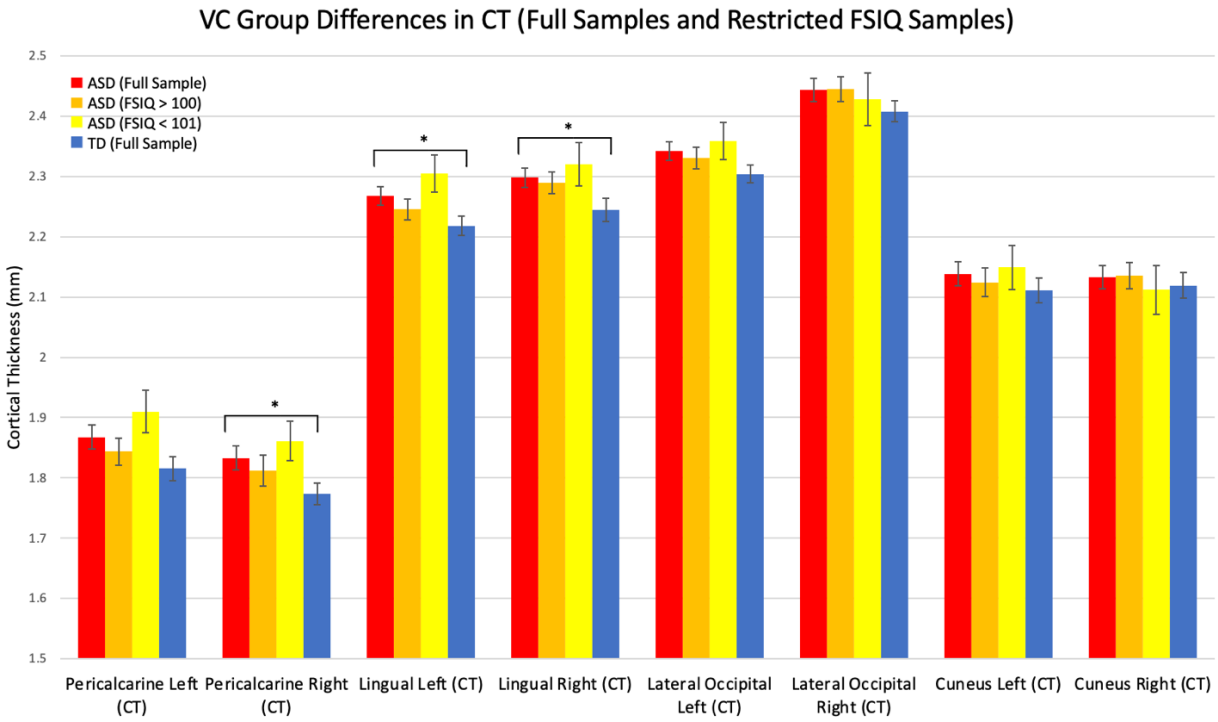

Figure 4.2: ASD vs. TD group differences in mean Visual Cortex (VC) Cortical Thickness (CT). Red = ASD (Full Sample); Orange = ASD (FSIQ > 100); Yellow = ASD (FSIQ $\leq$ 101); Blue = TD (Full Sample). Error bars depict the standard error of the each group mean. *notes a difference in means between the ASD (full sample) and TD (full sample) groups, significant at the threshold of $p < 0.05$, uncorrected.

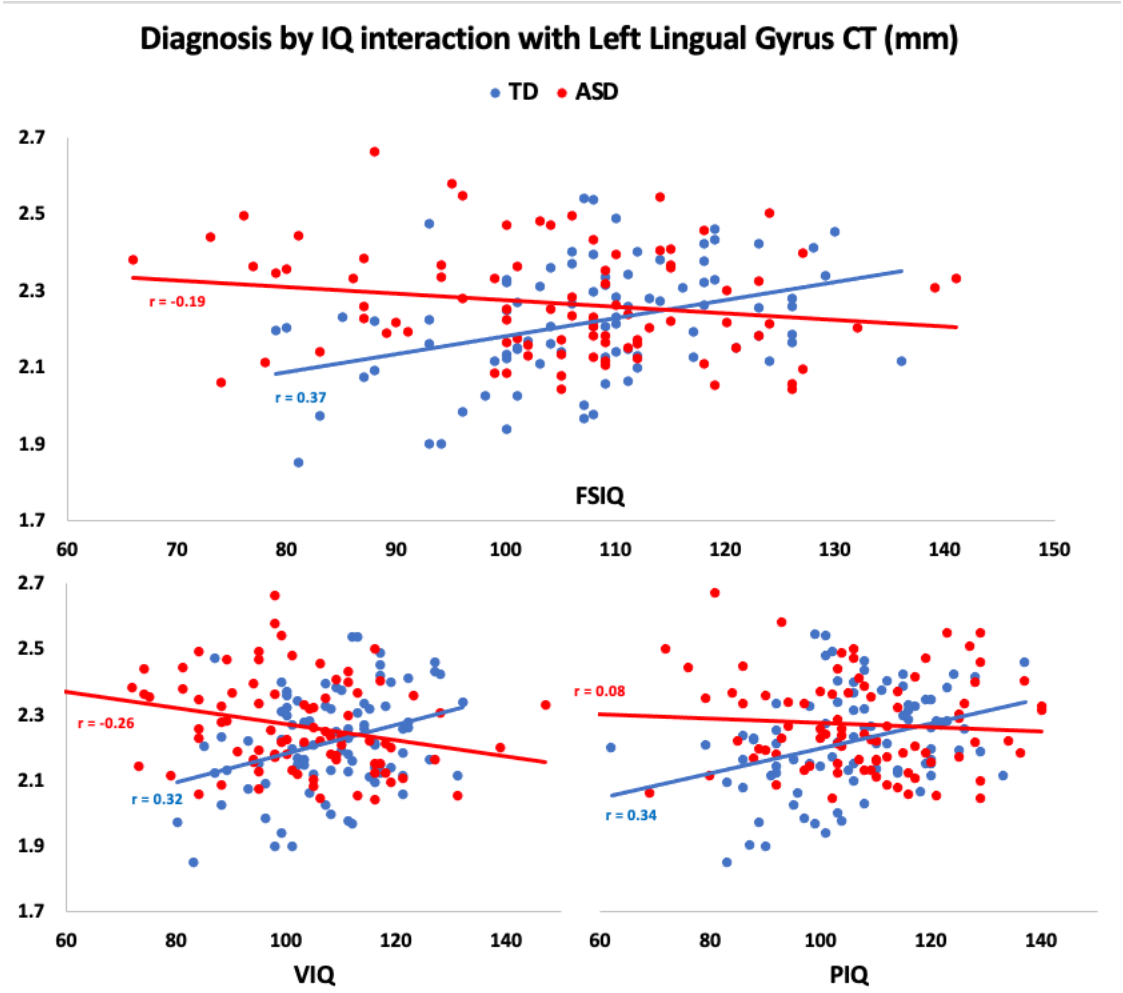

Figure 4.3: Diagnosis by IQ interactions with left Lingual Gyrus Cortical Thickness. Diagnosis by FSIQ interaction with Left Lingual Gyrus Cortical Thickness (top panel). Scatter plots in the bottom panels illustrate interactions involving Verbal (bottom left) and Performance (bottom right) IQ. Red = ASD. Blue = TD.

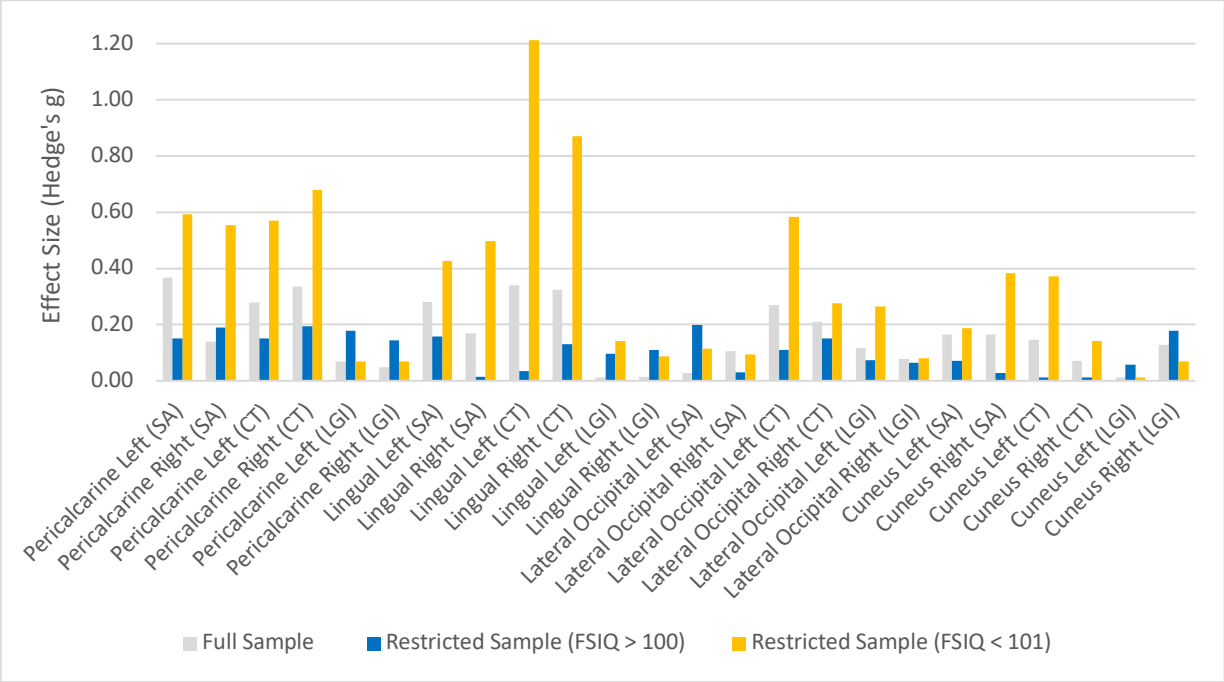

Figure 4.4: Effect sizes for (ASD vs. TD) group differences in VC Morphology in samples of differing CA. Gray = full sample; Blue = FSIQ > 100 sample; Orange = FSIQ < 101 sample.

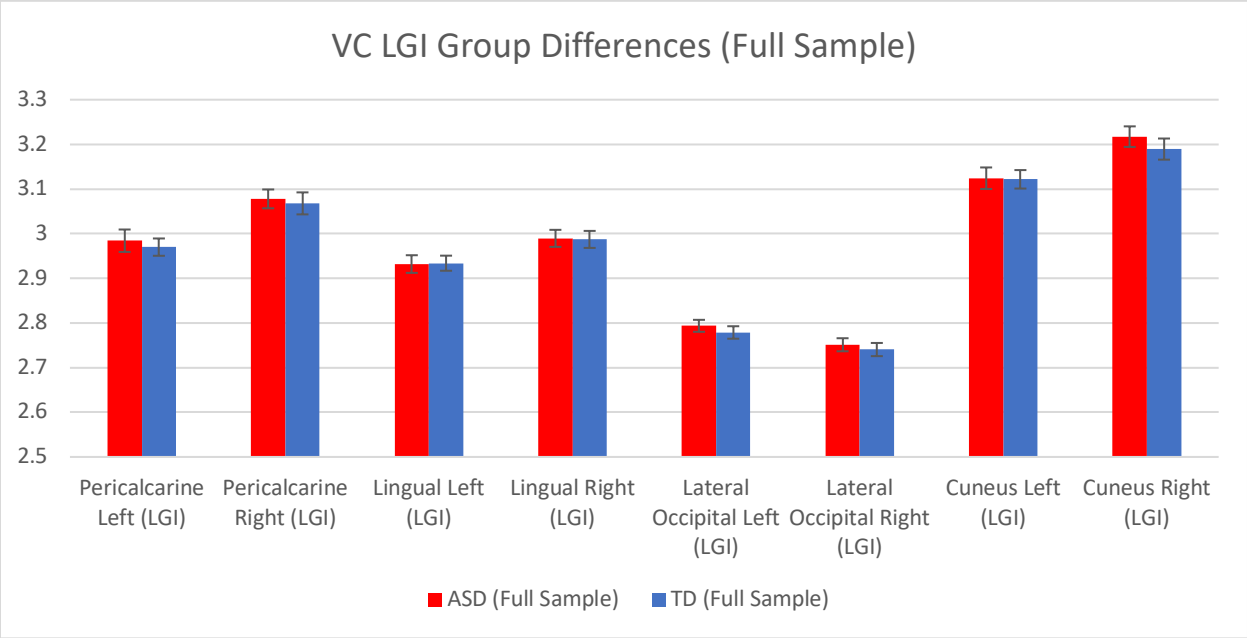

Supplemental Figure 4.S1: ASD vs. TD group Differences in VC Local Gyrification Index.

Chapter 5: General Discussion

Main Findings. Studies 1 through 3 included in this dissertation have explored relationships between CA (and, in the case of Study 2, potential developmental precursors to CA) and functional connectivity as well as morphology [SA, CT, and LGI]) in ASD. Studies 1-3 were motivated by the currently limited understanding of the neural correlates of CA in ASD, exacerbated by a near-absence of neuroimaging research in participants who have ASD and LCA or ID, although these individuals represent over 50% of the population with ASD (Maenner et al., 2020). Dearth of research on individuals with LCA continues to be a barrier to determining the extent to which the broad MRI and fMRI literature on ASD generalizes to individuals with LCA (a challenge of ecological validity). Given that cognitive abilities are related to quality of life in ASD (Ben-Itzchak & Zachor, 2020; Lord, McCauley, et al., 2020), but vary widely between individuals on the spectrum (Maenner et al., 2020), understanding the neural correlates of cognitive abilities in ASD is a public health priority. Each of the three studies comprising this dissertation presents an attempt to enhance our understanding of the neural underpinnings of cognitive abilities in ASD.

Study 1 provided a first glimpse into resting-state functional connectivity in children and adolescents with ASDs and below average CA (L-ASD), as there had been no research on resting-state functional connectivity in this population at the time it was published. One aim of the current dissertation was to test whether atypical functional connectivity in ASD was uniform across groups of differing cognitive abilities. We sought to examine whether connectivity differences from neurotypical controls exhibited by the L-ASD group would be similar to those exhibited by the H-ASD group, but simply more pronounced, or, whether the L-ASD group would show distinct patterns of atypical functional connectivity. In comparing the L-ASD and H-ASD groups to the

same control group, we showed that functional connectivity differences in ASD were not uniform across subsamples with differing CA. Furthermore, L-ASD and H-ASD subgroups differed in FC of regions most robustly implicated in atypical functional connectivity in ASD by prior research. Specifically, the L-ASD group showed decreased connectivity compared to the H-ASD group within the DMN as well as between pericalcarine visual cortex and the pSTS, bilaterally. Striking results linking connectivity of pericalcarine visual cortex with IQ in ASD led us to design Studies 2 and 3 to focus more systematically on relationships between CA and VC FC as well as between CA and VC neuroanatomy.

Study 2 sought to characterize functional connectivity of visual cortex at an earlier developmental stage (compared to Study 1), in toddlers and preschoolers with and without ASD, and to test links between visual cortex functional connectivity and early developmental cognitive abilities. Although Study 1 had tested whether group differences between the L-ASD and H-ASD group were related to age, no such relationships were observed. We thus hypothesized that the relationship between VC-pSTS functional connectivity and CA may emerge earlier in life. In Study 2, we were able to follow up on this hypothesis. Connectivity of VC (specifically right lateral occipital cortex) with the left pSTS was related to better developmental abilities in neurotypical children. The ASD group showed a notable absence of this relationship, involving similar regions to those linked to CA in ASD in Study 1 (between pericalcarine VC and pSTS, bilaterally). However, Study 2 did not, as hypothesized, provide evidence that this pattern emerges *during* toddler/preschool years (i.e., no significant diagnosis by age interactions with VC-pSTS functional connectivity). While detection of such effects was limited by sample size and lack of longitudinal data, the possibility that this pattern of atypical VC connectivity develops at an even earlier age cannot be ruled out, especially given that the visual system is one of the earliest networks to

develop (W. Gao et al., 2015; Gilmore et al., 2012). However, other atypical relationships between VC FC (i.e., not involving VC-pSTS connectivity) and age in ASD were observed in Study 2. Namely, VC connectivity with right somatosensory cortex was positively associated with age in TD preschoolers and this relationship was notably reversed in the ASD group. This suggests that in early childhood, FC between VC and other sensory cortices may be maturing atypically in ASD. Finally, examination of links between VC FC and ASD symptom severity revealed a negative relationship between FC within VC networks and higher ASD symptom severity, suggesting that FC of VC relates to core symptoms of autism early in life.

Study 3 attempted to examine the anatomy of VC regions identified in Study 1 as showing relationships between functional connectivity and CA in ASD, and tested for atypical relationships between cognitive abilities and VC neuroanatomy in children and adolescents with ASD. Results revealed differences in relationships between VC neuroanatomy and cognitive abilities in children with ASD as compared to TD peers. Specifically, a distinct relationship between left lingual gyrus CT and general CA was observed among children with ASD, with greater effect sizes of ASD v. TD differences found among children with ASD and relatively lower CA, for both SA and CT. This was in line with the functional connectivity findings observed in Study 1. These results suggest that individuals with ASD and LCA may show distinct VC neuroanatomy and functional connectivity patterns not observed in ASD and HCA.

Functional roles of the visual system in neurotypical development, and alterations in ASD. The current dissertation examined whether neural correlates of cognitive abilities differ between children with ASD and TD peers, with predominant focus on a potential role of visual cortex. Findings from Studies 2 & 3 also highlighted important relationships between visual cortex and cognitive abilities in typical development, and were consistent with the broader literature on

this topic in TD populations. Study 2 provided evidence that increased functional connectivity within visual networks was associated with greater developmental abilities in neurotypical toddlers and preschoolers, and that during these years connectivity between visual cortex and sensorimotor regions increases with age, consistent with previous studies by Chen et al. (2021) and Bruchhage et al. (2020). Results of Study 3 suggested that increased VC cortical thickness relates to higher cognitive abilities in neurotypical children and adolescents, which has also been observed by other groups (Schmitt et al., 2019; Shaw et al., 2006). Overall, findings presented in this dissertation, in line with limited prior research, speak to an important association between VC functional connectivity and neuroanatomy and normative cognitive development. Relationships between visual neural systems and cognitive abilities are readily interpretable given prior research. During the first years of life, many aspects of visual perception are dependent on experience-driven stimulation, which promotes further development (Siu & Murphy, 2018). Moreover, multisensory integration plays a crucial role in cognitive development across early childhood (Dionne-Dostie et al., 2015). The pSTS is a region involved in multisensory integration (Beauchamp et al., 2003; Pelphrey et al., 2005; Redcay, 2008; Redcay et al., 2008; Saygin et al., 2004). Thus, findings observed for the TD group in Study 2 (higher connectivity between visual cortex and the pSTS associated with better cognitive developmental abilities) are congruent with this developmental trajectory.

Studies 1 and 2 both showed, using similar methodologies in independent samples, across different developmental cohorts, that visual cortex functional connectivity with the pSTS relates atypically to cognitive development and/or abilities in ASD. Although additional longitudinal research is needed to draw any definitive conclusions regarding developmental trajectories, findings from Study 2 suggest a disruption in functioning of visual circuitry within the first years

of life in ASD. Findings from Study 1 suggest that such a disruption involving multisensory integration circuitry may still be evident into adolescence in ASD, when it is also associated with lower cognitive abilities. Atypical processing of visual information (including orienting, gaze, and joint attention) that is longitudinally predictive of poorer developmental abilities in later years (Kellerman et al., 2020; Thurm et al., 2007; Toth et al., 2006) is evident as early as the first year of life in ASD [e.g., see (Apicella et al., 2020; Gammer et al., 2015; Gangi et al., 2014; Gangi et al., 2018; Tanner & Dounavi, 2021)]. Thus, results presented in the current dissertation have high face validity, especially in light of robust evidence that ASD is associated with deficits in multisensory integration that are more pronounced earlier in life (Feldman et al., 2018).

Aggregating evidence to bolster the robustness of findings is one of the goals of multi-modal neuroimaging. In addition to shedding light on how VC neuroanatomy relates to cognitive abilities in ASD, Study 3 provided converging evidence of atypical involvement of VC in CA in ASD by revealing distinct relationships between neuroanatomy and cognitive abilities in children and adolescents with ASD. Studies 1-3 are impactful primarily in showing that relationships between visual cortex (both structure and function) and cognitive abilities differ in ASD during childhood and adolescence in comparison to TD peers, and that disruptions in neurotypical adaptive patterns of VC functional connectivity can be traced back to the first years of life in ASD. These three studies increased our understanding of the neural correlates of cognitive abilities in ASD, and provided additional insight into brain structure and functioning in individuals with lower cognitive abilities, fulfilling the primary aims of the current dissertation.

Addressing barriers to incorporating ASD participants with LCA or ID in MRI research. Barriers to incorporating participants with ASD and LCA or ID in neuroimaging research were enumerated in Chapter 1. Nevertheless, in the current dissertation it was ultimately

possible to include a sizable number of participants with ASD and LCA, through use of several strategies implemented in the experimental design. Studies 1 and 3 both used multi-site datasets in order to increase the number of participants with ASD and LCA, and both studies attempted to stratify ASD groups by CA for at least some of the analyses (for Study 1, we included an ASD group of 22 participants with FSIQ $\leq$ 85, and for Study 3, 10 participants with ASD had FSIQ $\leq$ 85]). Study 2 included toddlers and preschoolers with a full spectrum of developmental delays by scanning participants during natural sleep, which enabled us to acquire data from a less selective cohort of children with respect to cognitive developmental abilities and symptom severity. Multi-site data sharing efforts and stratification by CA as well as efforts to scan participants during natural sleep may facilitate future research efforts towards including more diverse (in terms of cognitive abilities) cohorts in autism research.

An additional motivation of the current dissertation was the need for more representative samples of individuals with ASD in terms of cognitive abilities as a step towards contributing to higher ecological validity of the neuroimaging research. Given the many conflicting findings in the neuroimaging literature on ASD, generation and evaluation of new hypotheses is important. However, hypothesis generation may be limited by the predominant inclusion of individuals with average or above average CA. By focusing on segments of the ASD population with lower CA in Study 1, we were able to observe striking differences in VC FC that helped prompt further research carried out in Studies 2 & 3. This dissertation has shown that inclusion of both individuals with above average and below average CA is extremely important – else differences in brain structure and functioning relating to this construct may remain obscured. Indeed, all three studies showed that experimental designs including underrepresented populations in research on ASD can potentially enhance our understanding of the general population.

Future research directions. Although this dissertation makes a first stride towards understanding the neural correlates of cognitive development and abilities in ASD, much additional research is warranted to follow-up on questions generated or left unanswered by Studies 1-3. Given that approximately 1/3 of individuals with ASD are diagnosed with intellectual disability (typically having an IQ score of 70 or below (American Psychiatric Association, 2013)), a limitation of Studies 1 & 3 was inclusion of very few participants with ASD and FSIQ < 70 (only 3 datasets in this FSIQ-range were available for Study 1, and only 1 for Study 3). Thus, even though the current dissertation aimed to be more representative of the ASD population (and succeeded in terms of representing more participants with LCA), those with lowest FSIQ scores were still underrepresented. Developing methods that could aid collection of imaging data from individuals with ID may be critical to enabling researchers to understand neural development in individuals with ASD and intellectual disability, and are currently under way (Nordahl et al., 2016).

Studying even younger participants than those included in Study 2 is also an important avenue of future research, as pinpointing the age at which atypical VC development emerges in ASD may have some bearing on potential intervention strategies and their optimal timing. For example, Study 2 showed that VC is related to cognitive developmental abilities in young neurotypical children. As this relationship was absent in ASD, we theorized that toddlers and preschoolers with ASD may have more difficulty integrating key visual input that stimulates cognitive and social development. Thus, development of interventions to increase exposure to visual stimuli (possibly with a social nature, e.g., facial expressions), or to improve multisensory integration early in life in ASD, may be useful at certain key ages. Development of such interventions can be aided by obtaining an improved understanding of how visual cortex relates to

cognitive development as early as possible in autism. Study 2 specifically hypothesized that atypical diagnosis by age interactions with VC functional connectivity would be observed during these ages. However, we found that some atypical VC connectivity patterns related to cognitive developmental abilities in ASD appeared to have already emerged in the cohort studied (i.e., no diagnosis by age interactions involving regions showing atypical relationships between FC and developmental abilities), while other diagnosis by age interactions with VC FC (between VC and somatosensory cortex) were observed in Study 2. Thus, experimental designs incorporating high-risk infants that aren't yet diagnosed with ASD may be helpful for gaining a more complete understanding of how atypical VC development unfolds in ASD. While such designs have their own limitations (e.g., very high initial induction needed given inevitable loss of sample size related to loss of participants who aren't eventually diagnosed with ASD, and an inherent bias towards heritable variants of ASD), they may still be very beneficial to further characterizing atypical VC developmental trajectories in ASD. Moreover, longitudinal research in infants and toddlers at risk for ASD is needed in order to make any conclusive determinations regarding atypical developmental trajectories in ASD.

Conclusions. Relationships between cognitive abilities and visual cortex functional connectivity and neuroanatomy may differ in ASD during childhood and adolescence, and may be detected as early as the first years of life. FMRI research carried out in this dissertation suggests an atypical relationship between functional connectivity of early visual cortex and higher order regions involved in multisensory integration (i.e., the pSTS). Initial research including children with ASD and lower cognitive abilities or intellectual disability in neuroimaging research suggests that individuals with ASD and lower cognitive abilities do not necessarily show the same pattern of differences from neurotypical controls as individuals with ASD and higher cognitive abilities.

Thus, neuroimaging studies on ASD incorporating mostly participants with higher CA may generate results that do not necessarily generalize to the broader ASD population or those with below-average CA. On the other hand, incorporating individuals with ASD and lower CA in autism research may lead to development of new theories and resolution of some of the conflicting findings portrayed in the broader literature (although heterogeneity along many other factors may still contribute to conflicting findings). Overall, the three studies included in the dissertation strongly suggest that stratification by CA and efforts to include participants with ASD and lower cognitive abilities or intellectual disability are critical to understanding how brain structure and functioning differ in ASD.

References

Abbott, A. E., Nair, A., Keown, C. L., Datko, M., Jahedi, A., Fishman, I., & Müller, R. A. (2016). Patterns of Atypical Functional Connectivity and Behavioral Links in Autism Differ Between Default, Salience, and Executive Networks. *Cerebral Cortex, 26*(10), 4034-4045.

Alaerts, K., Nayar, K., Kelly, C., Raithel, J., Milham, M. P., & Di Martino, A. (2015). Age-related changes in intrinsic function of the superior temporal sulcus in autism spectrum disorders. *Soc Cogn Affect Neurosci, 10*(10), 1413-1423.

Alaerts, K., Swinnen, S. P., & Wenderoth, N. (2016). Sex differences in autism: a resting-state fMRI investigation of functional brain connectivity in males and females. *Soc Cogn Affect Neurosci, 11*(6), 1002-1016.

Alaerts, K., Woolley, D. G., Steyaert, J., Di Martino, A., Swinnen, S. P., & Wenderoth, N. (2014). Underconnectivity of the superior temporal sulcus predicts emotion recognition deficits in autism. *Social Cognitive and Affective Neuroscience, 9*(10), 1589-1600.

Alloway, T. P. (2010). Working memory and executive function profiles of individuals with borderline intellectual functioning. *Journal of Intellectual Disability Research, 54*, 448-456.

American Psychiatric Association, D.-T. F. (2013). *Diagnostic and statistical manual of mental disorders: DSM-5TM* (5th ed. ed.): American Psychiatric Publishing, Inc.

Anderson, J. S., Nielsen, J. A., Froehlich, A. L., DuBray, M. B., Druzgal, T. J., Cariello, A. N., Cooperrider, J. R., Zielinski, B. A., Ravichandran, C., Fletcher, P. T., Alexander, A. L., Bigler, E. D., Lange, N., & Lainhart, J. E. (2011). Functional connectivity magnetic resonance imaging classification of autism. *Brain, 134*, 3739-3751.

Aoki, Y., Cortese, S., & Tansella, M. (2015). Neural bases of atypical emotional face processing in autism: A meta-analysis of fMRI studies. *World J Biol Psychiatry, 16*(5), 291-300.

APA. (2013). *Diagnostic and statistical manual of mental disorders (DSM-5®)*: American Psychiatric Pub.

Apicella, F., Costanzo, V., & Purpura, G. (2020). Are early visual behavior impairments involved in the onset of autism spectrum disorders? Insights for early diagnosis and intervention. *Eur J Pediatr, 179*(2), 225-234.

Assaf, M., Jagannathan, K., Calhoun, V. D., Miller, L., Stevens, M. C., Sahl, R., O'Boyle, J. G., Schultz, R. T., & Pearlson, G. D. (2010). Abnormal functional connectivity of default mode sub-networks in autism spectrum disorder patients. *Neuroimage, 53*(1), 247-256.

Balardin, J. B., Sato, J. R., Vieira, G., Feng, Y., Daly, E., Murphy, C., Consortium, M. A., Murphy, D., & Ecker, C. (2015). Relationship Between Surface-Based Brain Morphometric Measures and Intelligence in Autism Spectrum Disorders: Influence of History of Language Delay. *Autism Res, 8*(5), 556-566.

Banaji, M. R., Fiske, S. T., & Massey, D. S. (2021). Systemic racism: individuals and interactions, institutions and society. *Cogn Res Princ Implic, 6*(1), 82.

Baron-Cohen, S., Ring, H. A., Bullmore, E. T., Wheelwright, S., Ashwin, C., & Williams, S. C. (2000). The amygdala theory of autism. *Neurosci Biobehav Rev, 24*(3), 355-364.

Beauchamp, M. S., Lee, K. E., Haxby, J. V., & Martin, A. (2003). FMRI responses to video and point-light displays of moving humans and manipulable objects. *J Cogn Neurosci, 15*(7), 991-1001.

Bedford, R., Pickles, A., & Lord, C. (2016). Early gross motor skills predict the subsequent development of language in children with autism spectrum disorder. *Autism Res, 9*(9), 993-1001.

Bedford, S. A., Park, M. T. M., Devenyi, G. A., Tullo, S., Germann, J., Patel, R., Anagnostou, E., Baron-Cohen, S., Bullmore, E. T., Chura, L. R., Craig, M. C., Ecker, C., Floris, D. L., Holt, R. J., Lenroot, R., Lerch, J. P., Lombardo, M. V., Murphy, D. G. M., Raznahan, A., Ruigrok, A. N. V., Smith, E., Spencer, M. D., Suckling, J., Taylor, M. J., Thurm, A., Consortium, M. A., Lai, M. C., & Chakravarty, M. M. (2020). Large-scale analyses of the relationship between sex, age and intelligence quotient heterogeneity and cortical morphometry in autism spectrum disorder. *Mol Psychiatry, 25*(3), 614-628.

Behrmann, M., Thomas, C., & Humphreys, K. (2006). Seeing it differently: visual processing in autism. *Trends Cogn Sci, 10*(6), 258-264.

Behzadi, Y., Restom, K., Liau, J., & Liu, T. T. (2007). A component based noise correction method (CompCor) for BOLD and perfusion based fMRI. *Neuroimage, 37*(1), 90-101.

Ben-Itzchak, E., & Zachor, D. A. (2020). Toddlers to teenagers: Long-term follow-up study of outcomes in autism spectrum disorder. *Autism, 24*(1), 41-50.

Bethlehem, R. A. I., Seidlitz, J., White, S. R., Vogel, J. W., Anderson, K. M., Adamson, C., Adler, S., Alexopoulos, G. S., Anagnostou, E., Areces-Gonzalez, A., Astle, D. E., Auyeung, B., Ayub, M., Bae, J., Ball, G., Baron-Cohen, S., Beare, R., Bedford, S. A., Benegal, V., Beyer, F., Blangero, J., Blesa Cabez, M., Boardman, J. P., Borzage, M., Bosch-Bayard, J. F., Bourke, N., Calhoun, V. D., Chakravarty, M. M., Chen, C., Chertavian, C., Chetelat, G., Chong, Y. S., Cole, J. H., Corvin, A., Costantino, M., Courchesne, E., Crivello, F., Cropley, V. L., Crosbie, J., Crossley, N., Delarue, M., Delorme, R., Desrivieres, S., Devenyi, G. A., Di Biase, M. A., Dolan, R., Donald, K. A., Donohoe, G., Dunlop, K., Edwards, A. D., Elison, J. T., Ellis, C. T., Elman, J. A., Eyler, L., Fair, D. A., Feczko, E., Fletcher, P. C., Fonagy, P., Franz, C. E., Galan-Garcia, L., Gholipour, A., Giedd, J., Gilmore, J. H., Glahn, D. C., Goodyer, I. M., Grant, P. E., Groenewold, N. A., Gunning, F. M., Gur, R. E., Gur, R. C., Hammill, C. F., Hansson, O., Hedden, T., Heinz, A., Henson, R. N., Heuer, K., Hoare, J., Holla, B., Holmes, A. J., Holt, R., Huang, H., Im, K., Ipser, J., Jack, C. R., Jr., Jackowski, A. P., Jia, T., Johnson, K. A., Jones, P. B., Jones, D. T., Kahn, R. S., Karlsson, H., Karlsson, L., Kawashima, R., Kelley, E. A., Kern, S., Kim, K. W., Kitzbichler, M. G., Kremen, W. S., Lalonde, F., Landeau, B., Lee, S., Lerch, J., Lewis, J. D., Li, J., Liao, W., Liston, C., Lombardo, M. V., Lv, J., Lynch, C., Mallard, T. T., Marcelis, M., Markello, R. D., Mathias, S. R., Mazoyer, B., McGuire, P., Meaney, M. J., Mechelli, A., Medic, N., Misic, B., Morgan, S. E., Mothersill, D., Nigg, J., Ong, M. Q. W., Ortinau, C., Ossenkoppele, R., Ouyang, M., Palaniyappan, L., Paly, L., Pan, P. M., Pantelis, C., Park, M. M., Paus, T., Pausova, Z., Paz-Linares, D., Pichet Binette, A., Pierce, K., Qian, X., Qiu, J., Qiu, A., Raznahan, A., Rittman, T., Rodrigue, A., Rollins, C. K., Romero-Garcia, R., Ronan, L., Rosenberg, M. D., Rowitch, D. H., Salum, G. A., Satterthwaite, T. D., Schaare, H. L., Schachar, R. J., Schultz, A. P., Schumann, G., Scholl, M., Sharp, D., Shinohara, R. T., Skoog, I., Smyser, C. D., Sperling, R. A., Stein, D. J., Stolicyn, A., Suckling, J., Sullivan, G., Taki, Y., Thyreau, B., Toro, R., Traut, N., Tsvetanov, K. A., Turk-Browne, N. B., Tuulari, J. J., Tzourio, C., Vachon-Presseau, E., Valdes-Sosa, M. J., Valdes-Sosa, P. A., Valk, S. L., van Amelsvoort, T., Vandekar, S. N., Vasung, L., Victoria, L. W., Villeneuve, S., Villringer, A., Vertes, P. E., Wagstyl, K., Wang, Y. S., Warfield, S. K., Warrier, V., Westman, E., Westwater, M. L., Whalley, H. C., Witte, A. V., Yang, N., Yeo, B., Yun, H., Zalesky, A., Zar, H. J., Zettergren, A., Zhou, J. H., Ziauddeen, H., Zugman, A., Zuo, X. N., R, B., Aibl, Alzheimer's Disease Neuroimaging, I., Alzheimer's Disease Repository Without Borders, I., Team, C., Cam, C. A. N., Ccnp, Cobre, cVeda, Group, E. D. B. A. W., Developing Human Connectome, P., FinnBrain, Harvard Aging Brain, S., Imagen, Kne, Mayo Clinic Study of, A., Nspn, Pond, Group, P.-A. R., Vetsa, Bullmore, E. T., & Alexander-Bloch, A. F. (2022). Brain charts for the human lifespan. *Nature, 604*(7906), 525-533.

Bishop-Fitzpatrick, L., & Kind, A. J. H. (2017). A Scoping Review of Health Disparities in Autism Spectrum Disorder. *J Autism Dev Disord, 47*(11), 3380-3391.

Biswal, B., Yetkin, F. Z., Haughton, V. M., & Hyde, J. S. (1995). Functional Connectivity in the Motor Cortex of Resting Human Brain Using Echo-Planar Mri. *Magnetic Resonance in Medicine, 34*(4), 537-541.

Bonnet-Brilhault, F., Rajerison, T. A., Paillet, C., Guimard-Brunault, M., Saby, A., Ponson, L., Tripi, G., Malvy, J., & Roux, S. (2018). Autism is a prenatal disorder: Evidence from late gestation brain overgrowth. *Autism Res, 11*(12), 1635-1642.

Borich, M. R., Brodie, S. M., Gray, W. A., Ionta, S., & Boyd, L. A. (2015). Understanding the role of the primary somatosensory cortex: Opportunities for rehabilitation. *Neuropsychologia, 79*(Pt B), 246-255.

Brouwer, R. M., van Soelen, I. L., Swagerman, S. C., Schnack, H. G., Ehli, E. A., Kahn, R. S., Hulshoff Pol, H. E., & Boomsma, D. I. (2014). Genetic associations between intelligence and cortical thickness emerge at the start of puberty. *Hum Brain Mapp, 35*(8), 3760-3773.

Bruchhage, M. M. K., Ngo, G. C., Schneider, N., D'Sa, V., & Deoni, S. C. L. (2020). Functional connectivity correlates of infant and early childhood cognitive development. *Brain Struct Funct, 225*(2), 669-681.

Burgaleta, M., Johnson, W., Waber, D. P., Colom, R., & Karama, S. (2014). Cognitive ability changes and dynamics of cortical thickness development in healthy children and adolescents. *Neuroimage, 84*, 810-819.

Cascio, C. J. (2010). Somatosensory processing in neurodevelopmental disorders. *J Neurodev Disord, 2*(2), 62-69.

Center for Disease Control and Prevention. (2014). Prevalence of autism spectrum disorder among children aged 8 years - Autism and Developmental Disabilities Monitoring Network, 11 Sites, United States, 2010. *Morbidity and Mortality Weekly Reports, 63(SS02)*, 2-21.

Chakrabarti, B. (2017). Commentary: Critical considerations for studying low-functioning autism. *Journal of Child Psychology and Psychiatry, 58*(4), 436-438.

Chen, B., Linke, A., Olson, L., Ibarra, C., Kinnear, M., & Fishman, I. (2021). Resting state functional networks in 1-to-3-year-old typically developing children. *Dev Cogn Neurosci, 51*, 100991.

Chen, B., Linke, A., Olson, L., Ibarra, C., Reynolds, S., Müller, R. A., Kinnear, M., & Fishman, I. (2021). Greater functional connectivity between sensory networks is related to symptom severity in toddlers with autism spectrum disorder. *J Child Psychol Psychiatry*.

Chiurazzi, P., Kiani, A. K., Miertus, J., Paolacci, S., Barati, S., Manara, E., Stuppia, L., Gurrieri, F., & Bertelli, M. (2020). Genetic analysis of intellectual disability and autism. *Acta Biomed, 91*(13-S), e2020003.

Chung, S., & Son, J. W. (2020). Visual Perception in Autism Spectrum Disorder: A Review of Neuroimaging Studies. *Soa Chongsonyon Chongsin Uihak, 31*(3), 105-120.

Courchesne, E., Campbell, K., & Solso, S. (2011). Brain growth across the life span in autism: age-specific changes in anatomical pathology. *Brain Res, 1380*, 138-145.

Courchesne, E., Carper, R., & Akshoomoff, N. (2003). Evidence of brain overgrowth in the first year of life in autism. *JAMA, 290*(3), 337-344.

Courchesne, E., Gazestani, V. H., & Lewis, N. E. (2020). Prenatal Origins of ASD: The When, What, and How of ASD Development. *Trends Neurosci, 43*(5), 326-342.

Cox, A. D., Virues-Ortega, J., Julio, F., & Martin, T. L. (2017). Establishing motion control in children with autism and intellectual disability: Applications for anatomical and functional MRI. *J Appl Behav Anal, 50*(1), 8-26.

Cox, R. W. (1996). AFNI: Software for analysis and visualization of functional magnetic resonance neuroimages. *Computers and Biomedical Research, 29*(3), 162-173.

Cox, R. W., Chen, G., Glen, D. R., Reynolds, R. C., & Taylor, P. A. (2017). FMRI Clustering in AFNI: False-Positive Rates Redux. *Brain Connect, 7*(3), 152-171.

Crocker, N., Riley, E. P., & Mattson, S. N. (2015). Visual-Spatial Abilities Relate to Mathematics Achievement in Children With Heavy Prenatal Alcohol Exposure. *Neuropsychology, 29*(1), 108-116.

D'Mello, A. M., & Stoodley, C. J. (2015). Cerebro-cerebellar circuits in autism spectrum disorder. *Frontiers in Neuroscience, 9*.

Dale, A. M., Fischl, B., & Sereno, M. I. (1999). Cortical surface-based analysis. I. Segmentation and surface reconstruction. *Neuroimage, 9*(2), 179-194.

Desikan, R. S., Segonne, F., Fischl, B., Quinn, B. T., Dickerson, B. C., Blacker, D., Buckner, R. L., Dale, A. M., Maguire, R. P., Hyman, B. T., Albert, M. S., & Killiany, R. J. (2006). An

automated labeling system for subdividing the human cerebral cortex on MRI scans into gyral based regions of interest. *Neuroimage, 31*(3), 968-980.

Di Martino, A., O'Connor, D., Chen, B., Alaerts, K., Anderson, J. S., Assaf, M., Balsters, J. H., Baxter, L., Beggiato, A., Bernaerts, S., Blanken, L. M., Bookheimer, S. Y., Braden, B. B., Byrge, L., Castellanos, F. X., Dapretto, M., Delorme, R., Fair, D. A., Fishman, I., Fitzgerald, J., Gallagher, L., Keehn, R. J., Kennedy, D. P., Lainhart, J. E., Luna, B., Mostofsky, S. H., Müller, R. A., Nebel, M. B., Nigg, J. T., O'Hearn, K., Solomon, M., Toro, R., Vaidya, C. J., Wenderoth, N., White, T., Craddock, R. C., Lord, C., Leventhal, B., & Milham, M. P. (2017a). Enhancing studies of the connectome in autism using the autism brain imaging data exchange II. *Scientific Data, 4*, 170010.

Di Martino, A., O'Connor, D., Chen, B., Alaerts, K., Anderson, J. S., Assaf, M., Balsters, J. H., Baxter, L., Beggiato, A., Bernaerts, S., Blanken, L. M. E., Bookheimer, S. Y., Braden, B. B., Byrge, L., Castellanos, F. X., Dapretto, M., Delorme, R., Fair, D. A., Fishman, I., Fitzgerald, J., Gallagher, L., Keehn, R. J. J., Kennedy, D. P., Lainhart, J. E., Luna, B., Mostofsky, S. H., Müller, R. A., Nebel, M. B., Nigg, J. T., O'Hearn, K., Solomon, M., Toro, R., Vaidya, C. J., Wenderoth, N., White, T., Craddock, R. C., Lord, C., Leventhal, B., & Milham, M. P. (2017). Data Descriptor: Enhancing studies of the connectome in autism using the autism brain imaging data exchange II. *Scientific Data, 4*.

Di Martino, A., Yan, C. G., Li, Q., Denio, E., Castellanos, F. X., Alaerts, K., Anderson, J. S., Assaf, M., Bookheimer, S. Y., Dapretto, M., Deen, B., Delmonte, S., Dinstein, I., Ertl-Wagner, B., Fair, D. A., Gallagher, L., Kennedy, D. P., Keown, C. L., Keysers, C., Lainhart, J. E., Lord, C., Luna, B., Menon, V., Minshew, N. J., Monk, C. S., Mueller, S., Müller, R. A., Nebel, M. B., Nigg, J. T., O'Hearn, K., Pelphrey, K. A., Peltier, S. J., Rudie, J. D., Sunaert, S., Thioux, M., Tyszka, J. M., Uddin, L. Q., Verhoeven, J. S., Wenderoth, N., Wiggins, J. L., Mostofsky, S. H., & Milham, M. P. (2014). The autism brain imaging data exchange: towards a large-scale evaluation of the intrinsic brain architecture in autism. *Mol Psychiatry, 19*(6), 659-667.

Dichter, G. S. (2012). Functional magnetic resonance imaging of autism spectrum disorders. *Dialogues Clin Neurosci, 14*(3), 319-351.

Dinstein, I., Pierce, K., Eyler, L., Solso, S., Malach, R., Behrmann, M., & Courchesne, E. (2011). Disrupted Neural Synchronization in Toddlers with Autism. *Neuron, 70*(6), 1218-1225.

Dionne-Dostie, E., Paquette, N., Lassonde, M., & Gallagher, A. (2015). Multisensory integration and child neurodevelopment. *Brain Sci, 5*(1), 32-57.

Donovan, A. P., & Basson, M. A. (2017). The neuroanatomy of autism - a developmental perspective. *J Anat, 230*(1), 4-15.

Doyle-Thomas, K. A., Lee, W., Foster, N. E., Tryfon, A., Ouimet, T., Hyde, K. L., Evans, A. C., Lewis, J., Zwaigenbaum, L., Anagnostou, E., & NeuroDevNet, A. S. D. I. G. (2015). Atypical functional brain connectivity during rest in autism spectrum disorders. *Ann Neurol, 77*(5), 866-876.

Ecker, C. (2017). The neuroanatomy of autism spectrum disorder: An overview of structural neuroimaging findings and their translatability to the clinical setting. *Autism, 21*(1), 18-28.

Edirisooriya, M., Dykiert, D., & Auyeung, B. (2021). IQ and Internalising Symptoms in Adolescents with ASD. *J Autism Dev Disord, 51*(11), 3887-3907.

Eggebrecht, A. T., Elison, J. T., Feczko, E., Todorov, A., Wolff, J. J., Kandala, S., Adams, C. M., Snyder, A. Z., Lewis, J. D., Estes, A. M., Zwaigenbaum, L., Botteron, K. N., McKinstry, R. C., Constantino, J. N., Evans, A., Hazlett, H. C., Dager, S., Paterson, S. J., Schultz, R. T., Styner, M. A., Gerig, G., Das, S., Kostopoulos, P., Schlaggar, B. L., Petersen, S. E., Piven, J., Pruett, J. R., & Network, I. (2017). Joint Attention and Brain Functional Connectivity in Infants and Toddlers. *Cerebral Cortex, 27*(3), 1709-1720.

Eklund, A., Nichols, T. E., & Knutsson, H. (2016). Cluster failure: Why fMRI inferences for spatial extent have inflated false-positive rates. *Proc Natl Acad Sci U S A, 113*(28), 7900-7905.

Erbetta, A., Bulgheroni, S., Contarino, V. E., Chiapparini, L., Esposito, S., Annunziata, S., & Riva, D. (2015). Low-Functioning Autism and Nonsyndromic Intellectual Disability: Magnetic Resonance Imaging (MRI) Findings. *J Child Neurol, 30*(12), 1658-1663.

Eyler, L. T., Pierce, K., & Courchesne, E. (2012). A failure of left temporal cortex to specialize for language is an early emerging and fundamental property of autism. *Brain, 135*, 949-960.

Falahpour, M., Thompson, W. K., Abbott, A. E., Jahedi, A., Mulvey, M. E., Datko, M., Liu, T. T., & Müller, R. A. (2016). Underconnected, But Not Broken? Dynamic Functional Connectivity MRI Shows Underconnectivity in Autism Is Linked to Increased Intra-Individual Variability Across Time. *Brain Connectivity, 6*(5), 403-413.

Feldman, J. I., Dunham, K., Cassidy, M., Wallace, M. T., Liu, Y., & Woynaroski, T. G. (2018). Audiovisual multisensory integration in individuals with autism spectrum disorder: A systematic review and meta-analysis. *Neurosci Biobehav Rev, 95*, 220-234.

Fields, R. D. (2010). Neuroscience. Change in the brain's white matter. *Science, 330*(6005), 768-769.

Fischl, B., Sereno, M. I., & Dale, A. M. (1999). Cortical surface-based analysis. II: Inflation, flattening, and a surface-based coordinate system. *Neuroimage, 9*(2), 195-207.

Fishman, I., Datko, M., Cabrera, Y., Carper, R. A., & Müller, R. A. (2015). Reduced Integration and Differentiation of the Imitation Network in Autism: A Combined Functional Connectivity Magnetic Resonance Imaging and Diffusion-Weighted Imaging Study. *Annals of Neurology, 78*(6), 958-969.

Fishman, I., Keown, C. L., Lincoln, A. J., Pineda, J. A., & Müller, R. A. (2014). Atypical cross talk between mentalizing and mirror neuron networks in autism spectrum disorder. *Jama Psychiatry, 71*(7), 751-760.

Fishman, I., Linke, A. C., Hau, J., Carper, R. A., & Müller, R. A. (2018). Atypical Functional Connectivity of Amygdala Related to Reduced Symptom Severity in Children With Autism. *J Am Acad Child Adolesc Psychiatry, 57*(10), 764-774 e763.

Fortin, J. P., Cullen, N., Sheline, Y. I., Taylor, W. D., Aselcioglu, I., Cook, P. A., Adams, P., Cooper, C., Fava, M., McGrath, P. J., McInnis, M., Phillips, M. L., Trivedi, M. H., Weissman, M. M., & Shinohara, R. T. (2018). Harmonization of cortical thickness measurements across scanners and sites. *Neuroimage, 167*, 104-120.

Frangou, S., Modabbernia, A., Williams, S. C. R., Papachristou, E., Doucet, G. E., Agartz, I., Aghajani, M., Akudjedu, T. N., Albajes-Eizagirre, A., Alnaes, D., Alpert, K. I., Andersson, M., Andreasen, N. C., Andreassen, O. A., Asherson, P., Banaschewski, T., Bargallo, N., Baumeister, S., Baur-Streubel, R., Bertolino, A., Bonvino, A., Boomsma, D. I., Borgwardt, S., Bourque, J., Brandeis, D., Breier, A., Brodaty, H., Brouwer, R. M., Buitelaar, J. K., Busatto, G. F., Buckner, R. L., Calhoun, V., Canales-Rodriguez, E. J., Cannon, D. M., Caseras, X., Castellanos, F. X., Cervenka, S., Chaim-Avancini, T. M., Ching, C. R. K., Chubar, V., Clark, V. P., Conrod, P., Conzelmann, A., Crespo-Facorro, B., Crivello, F., Crone, E. A., Dale, A. M., Dannlowski, U., Davey, C., de Geus, E. J. C., de Haan, L., de Zubicaray, G. I., den Braber, A., Dickie, E. W., Di Giorgio, A., Doan, N. T., Dorum, E. S., Ehrlich, S., Erk, S., Espeseth, T., Fatouros-Bergman, H., Fisher, S. E., Fouche, J. P., Franke, B., Frodl, T., Fuentes-Claramonte, P., Glahn, D. C., Gotlib, I. H., Grabe, H. J., Grimm, O., Groenewold, N. A., Grotegerd, D., Gruber, O., Gruner, P., Gur, R. E., Gur, R.

C., Hahn, T., Harrison, B. J., Hartman, C. A., Hatton, S. N., Heinz, A., Heslenfeld, D. J., Hibar, D. P., Hickie, I. B., Ho, B. C., Hoekstra, P. J., Hohmann, S., Holmes, A. J., Hoogman, M., Hosten, N., Howells, F. M., Hulshoff Pol, H. E., Huyser, C., Jahanshad, N., James, A., Jernigan, T. L., Jiang, J., Jonsson, E. G., Joska, J. A., Kahn, R., Kalnin, A., Kanai, R., Klein, M., Klyushnik, T. P., Koenders, L., Koops, S., Kramer, B., Kuntsi, J., Lagopoulos, J., Lazaro, L., Lebedeva, I., Lee, W. H., Lesch, K. P., Lochner, C., Machielsen, M. W. J., Maingault, S., Martin, N. G., Martinez-Zalacain, I., Mataix-Cols, D., Mazoyer, B., McDonald, C., McDonald, B. C., McIntosh, A. M., McMahon, K. L., McPhilemy, G., Meinert, S., Menchon, J. M., Medland, S. E., Meyer-Lindenberg, A., Naaijen, J., Najt, P., Nakao, T., Nordvik, J. E., Nyberg, L., Oosterlaan, J., de la Foz, V. O., Paloyelis, Y., Pauli, P., Pergola, G., Pomarol-Clotet, E., Portella, M. J., Potkin, S. G., Radua, J., Reif, A., Rinker, D. A., Roffman, J. L., Rosa, P. G. P., Sacchet, M. D., Sachdev, P. S., Salvador, R., Sanchez-Juan, P., Sarro, S., Satterthwaite, T. D., Saykin, A. J., Serpa, M. H., Schmaal, L., Schnell, K., Schumann, G., Sim, K., Smoller, J. W., Sommer, I., Soriano-Mas, C., Stein, D. J., Strike, L. T., Swagerman, S. C., Tamnes, C. K., Temmingh, H. S., Thomopoulos, S. I., Tomyshev, A. S., Tordesillas-Gutierrez, D., Trollor, J. N., Turner, J. A., Uhlmann, A., van den Heuvel, O. A., van den Meer, D., van der Wee, N. J. A., van Haren, N. E. M., van 't Ent, D., van Erp, T. G. M., Veer, I. M., Veltman, D. J., Voineskos, A., Volzke, H., Walter, H., Walton, E., Wang, L., Wang, Y., Wassink, T. H., Weber, B., Wen, W., West, J. D., Westlye, L. T., Whalley, H., Wierenga, L. M., Wittfeld, K., Wolf, D. H., Worker, A., Wright, M. J., Yang, K., Yoncheva, Y., Zanetti, M. V., Ziegler, G. C., Karolinska Schizophrenia, P., Thompson, P. M., & Dima, D. (2022). Cortical thickness across the lifespan: Data from 17,075 healthy individuals aged 3-90 years. *Hum Brain Mapp, 43*(1), 431-451.

Gabrielsen, T. P., Anderson, J. S., Stephenson, K. G., Beck, J., King, J. B., Kellems, R., Top, D. N., Jr., Russell, N. C. C., Anderberg, E., Lundwall, R. A., Hansen, B., & South, M. (2018). Functional MRI connectivity of children with autism and low verbal and cognitive performance. *Mol Autism, 9*, 67.

Gaffrey, M. S., Kleinhans, N. M., Haist, F., Akshoomoff, N., Campbell, A., Courchesne, E., & Müller, R. A. (2007). Atypical participation of visual cortex during word processing in autism: An fMRI study of semantic decision (vol 45, pg 1672, 2007). *Neuropsychologia, 45*(11), 2644-2644.

Gammer, I., Bedford, R., Elsabbagh, M., Garwood, H., Pasco, G., Tucker, L., Volein, A., Johnson, M. H., Charman, T., & Team, B. (2015). Behavioural markers for autism in infancy: scores on the Autism Observational Scale for Infants in a prospective study of at-risk siblings. *Infant Behavior & Development, 38*, 107-115.

Gangi, D. N., Ibanez, L. V., & Messinger, D. S. (2014). Joint attention initiation with and without positive affect: risk group differences and associations with ASD symptoms. *J Autism Dev Disord, 44*(6), 1414-1424.

Gangi, D. N., Schwichtenberg, A. J., Iosif, A. M., Young, G. S., Baguio, F., & Ozonoff, S. (2018). Gaze to faces across interactive contexts in infants at heightened risk for autism. *Autism, 22*(6), 763-768.

Gao, W., Alcauter, S., Smith, J. K., Gilmore, J. H., & Lin, W. (2015). Development of human brain cortical network architecture during infancy. *Brain Struct Funct, 220*(2), 1173-1186.

Gao, Y., Linke, A., Jao Keehn, R. J., Punyamurthula, S., Jahedi, A., Gates, K., Fishman, I., & Müller, R. A. (2019). The language network in autism: Atypical functional connectivity with default mode and visual regions. *Autism Res, 12*(9), 1344-1355.

Geschwind, D. H., & Rakic, P. (2013). Cortical evolution: judge the brain by its cover. *Neuron, 80*(3), 633-647.

Gilmore, J. H., Shi, F., Woolson, S. L., Knickmeyer, R. C., Short, S. J., Lin, W., Zhu, H., Hamer, R. M., Styner, M., & Shen, D. (2012). Longitudinal development of cortical and subcortical gray matter from birth to 2 years. *Cerebral Cortex, 22*(11), 2478-2485.

Girault, J. B., Langworthy, B. W., Goldman, B. D., Stephens, R. L., Cornea, E., Reznick, J. S., Fine, J., & Gilmore, J. H. (2018). The predictive value of developmental assessments at 1 and 2 for intelligence quotients at 6. *Intelligence, 68*, 58-65.

Girault, J. B., & Piven, J. (2020). The Neurodevelopment of Autism from Infancy Through Toddlerhood. *Neuroimaging Clin N Am, 30*(1), 97-114.

Gogtay, N., & Thompson, P. M. (2010). Mapping gray matter development: implications for typical development and vulnerability to psychopathology. *Brain Cogn, 72*(1), 6-15.

Gotham, K., Risi, S., Pickles, A., & Lord, C. (2007). The autism diagnostic observation schedule: Revised algorithms for improved diagnostic validity. *Journal of Autism and Developmental Disorders, 37*(4), 613-627.

Gould, S. J. (2008). *The mismeasure of man* (Rev. and expanded, with a new introduction. ed.). New York: W.W. Norton.

Green, S. A., Hernandez, L., Tottenham, N., Krasileva, K., Bookheimer, S. Y., & Dapretto, M. (2015). Neurobiology of Sensory Overresponsivity in Youth With Autism Spectrum Disorders. *Jama Psychiatry, 72*(8), 778-786.

Hadjikhani, N., Chabris, C. F., Joseph, R. M., Clark, J., McGrath, L., Aharon, I., Feczko, E., Tager-Flusberg, H., & Harris, G. J. (2004). Early visual cortex organization in autism: an fMRI study. *Neuroreport, 15*(2), 267-270.

Hadjikhani, N., Joseph, R. M., Snyder, J., & Tager-Flusberg, H. (2006). Anatomical differences in the mirror neuron system and social cognition network in autism. *Cerebral Cortex, 16*(9), 1276-1282.

Hampson, M., Driesen, N., Roth, J. K., Gore, J. C., & Constable, R. T. (2010). Functional connectivity between task-positive and task-negative brain areas and its relation to working memory performance. *Magnetic Resonance Imaging, 28*(8), 1051-1057.

Hand, B. N., Angell, A. M., Harris, L., & Carpenter, L. A. (2020). Prevalence of physical and mental health conditions in Medicare-enrolled, autistic older adults. *Autism, 24*(3), 755-764.

Hardan, A. Y., Muddasani, S., Vemulapalli, M., Keshavan, M. S., & Minshew, N. J. (2006). An MRI study of increased cortical thickness in autism. *American Journal of Psychiatry, 163*(7), 1290-1292.

Hazlett, H. C., Poe, M. D., Gerig, G., Styner, M., Chappell, C., Smith, R. G., Vachet, C., & Piven, J. (2011). Early Brain Overgrowth in Autism Associated With an Increase in Cortical Surface Area Before Age 2 Years. *Archives of General Psychiatry, 68*(5), 467-476.

He, Y., Byrge, L., & Kennedy, D. P. (2020). Nonreplication of functional connectivity differences in autism spectrum disorder across multiple sites and denoising strategies. *Hum Brain Mapp, 41*(5), 1334-1350.

Hossain, M. M., Khan, N., Sultana, A., Ma, P., McKyer, E. L. J., Ahmed, H. U., & Purohit, N. (2020). Prevalence of comorbid psychiatric disorders among people with autism spectrum disorder: An umbrella review of systematic reviews and meta-analyses. *Psychiatry Res, 287*, 112922.

Huijbers, W., Van Dijk, K. R. A., Boenniger, M. M., Stirnberg, R., & Breteler, M. M. B. (2016). Less head motion during MRI under task than resting-state conditions. *Neuroimage, 147*, 111-120.

Hull, J. V., Jacokes, Z. J., Torgerson, C. M., Irimia, A., & Van Horn, J. D. (2017). Resting-State Functional Connectivity in Autism Spectrum Disorders: A Review. *Front Psychiatry, 7*, 205.

Hull, J. V., Jacokes, Z. J., Torgerson, C. M., Irimia, A., Van Horn, J. D., & Consortium, G. R. (2017). Resting-State Functional Connectivity in Autism Spectrum Disorders: A Review. *Frontiers in Psychiatry, 7*.

Hyde, K. L., Samson, F., Evans, A. C., & Mottron, L. (2010). Neuroanatomical Differences in Brain Areas Implicated in Perceptual and Other Core Features of Autism Revealed by Cortical Thickness Analysis and Voxel-Based Morphometry. *Human Brain Mapping, 31*(4), 556-566.

Iakoucheva, L. M., Muotri, A. R., & Sebat, J. (2019). Getting to the Cores of Autism. *Cell, 178*(6), 1287-1298.

Jack, A., & Pelphrey, K. A. (2017). Annual Research Review: Understudied populations within the autism spectrum - current trends and future directions in neuroimaging research. *J Child Psychol Psychiatry, 58*(4), 411-435.

Jarrold, C., & Brock, J. (2004). To match or not to match? Methodological issues in autism-related research. *Journal of Autism and Developmental Disorders, 34*(1), 81-86.

Jiao, Y., Chen, R., Ke, X. Y., Chu, K. K., Lu, Z. H., & Herskovits, E. H. (2010). Predictive models of autism spectrum disorder based on brain regional cortical thickness. *Neuroimage, 50*(2), 589-599.

Joseph, R. M., Tager-Flusberg, H., & Lord, C. (2002). Cognitive profiles and social-communicative functioning in children with autism spectrum disorder. *J Child Psychol Psychiatry, 43*(6), 807-821.

Joshi, G., Gabrieli, J., Biederman, J., & Whitfield-Gabrieli, S. (2015). Integration and segregation of default mode network resting-state functional connectivity in high-functioning autism spectrum disorder. *European Neuropsychopharmacology, 25*, S190-S191.

Jung, M., Kosaka, H., Saito, D. N., Ishitobi, M., Morita, T., Inohara, K., Asano, M., Arai, S., Munesue, T., Tomoda, A., Wada, Y., Sadato, N., Okazawa, H., & Iidaka, T. (2014). Default mode network in young male adults with autism spectrum disorder: relationship with autism spectrum traits. *Mol Autism, 5*, 35.

Just, M. A., Cherkassky, V. L., Keller, T. A., & Minshew, N. J. (2004). Cortical activation and synchronization during sentence comprehension in high-functioning autism: evidence of underconnectivity. *Brain, 127*(Pt 8), 1811-1821.

Kanner, L. (1943). Autistic disturbances of affective contact. *Nervous child*.

Keehn, R. J. J., Sanchez, S. S., Stewart, C. R., Zhao, W. Q., Grenesko-Stevens, E. L., Keehn, B., & Müller, R. A. (2017). Impaired downregulation of visual cortex during auditory processing is associated with autism symptomatology in children and adolescents with autism spectrum disorder. *Autism Research, 10*(1), 130-143.

Kellerman, A. M., Schwichtenberg, A. J., Abu-Zhaya, R., Miller, M., Young, G. S., & Ozonoff, S. (2020). Dyadic Synchrony and Responsiveness in the First Year: Associations with Autism Risk. *Autism Research, 13*(12), 2190-2201.

Kennedy, D. P., Redcay, E., & Courchesne, E. (2006). Failing to deactivate: resting functional abnormalities in autism. *Proceedings of the National Academy of Sciences of the United States of America, 103*(21), 8275-8280.

Kim, J. I., Bang, S., Yang, J. J., Kwon, H., Jang, S., Roh, S., Kim, S. H., Kim, M. J., Lee, H. J., Lee, J. M., & Kim, B. N. (2022). Classification of Preschoolers with Low-Functioning Autism Spectrum Disorder Using Multimodal MRI Data. *J Autism Dev Disord*.

King, J. B., Prigge, M. B. D., King, C. K., Morgan, J., Weathersby, F., Fox, J. C., Dean, D. C., 3rd, Freeman, A., Villaruz, J. A. M., Kane, K. L., Bigler, E. D., Alexander, A. L., Lange, N., Zielinski, B., Lainhart, J. E., & Anderson, J. S. (2019). Generalizability and reproducibility of functional connectivity in autism. *Mol Autism, 10*, 27.

Kissine, M., Bertels, J., Deconinck, N., Passeri, G., & Deliens, G. (2021). Audio-visual integration in nonverbal or minimally verbal young autistic children. *J Exp Psychol Gen, 150*(10), 2137-2157.

Kleinhans, N. M., Reiter, M. A., Neuhaus, E., Pauley, G., Martin, N., Dager, S., & Estes, A. (2016). Subregional differences in intrinsic amygdala hyperconnectivity and hypoconnectivity in autism spectrum disorder. *Autism Res, 9*(7), 760-772.

Kohli, J. S., Kinnear, M. K., Fong, C. H., Fishman, I., Carper, R. A., & Müller, R. A. (2019). Local Cortical Gyrification is Increased in Children With Autism Spectrum Disorders, but Decreases Rapidly in Adolescents. *Cerebral Cortex, 29*(6), 2412-2423.

Korhonen, V., Kärnä, E., & Räty, H. (2014). Autism spectrum disorder and impaired joint attention: A review of joint attention research from the past decade. *Nordic Psychology, 66*(2), 94-107.

Lai, G., Pantazatos, S. P., Schneider, H., & Hirsch, J. (2012). Neural systems for speech and song in autism. *Brain, 135*, 961-975.

Laidi, C., Boisgontier, J., de Pierrefeu, A., Duchesnay, E., Hotier, S., d'Albis, M. A., Delorme, R., Bolognani, F., Czech, C., Bouquet, C., Amestoy, A., Petit, J., Holiga, S., Dukart, J., Gaman, A., Toledano, E., Ly-Le Moal, M., Scheid, I., Leboyer, M., & Houenou, J. (2019). Decreased Cortical Thickness in the Anterior Cingulate Cortex in Adults with Autism. *Journal of Autism and Developmental Disorders, 49*(4), 1402-1409.

Lange, N., Travers, B. G., Bigler, E. D., Prigge, M. B. D., Froehlich, A. L., Nielsen, J. A., Cariello, A. N., Zielinski, B. A., Anderson, J. S., Fletcher, P. T., Alexander, A. A., & Lainhart, J. E. (2015). Longitudinal Volumetric Brain Changes in Autism Spectrum Disorder Ages 6-35 Years. *Autism Research, 8*(1), 82-93.

Lenroot, R. K., & Yeung, P. K. (2013). Heterogeney within autism spectrum disorders: what have we learned from neuroimaging studies? *Frontiers in Human Neuroscience, 7*.

Lerch, J. P., van der Kouwe, A. J., Raznahan, A., Paus, T., Johansen-Berg, H., Miller, K. L., Smith, S. M., Fischl, B., & Sotiropoulos, S. N. (2017). Studying neuroanatomy using MRI. *Nature Neuroscience, 20*(3), 314-326.

Leyfer, O. T., Folstein, S. E., Bacalman, S., Davis, N. O., Dinh, E., Morgan, J., Tager-Flusberg, H., & Lainhart, J. E. (2006). Comorbid psychiatric disorders in children with autism: interview development and rates of disorders. *J Autism Dev Disord, 36*(7), 849-861.

Li, C., & Tian, L. (2014). Association between Resting-State Coactivation in the Parieto-Frontal Network and Intelligence during Late Childhood and Adolescence. *American Journal of Neuroradiology, 35*(6), 1150-1156.

Li, G., Rossbach, K., Jiang, W., & Du, Y. (2018). Resting-state brain activity in Chinese boys with low functioning autism spectrum disorder. *Ann Gen Psychiatry, 17*, 47.

Linke, A. C., Olson, L., Gao, Y., Fishman, I., & Müller, R. A. (2017). Psychotropic medication use in autism spectrum disorders may affect functional brain connectivity. *Biol Psychiatry Cogn Neurosci Neuroimaging, 2*(6), 518-527.

Lombardo, M. V., Eyler, L., Moore, A., Datko, M., Carter Barnes, C., Cha, D., Courchesne, E., & Pierce, K. (2019). Default mode-visual network hypoconnectivity in an autism subtype with pronounced social visual engagement difficulties. *Elife, 8*.

Lombardo, M. V., Lai, M. C., & Baron-Cohen, S. (2019). Big data approaches to decomposing heterogeneity across the autism spectrum. *Mol Psychiatry, 24*(10), 1435-1450.

Lombardo, M. V., Pierce, K., Eyler, L. T., Barnes, C. C., Ahrens-Barbeau, C., Solso, S., Campbell, K., & Courchesne, E. (2015). Different Functional Neural Substrates for Good and Poor Language Outcome in Autism. *Neuron, 86*(2), 567-577.

Lord, C., Brugha, T. S., Charman, T., Cusack, J., Dumas, G., Frazier, T., Jones, E. J. H., Jones, R. M., Pickles, A., State, M. W., Taylor, J. L., & Veenstra-VanderWeele, J. (2020). Autism spectrum disorder. *Nat Rev Dis Primers, 6*(1), 5.

Lord, C., Elsabbagh, M., Baird, G., & Veenstra-Vanderweele, J. (2018). Autism spectrum disorder. *Lancet, 392*(10146), 508-520.

Lord, C., McCauley, J. B., Pepa, L. A., Huerta, M., & Pickles, A. (2020). Work, living, and the pursuit of happiness: Vocational and psychosocial outcomes for young adults with autism. *Autism, 24*(7), 1691-1703.

Lord, C., Rutter, M., D'iLavore, P. C., Risi, S., Gotham, K., & Bishop, S. (2012). *Autism diagnostic observation schedule, second edition*. Torrance, CA: Western Psychological Services.

Lord, C., Rutter, M., Goode, S., Heemsbergen, J., Jordan, H., Mawhood, L., & Schopler, E. (1989). Autism diagnostic observation schedule: a standardized observation of communicative and social behavior. *J Autism Dev Disord, 19*(2), 185-212.

Lord, C., Rutter, M., & Le Couteur, A. (1994). Autism Diagnostic Interview-Revised: a revised version of a diagnostic interview for caregivers of individuals with possible pervasive developmental disorders. *J Autism Dev Disord, 24*(5), 659-685.

Lundstrom, S., Reichenberg, A., Anckarsater, H., Lichtenstein, P., & Gillberg, C. (2015). Autism phenotype versus registered diagnosis in Swedish children: prevalence trends over 10 years in general population samples. *BMJ, 350*, h1961.

Lynch, C. J., Uddin, L. Q., Supekar, K., Khouzam, A., Phillips, J., & Menon, V. (2013). Default mode network in childhood autism: posteromedial cortex heterogeneity and relationship with social deficits. *Biol Psychiatry, 74*(3), 212-219.

Maenner, M. J., Shaw, K. A., Bak, J., Washington, A., Patrick, M., DiRienzo, M., Christensen, D. L., Wiggins, L. D., Pettygrove, S., Andrews, J. G., Lopez, M., Hudson, A., Baroud, T., Schwenk, Y., White, T., Rosenberg, C. R., Lee, L. C., Harrington, R. A., Huston, M., Hewitt, A., Esler, A., Hall-Lande, J., Poynter, J. N., Hallas-Muchow, L., Constantino, J. N., Fitzgerald, R. T., Zahorodny, W., Shenouda, J., Daniels, J. L., Warren, Z., Vehorn, A., Salinas, A., Durkin, M. S., & Dietz, P. M. (2020). Prevalence of Autism Spectrum Disorder Among Children Aged 8 Years - Autism and Developmental Disabilities Monitoring Network, 11 Sites, United States, 2016. *Mmwr Surveillance Summaries, 69*(4), 1-+.

Malikovic, A., Amunts, K., Schleicher, A., Mohlberg, H., Kujovic, M., Palomero-Gallagher, N., Eickhoff, S. B., & Zilles, K. (2016). Cytoarchitecture of the human lateral occipital cortex: mapping of two extrastriate areas hOc4la and hOc4lp. *Brain Struct Funct, 221*(4), 1877-1897.

Mash, L. E., Reiter, M. A., Linke, A. C., Townsend, J., & Müller, R. A. (2018). Multimodal approaches to functional connectivity in autism spectrum disorders: An integrative perspective. *Dev Neurobiol, 78*(5), 456-473.

Matson, J. L., & Shoemaker, M. (2009). Intellectual disability and its relationship to autism spectrum disorders. *Res Dev Disabil, 30*(6), 1107-1114.

Menon, V. (2011). Large-scale brain networks and psychopathology: a unifying triple network model. *Trends Cogn Sci, 15*(10), 483-506.

Mensen, V. T., Wierenga, L. M., van Dijk, S., Rijks, Y., Oranje, B., Mandl, R. C., & Durston, S. (2017). Development of cortical thickness and surface area in autism spectrum disorder. *Neuroimage Clin, 13*, 215-222.

Miller, D. J., Duka, T., Stimpson, C. D., Schapiro, S. J., Baze, W. B., McArthur, M. J., Fobbs, A. J., Sousa, A. M., Sestan, N., Wildman, D. E., Lipovich, L., Kuzawa, C. W., Hof, P. R., & Sherwood, C. C. (2012). Prolonged myelination in human neocortical evolution. *Proc Natl Acad Sci U S A, 109*(41), 16480-16485.

Misaki, M., Wallace, G. L., Dankner, N., Martin, A., & Bandettini, P. A. (2012). Characteristic cortical thickness patterns in adolescents with autism spectrum disorders: interactions with age and intellectual ability revealed by canonical correlation analysis. *Neuroimage, 60*(3), 1890-1901.

Mohd Nordin, A., Ismail, J., & Kamal Nor, N. (2021). Motor Development in Children With Autism Spectrum Disorder. *Front Pediatr, 9*, 598276.

Molnar-Szakacs, I., Kupis, L., & Uddin, L. Q. (2021). Neuroimaging Markers of Risk and Pathways to Resilience in Autism Spectrum Disorder. *Biol Psychiatry Cogn Neurosci Neuroimaging, 6*(2), 200-210.

Monk, C. S., Peltier, S. J., Wiggins, J. L., Weng, S. J., Carrasco, M., Risi, S., & Lord, C. (2009). Abnormalities of intrinsic functional connectivity in autism spectrum disorders. *Neuroimage, 47*(2), 764-772.

Moradi, E., Khundrakpam, B., Lewis, J. D., Evans, A. C., & Tohka, J. (2017). Predicting symptom severity in autism spectrum disorder based on cortical thickness measures in agglomerative data. *Neuroimage, 144*(Pt A), 128-141.

Mottron, L., Dawson, M., Soulieres, I., Hubert, B., & Burack, J. (2006). Enhanced perceptual functioning in autism: an update, and eight principles of autistic perception. *J Autism Dev Disord, 36*(1), 27-43.

Mullen, E. M. (1995). *Mullen scales of early learning*. Circle Pines, MN: American Guidance Service.

Müller, R. A., Shih, P., Keehn, B., Deyoe, J. R., Leyden, K. M., & Shukla, D. K. (2011). Underconnected, but how? A survey of functional connectivity MRI studies in autism spectrum disorders. *Cerebral Cortex, 21*(10), 2233-2243.

Mundy, P., Sullivan, L., & Mastergeorge, A. M. (2009). A Parallel and Distributed-Processing Model of Joint Attention, Social Cognition and Autism. *Autism Research, 2*(1), 2-21.

Myers, S. M., Challman, T. D., Bernier, R., Bourgeron, T., Chung, W. K., Constantino, J. N., Eichler, E. E., Jacquemont, S., Miller, D. T., Mitchell, K. J., Zoghbi, H. Y., Martin, C. L., & Ledbetter, D. H. (2020). Insufficient Evidence for "Autism-Specific" Genes. *American Journal of Human Genetics, 106*(5), 587-595.

Nagy, Z., Westerberg, H., & Klingberg, T. (2004). Maturation of white matter is associated with the development of cognitive functions during childhood. *J Cogn Neurosci, 16*(7), 1227-1233.

Nair, S., Jao Keehn, R. J., Berkebile, M. M., Maximo, J. O., Witkowska, N., & Müller, R. A. (2017). Local resting state functional connectivity in autism: site and cohort variability and the effect of eye status. *Brain Imaging Behav*.

Narr, K. L., Woods, R. P., Thompson, P. M., Szeszko, P., Robinson, D., Dimtcheva, T., Gurbani, M., Toga, A. W., & Bilder, R. M. (2007). Relationships between IQ and regional cortical gray matter thickness in healthy adults. *Cerebral Cortex, 17*(9), 2163-2171.

Natu, V. S., Gomez, J., Barnett, M., Jeska, B., Kirilina, E., Jaeger, C., Zhen, Z., Cox, S., Weiner, K. S., Weiskopf, N., & Grill-Spector, K. (2019). Apparent thinning of human visual cortex during childhood is associated with myelination. *Proc Natl Acad Sci U S A, 116*(41), 20750-20759.

Nielsen, J. A., Zielinski, B. A., Fletcher, P. T., Alexander, A. L., Lange, N., Bigler, E. D., Lainhart, J. E., & Anderson, J. S. (2013). Multisite functional connectivity MRI classification of autism: ABIDE results. *Frontiers in Human Neuroscience, 7*.

Nomi, J. S., Molnar-Szakacs, I., & Uddin, L. Q. (2019). Insular function in autism: Update and future directions in neuroimaging and interventions. *Prog Neuropsychopharmacol Biol Psychiatry, 89*, 412-426.

Nomi, J. S., & Uddin, L. Q. (2015). Developmental changes in large-scale network connectivity in autism. *Neuroimage-Clinical, 7*, 732-741.

Nordahl, C. W., Dierker, D., Mostafavi, I., Schumann, C. M., Rivera, S. M., Amaral, D. G., & Van Essen, D. C. (2007). Cortical folding abnormalities in autism revealed by surface-based morphometry. *J Neurosci, 27*(43), 11725-11735.

Nordahl, C. W., Mello, M., Shen, A. M., Shen, M. D., Vismara, L. A., Li, D. A., Harrington, K., Tanase, C., Goodlin-Jones, B., Rogers, S., Abbeduto, L., & Amaral, D. G. (2016). Methods for acquiring MRI data in children with autism spectrum disorder and intellectual impairment without the use of sedation. *Journal of Neurodevelopmental Disorders, 8*.

O'Riordan, M. A., Plaisted, K. C., Driver, J., & Baron-Cohen, S. (2001). Superior visual search in autism. *Journal of Experimental Psychology-Human Perception and Performance, 27*(3), 719-730.

Odriozola, P., Uddin, L. Q., Lynch, C. J., Kochalka, J., Chen, T., & Menon, V. (2016). Insula response and connectivity during social and non-social attention in children with autism. *Soc Cogn Affect Neurosci, 11*(3), 433-444.

Ogawa, S., Lee, T. M., Kay, A. R., & Tank, D. W. (1990). Brain Magnetic-Resonance-Imaging with Contrast Dependent on Blood Oxygenation. *Proceedings of the National Academy of Sciences of the United States of America, 87*(24), 9868-9872.

Olson, L., Chen, B., & Fishman, I. (2021). Neural correlates of socioeconomic status in early childhood: a systematic review of the literature. *Child Neuropsychol, 27*(3), 390-423.

Olson, L. A., Mash, L. E., Linke, A., Fong, C. H., Müller, R. A., & Fishman, I. (2020). Sex-related patterns of intrinsic functional connectivity in children and adolescents with autism spectrum disorders. *Autism, 24*(8), 2190-2201.

Ozonoff, S., Young, G. S., Landa, R. J., Brian, J., Bryson, S., Charman, T., Chawarska, K., Macari, S. L., Messinger, D., Stone, W. L., Zwaigenbaum, L., & Iosif, A. M. (2015). Diagnostic stability in young children at risk for autism spectrum disorder: a baby siblings research consortium study. *J Child Psychol Psychiatry, 56*(9), 988-998.

Padmanabhan, A., Lynch, C. J., Schaer, M., & Menon, V. (2017). The Default Mode Network in Autism. *Biol Psychiatry Cogn Neurosci Neuroimaging, 2*(6), 476-486.

Pagnozzi, A. M., Conti, E., Calderoni, S., Fripp, J., & Rose, S. E. (2018). A systematic review of structural MRI biomarkers in autism spectrum disorder: A machine learning perspective. *Int J Dev Neurosci, 71*, 68-82.

Pelphrey, K. A., Morris, J. P., Michelich, C. R., Allison, T., & McCarthy, G. (2005). Functional anatomy of biological motion perception in posterior temporal cortex: an FMRI study of eye, mouth and hand movements. *Cerebral Cortex, 15*(12), 1866-1876.

Pierce, K., Gazestani, V. H., Bacon, E., Barnes, C. C., Cha, D., Nalabolu, S., Lopez, L., Moore, A., Pence-Stophaeros, S., & Courchesne, E. (2019). Evaluation of the Diagnostic Stability of the Early Autism Spectrum Disorder Phenotype in the General Population Starting at 12 Months. *Jama Pediatrics, 173*(6), 578-587.

Power, J. D., Mitra, A., Laumann, T. O., Snyder, A. Z., Schlaggar, B. L., & Petersen, S. E. (2014). Methods to detect, characterize, and remove motion artifact in resting state fMRI. *Neuroimage, 84*, 320-341.

Prasad, S., & Galetta, S. L. (2011). Anatomy and physiology of the afferent visual system. *Handb Clin Neurol, 102*, 3-19.

Prigge, M. B. D., Lange, N., Bigler, E. D., King, J. B., Dean, D. C., 3rd, Adluru, N., Alexander, A. L., Lainhart, J. E., & Zielinski, B. A. (2021). A 16-year study of longitudinal volumetric brain development in males with autism. *Neuroimage, 236*, 118067.

Raichle, M. E., MacLeod, A. M., Snyder, A. Z., Powers, W. J., Gusnard, D. A., & Shulman, G. L. (2001). A default mode of brain function. *Proceedings of the National Academy of Sciences of the United States of America, 98*(2), 676-682.

Rakic, P. (1988). Specification of cerebral cortical areas. *Science, 241*(4862), 170-176.

Redcay, E. (2008). The superior temporal sulcus performs a common function for social and speech perception: implications for the emergence of autism. *Neurosci Biobehav Rev, 32*(1), 123-142.

Redcay, E., & Courchesne, E. (2008). Deviant functional magnetic resonance imaging patterns of brain activity to speech in 2-3-year-old children with autism spectrum disorder. *Biol Psychiatry, 64*(7), 589-598.

Redcay, E., Haist, F., & Courchesne, E. (2008). Functional neuroimaging of speech perception during a pivotal period in language acquisition. *Developmental Science, 11*(2), 237-252.

Reiter, M. A., Jahedi, A., Jac Fredo, A. R., Fishman, I., Bailey, B., & Müller, R. A. (2021). Performance of machine learning classification models of autism using resting-state fMRI is contingent on sample heterogeneity. *Neural Comput Appl, 33*(8), 3299-3310.

Reiter, M. A., Mash, L. E., Linke, A. C., Fong, C. H., Fishman, I., & Müller, R. A. (2018). Distinct Patterns of Atypical Functional Connectivity in Lower-Functioning Autism. *Biol Psychiatry Cogn Neurosci Neuroimaging, 4*(3), 251-259.

Rudie, J. D., Brown, J. A., Beck-Pancer, D., Hernandez, L. M., Dennis, E. L., Thompson, P. M., Bookheimer, S. Y., & Dapretto, M. (2013). Altered functional and structural brain network organization in autism. *Neuroimage-Clinical, 2*, 79-94.

Rudie, J. D., Shehzad, Z., Hernandez, L. M., Colich, N. L., Bookheimer, S. Y., Iacoboni, M., & Dapretto, M. (2012). Reduced functional integration and segregation of distributed neural systems underlying social and emotional information processing in autism spectrum disorders. *Cerebral Cortex, 22*(5), 1025-1037.

Rutter, M., Bailey, A., & Lord, C. (2003). *Social Communication Questionnaire.* Los Angeles, CA: Western Psychological Services.

Rylaarsdam, L., & Guemez-Gamboa, A. (2019). Genetic Causes and Modifiers of Autism Spectrum Disorder. *Front Cell Neurosci, 13*, 385.

Salmi, J., Roine, U., Glerean, E., Lahnakoski, J., Nieminen-von Wendt, T., Tani, P., Leppamaki, S., Nummenmaa, L., Jaaskelainen, I. P., Carlson, S., Rintahaka, P., & Sams, M. (2013). The brains of high functioning autistic individuals do not synchronize with those of others. *Neuroimage-Clinical, 3*, 489-497.

Samson, F., Mottron, L., Soulieres, I., & Zeffiro, T. A. (2012). Enhanced visual functioning in autism: an ALE meta-analysis. *Human Brain Mapping, 33*(7), 1553-1581.

Satterthwaite, T. D., Elliott, M. A., Gerraty, R. T., Ruparel, K., Loughead, J., Calkins, M. E., Eickhoff, S. B., Hakonarson, H., Gur, R. C., Gur, R. E., & Wolf, D. H. (2013). An improved framework for confound regression and filtering for control of motion artifact in the preprocessing of resting-state functional connectivity data. *Neuroimage, 64*, 240-256.

Sattler J.M, & J.J., R. (2009). *Assessment with the WAIS-IV*. San Diego, CA: Jerome M. Sattler, Publisher, Inc.

Saygin, A. P., Wilson, S. M., Hagler, D. J., Jr., Bates, E., & Sereno, M. I. (2004). Point-light biological motion perception activates human premotor cortex. *J Neurosci, 24*(27), 6181-6188.

Schaer, M., Cuadra, M. B., Schmansky, N., Fischl, B., Thiran, J. P., & Eliez, S. (2012). How to measure cortical folding from MR images: a step-by-step tutorial to compute local gyrification index. *J Vis Exp*(59), e3417.

Schaer, M., Cuadra, M. B., Tamarit, L., Lazeyras, F., Eliez, S., & Thiran, J. P. (2008). A surface-based approach to quantify local cortical gyrification. *IEEE Trans Med Imaging, 27*(2), 161-170.

Schmitt, J. E., Raznahan, A., Clasen, L. S., Wallace, G. L., Pritikin, J. N., Lee, N. R., Giedd, J. N., & Neale, M. C. (2019). The Dynamic Associations Between Cortical Thickness and General Intelligence are Genetically Mediated. *Cerebral Cortex, 29*(11), 4743-4752.

Schnack, H. G., van Haren, N. E., Brouwer, R. M., Evans, A., Durston, S., Boomsma, D. I., Kahn, R. S., & Hulshoff Pol, H. E. (2015). Changes in thickness and surface area of the human cortex and their relationship with intelligence. *Cerebral Cortex, 25*(6), 1608-1617.

Schumann, C. M., Barnes, C. C., Lord, C., & Courchesne, E. (2009). Amygdala enlargement in toddlers with autism related to severity of social and communication impairments. *Biol Psychiatry, 66*(10), 942-949.

Schumann, C. M., & Nordahl, C. W. (2011). Bridging the gap between MRI and postmortem research in autism. *Brain Res, 1380*, 175-186.

Shaw, P., Greenstein, D., Lerch, J., Clasen, L., Lenroot, R., Gogtay, N., Evans, A., Rapoport, J., & Giedd, J. (2006). Intellectual ability and cortical development in children and adolescents. *Nature, 440*(7084), 676-679.

Shen, M. D., Kim, S. H., McKinstry, R. C., Gu, H., Hazlett, H. C., Nordahl, C. W., Emerson, R. W., Shaw, D., Elison, J. T., Swanson, M. R., Fonov, V. S., Gerig, G., Dager, S. R., Botteron, K. N., Paterson, S., Schultz, R. T., Evans, A. C., Estes, A. M., Zwaigenbaum, L., Styner, M. A., Amaral, D. G., Piven, J., Hazlett, H. C., Chappell, C., Dager, S., Estes, A., Shaw, D., Botteron, K., McKinstry, R., Constantino, J., Pruett, J., Schultz, R., Zwaigenbaum, L., Elison, J., Evans, A. C., Collins, D. L., Pike, G. B., Fonov, V., Kostopoulos, P., Das, S., Gerig, G., Styner, M., Gu, H., Piven, J., & Infant Brain Imaging Study, N. (2017). Increased Extra-axial Cerebrospinal Fluid in High-Risk Infants Who Later Develop Autism. *Biol Psychiatry, 82*(3), 186-193.

Shen, M. D., Li, D. D., Keown, C. L., Lee, A., Johnson, R. T., Angkustsiri, K., Rogers, S. J., Müller, R. A., Amaral, D. G., & Nordahl, C. W. (2016). Functional Connectivity of the Amygdala Is Disrupted in Preschool-Aged Children With Autism Spectrum Disorder. *Journal of the American Academy of Child and Adolescent Psychiatry, 55*(9), 817-824.

Shen, M. D., Nordahl, C. W., Young, G. S., Wootton-Gorges, S. L., Lee, A., Liston, S. E., Harrington, K. R., Ozonoff, S., & Amaral, D. G. (2013). Early brain enlargement and elevated extra-axial fluid in infants who develop autism spectrum disorder. *Brain, 136*(Pt 9), 2825-2835.

Shih, P., Keehn, B., Oram, J. K., Leyden, K. M., Keown, C. L., & Müller, R. A. (2011). Functional differentiation of posterior superior temporal sulcus in autism: a functional connectivity magnetic resonance imaging study. *Biol Psychiatry, 70*(3), 270-277.

Shimony, J. S., Smyser, C. D., Wideman, G., Alexopoulos, D., Hill, J., Harwell, J., Dierker, D., Van Essen, D. C., Inder, T. E., & Neil, J. J. (2016). Comparison of cortical folding measures for evaluation of developing human brain. *Neuroimage, 125*, 780-790.

Simmons, D. R., Robertson, A. E., McKay, L. S., Toal, E., McAleer, P., & Pollick, F. E. (2009). Vision in autism spectrum disorders. *Vision Research, 49*(22), 2705-2739.

Simonoff, E., Pickles, A., Charman, T., Chandler, S., Loucas, T., & Baird, G. (2008). Psychiatric disorders in children with autism spectrum disorders: prevalence, comorbidity, and

associated factors in a population-derived sample. *J Am Acad Child Adolesc Psychiatry, 47*(8), 921-929.

Siu, C. R., & Murphy, K. M. (2018). The development of human visual cortex and clinical implications. *Eye Brain, 10*, 25-36.

Smith, S. M., Fox, P. T., Miller, K. L., Glahn, D. C., Fox, P. M., Mackay, C. E., Filippini, N., Watkins, K. E., Toro, R., Laird, A. R., & Beckmann, C. F. (2009). Correspondence of the brain's functional architecture during activation and rest. *Proceedings of the National Academy of Sciences of the United States of America, 106*(31), 13040-13045.

Smith, S. M., Jenkinson, M., Woolrich, M. W., Beckmann, C. F., Behrens, T. E. J., Johansen-Berg, H., Bannister, P. R., De Luca, M., Drobnjak, I., Flitney, D. E., Niazy, R. K., Saunders, J., Vickers, J., Zhang, Y. Y., De Stefano, N., Brady, J. M., & Matthews, P. M. (2004). Advances in functional and structural MR image analysis and implementation as FSL. *Neuroimage, 23*, S208-S219.

Song, D. Y., Topriceanu, C. C., Ilie-Ablachim, D. C., Kinali, M., & Bisdas, S. (2021). Machine learning with neuroimaging data to identify autism spectrum disorder: a systematic review and meta-analysis. *Neuroradiology, 63*(12), 2057-2072.

Soulieres, I., Dawson, M., Samson, F., Barbeau, E. B., Sahyoun, C. P., Strangman, G. E., Zeffiro, T. A., & Mottron, L. (2009). Enhanced visual processing contributes to matrix reasoning in autism. *Hum Brain Mapp, 30*(12), 4082-4107.

Sparrow, S. S., Cicchetti, D. V., & Balla, D. A. (2005). *Vineland adaptive behavior scales: Second edition (Vineland II), survey interview form/caregiver rating form.* . Livonia, MN: Pearson Assessments.

Sridharan, D., Levitin, D. J., & Menon, V. (2008). A critical role for the right fronto-insular cortex in switching between central-executive and default-mode networks. *Proceedings of the National Academy of Sciences of the United States of America, 105*(34), 12569-12574.

Srivastava, A. K., & Schwartz, C. E. (2014). Intellectual disability and autism spectrum disorders: causal genes and molecular mechanisms. *Neurosci Biobehav Rev, 46 Pt 2*, 161-174.

Stanfield, A. C., McIntosh, A. M., Spencer, M. D., Philip, R., Gaur, S., & Lawrie, S. M. (2008). Towards a neuroanatomy of autism: A systematic review and meta-analysis of structural magnetic resonance imaging studies. *European Psychiatry, 23*(4), 289-299.

Steinhausen, H. C., Jensen, C. M., & Lauritsen, M. B. (2016). A systematic review and meta-analysis of the long-term overall outcome of autism spectrum disorders in adolescence and adulthood. *Acta Psychiatrica Scandinavica, 133*(6), 445-452.

Stevenson, J. L., & Gernsbacher, M. A. (2013). Abstract Spatial Reasoning as an Autistic Strength. *Plos One, 8*(3).

Stevenson, R. A., Segers, M., Ncube, B. L., Black, K. R., Bebko, J. M., Ferber, S., & Barense, M. D. (2018). The cascading influence of multisensory processing on speech perception in autism. *Autism, 22*(5), 609-624.

Stevenson, R. A., Siemann, J. K., Woynaroski, T. G., Schneider, B. C., Eberly, H. E., Camarata, S. M., & Wallace, M. T. (2014). Brief report: Arrested development of audiovisual speech perception in autism spectrum disorders. *J Autism Dev Disord, 44*(6), 1470-1477.

Stiles, J., & Jernigan, T. L. (2010). The basics of brain development. *Neuropsychol Rev, 20*(4), 327-348.

Storsve, A. B., Fjell, A. M., Tamnes, C. K., Westlye, L. T., Overbye, K., Aasland, H. W., & Walhovd, K. B. (2014). Differential longitudinal changes in cortical thickness, surface area and volume across the adult life span: regions of accelerating and decelerating change. *J Neurosci, 34*(25), 8488-8498.

Tager-Flusberg, H., Paul, R., & Lord, C. (2005). Language and communication in autism *Handbook of Autism and Pervasive Developmental Disorders* (3 ed., Vol. 1).

Tahedl, M. (2020). Towards individualized cortical thickness assessment for clinical routine. *J Transl Med, 18*(1), 151.

Tamnes, C. K., Herting, M. M., Goddings, A. L., Meuwese, R., Blakemore, S. J., Dahl, R. E., Guroglu, B., Raznahan, A., Sowell, E. R., Crone, E. A., & Mills, K. L. (2017). Development of the Cerebral Cortex across Adolescence: A Multisample Study of Inter-Related Longitudinal Changes in Cortical Volume, Surface Area, and Thickness. *J Neurosci, 37*(12), 3402-3412.

Tanner, A., & Dounavi, K. (2021). The Emergence of Autism Symptoms Prior to 18 Months of Age: A Systematic Literature Review. *J Autism Dev Disord, 51*(3), 973-993.

Thompson, A., Murphy, D., Dell'Acqua, F., Ecker, C., McAlonan, G., Howells, H., Baron-Cohen, S., Lai, M. C., Lombardo, M. V., Consortium, M. A., & Marco, C. (2017). Impaired Communication Between the Motor and Somatosensory Homunculus Is Associated With Poor Manual Dexterity in Autism Spectrum Disorder. *Biol Psychiatry, 81*(3), 211-219.

Thurm, A., Lord, C., Lee, L. C., & Newschaffer, C. (2007). Predictors of language acquisition in preschool children with autism spectrum disorders. *J Autism Dev Disord, 37*(9), 1721-1734.

Toth, K., Munson, J., Meltzoff, A. N., & Dawson, G. (2006). Early predictors of communication development in young children with autism spectrum disorder: joint attention, imitation, and toy play. *J Autism Dev Disord, 36*(8), 993-1005.

Turesky, T. K., Vanderauwera, J., & Gaab, N. (2021). Imaging the rapidly developing brain: Current challenges for MRI studies in the first five years of life. *Dev Cogn Neurosci, 47*, 100893.

Uddin, L. Q., Dajani, D. R., Voorhies, W., Bednarz, H., & Kana, R. K. (2017). Progress and roadblocks in the search for brain-based biomarkers of autism and attention-deficit/hyperactivity disorder. *Transl Psychiatry, 7*(8), e1218.

Uddin, L. Q., Kelly, A. M., Biswal, B. B., Castellanos, F. X., & Milham, M. P. (2009). Functional connectivity of default mode network components: correlation, anticorrelation, and causality. *Hum Brain Mapp, 30*(2), 625-637.

Uddin, L. Q., & Menon, V. (2009). The anterior insula in autism: under-connected and under-examined. *Neurosci Biobehav Rev, 33*(8), 1198-1203.

Uddin, L. Q., Supekar, K., Lynch, C. J., Cheng, K. M., Odriozola, P., Barth, M. E., Phillips, J., Feinstein, C., Abrams, D. A., & Menon, V. (2015). Brain State Differentiation and Behavioral Inflexibility in Autism. *Cereb Cortex, 25*(12), 4740-4747.

Uddin, L. Q., Supekar, K., & Menon, V. (2013). Reconceptualizing functional brain connectivity in autism from a developmental perspective. *Front Hum Neurosci, 7*, 458.

Ungerleider, L. G., & Haxby, J. V. (1994). 'What' and 'where' in the human brain. *Current Biology, 4*(1), 157-165.

Van Dijk, K. R. A., Hedden, T., Venkataraman, A., Evans, K. C., Lazar, S. W., & Buckner, R. L. (2010). Intrinsic Functional Connectivity As a Tool For Human Connectomics: Theory, Properties, and Optimization. *Journal of Neurophysiology, 103*(1), 297-321.

van Rooij, D., Anagnostou, E., Arango, C., Auzias, G., Behrmann, M., Busatto, G. F., Calderoni, S., Daly, E., Deruelle, C., Di Martino, A., Dinstein, I., Duran, F. L. S., Durston, S., Ecker, C., Fair, D., Fedor, J., Fitzgerald, J., Freitag, C. M., Gallagher, L., Gori, I., Haar, S., Hoekstra, L., Jahanshad, N., Jalbrzikowski, M., Janssen, J., Lerch, J., Luna, B., Martinho, M. M., McGrath, J., Muratori, F., Murphy, C. M., Murphy, D. G. M., O'Hearn, K., Oranje, B., Parellada, M., Retico, A., Rosa, P., Rubia, K., Shook, D., Taylor, M., Thompson, P. M., Tosetti, M., Wallace, G. L., Zhou, F., & Buitelaar, J. K. (2018). Cortical and Subcortical Brain Morphometry Differences Between Patients With Autism Spectrum Disorder and Healthy Individuals Across the Lifespan: Results From the ENIGMA ASD Working Group. *Am J Psychiatry, 175*(4), 359-369.

Veldman, S. L. C., Santos, R., Jones, R. A., Sousa-Sa, E., & Okely, A. D. (2019). Associations between gross motor skills and cognitive development in toddlers. *Early Hum Dev, 132*, 39-44.

Washington, S. D., Gordon, E. M., Brar, J., Warburton, S., Sawyer, A. T., Wolfe, A., Mease-Ference, E. R., Girton, L., Hailu, A., Mbwana, J., Gaillard, W. D., Kalbfleisch, M. L., & VanMeter, J. W. (2014). Dysmaturation of the Default Mode Network in Autism. *Human Brain Mapping, 35*(4), 1284-1296.

Wechsler, D. (1999). *Wechsler Abbreviated Scale of Intelligence*. San Antonio, TX: The Psychological Corporation.

Weitzman, C., & Wegner, L. (2015). Promoting optimal development: screening for behavioral and emotional problems. *Pediatrics, 135*(2), 384-395.

Weng, S. J., Wiggins, J. L., Peltier, S. J., Carrasco, M., Risi, S., Lord, C., & Monk, C. S. (2010a). Alterations of resting state functional connectivity in the default network in adolescents with autism spectrum disorders. *Brain Research, 1313*, 202-214.

White, N., Roddey, C., Shankaranarayanan, A., Han, E., Rettmann, D., Santos, J., Kuperman, J., & Dale, A. (2010). PROMO: Real-time prospective motion correction in MRI using image-based tracking. *Magn Reson Med, 63*(1), 91-105.

Whitfield-Gabrieli, S., & Ford, J. M. (2012). Default mode network activity and connectivity in psychopathology. *Annu Rev Clin Psychol, 8*, 49-76.

Whitfield-Gabrieli, S., & Nieto-Castanon, A. (2012). Conn: A Functional Connectivity Toolbox for Correlated and Anticorrelated Brain Networks. *Brain Connectivity, 2*(3), 125-141.

Wolff, J. J., Jacob, S., & Elison, J. T. (2018). The journey to autism: Insights from neuroimaging studies of infants and toddlers. *Dev Psychopathol, 30*(2), 479-495.

Xiao, X., Fang, H., Wu, J. S., Xiao, C. Y., Xiao, T., Qian, L., Liang, F. J., Xiao, Z., Chu, K. K., & Ke, X. Y. (2017). Diagnostic model generated by MRI-derived brain features in toddlers with autism spectrum disorder. *Autism Research, 10*(4), 620-630.

Yang, D. Y., Rosenblau, G., Keifer, C., & Pelphrey, K. A. (2015). An integrative neural model of social perception, action observation, and theory of mind. *Neurosci Biobehav Rev, 51*, 263-275.

Yerys, B. E., Gordon, E. M., Abrams, D. N., Satterthwaite, T. D., Weinblatt, R., Jankowski, K. F., Strang, J., Kenworthy, L., Gaillard, W. D., & Vaidya, C. J. (2015). Default mode network segregation and social deficits in autism spectrum disorder: Evidence from non-medicated children. *Neuroimage Clin, 9*, 223-232.

Zatorre, R. J., Fields, R. D., & Johansen-Berg, H. (2012). Plasticity in gray and white: neuroimaging changes in brain structure during learning. *Nature Neuroscience, 15*(4), 528-536.